ABSTRACT

VITCHULI GANGADHARAN, NARENDIRAN. Atmospheric Pressure Plasma-Electrospinning Hybrid Process for Protective Applications. (Under the direction of Dr Xiangwu Zhang and Dr.Marian G McCord.)

Chemical and biological (C-B) warfare agents like sarin, sulfur mustard, anthrax are usually dispersed into atmosphere in the form of micro aerosols. They are considered to be dangerous weapon of mass destruction next to nuclear weapons. The airtight protective clothing materials currently available are able to stop the diffusion of threat agents but not good enough to detoxify them, which endangers the wearers. Extensive research efforts are being made to prepare advanced protective clothing materials that not only prevent the diffusion of C-B agents, but also detoxify them into harmless products thus ensuring the safety and comfort of the wearer. Electrospun nanofiber mats are considered to have effective filtration characteristics to stop the diffusion of submicron level particulates without sacrificing air permeability characteristics and could be used in protective application as barrier material. In addition, functional nanofibers could be potentially developed to detoxify the C-B warfare threats into harmless products. In this research, electrospun nanofibers were deposited on fabric surface to improve barrier efficiency without sacrificing comfort-related properties of the fabrics. Multi-functional nanofibers were fabricated through an electrospinning-electrospraying hybrid process and their ability to detoxify simulants of C-B agents was evaluated. Nanofibers were also deposited onto plasma-pretreated woven fabric substrate through a newly developed plasma-electrospinning hybrid process, to improve the adhesive properties of nanofibers on the fabric surface. The nanofiber adhesion and durability properties were evaluated by peel test, flex and abrasion resistance tests.

In this research work, following tasks have been carried out:

i) *Controlled deposition of nanofiber mat onto woven fabric substrate*

Electrospun Nylon 6 fiber mats were deposited onto woven 50/50 Nylon/Cotton fabric with the motive of making them into protective material against submicron-level aerosol chemical and biological threats. Polymer solution concentration, electrospinning voltage, and deposition areal density were varied to establish the relationship of processing-structure-filtration efficiency for electrospun fiber mats. A high barrier efficiency of greater than 99.5% was achieved on electrospun fiber mats without sacrificing air permeability and pressure drop.

ii) *Fabrication and Characterization of Multifunctional ZnO/Nylon 6 nanofibers*

ZnO/Nylon 6 nanofiber mats were prepared by an electrospinning-electrospraying hybrid process, The electrospinning of polymer solution and electrospraying of ZnO particles were carried out simultaneously such that the ZnO nanoparticles were dispersed on the surface of Nylon 6 nanofibers. The prepared ZnO/Nylon 6 nanofiber mats were tested for detoxifying characteristics against simulants of C-B agents. The results showed that ZnO/Nylon 6 functional nanofiber mats exhibited good detoxification action against paraoxon and have antibacterial efficiency over 99.99% against both the gram-negative *E. coli* and gram positive *B. cereus* bacteria.

iii) *Improving adhesion of electrospun nanofiber mat onto woven fabric by plasma pretreatment of substrate fabric and plasma-electrospinning hybrid process*

Electrospun nanofibers were deposited onto plasma-pretreated woven fabric to improve the adhesion. In addition, the plasma-electrospinning hybrid process was developed and used in which the nanofibers were subjected to *in-situ* plasma treatment during electrospinning. The effects of plasma treatement on substrate fabric and electrospun fibers were characterized by water contact angle test, XPS analyses. The improvement of nanofiber adhesive properties on fabric substrate was evaluated by peel test, flex resistance test and abrasion resistance test. The test results showed that the plasma treatment caused introduction of active chemical groups on substrate fabric and electrospun nanofibers. These active chemical assisted in possible cross-linking formation between nanofiber mat and substrate fabric, and this hypothesis was supported by improved adhesion strength, flex resistance and abrasion resistance of nanofiber mat.

Atmospheric Pressure Plasma-Electrospin Hybrid Process for Protective Applications

by
Narendiran Vitchuli Gangadharan

A dissertation submitted to the Graduate Faculty of
North Carolina State University
in partial fulfillment of the
requirements for the degree of
Doctor of Philosophy

Fiber and Polymer Science

Raleigh, North Carolina

2011

APPROVED BY:

_____	_____
Dr Xiangwu Zhang Committee Chair	Dr Marian McCord Committee Co-Chair
_____	_____
Prof Mohamed Bourham Committee Member	Prof Yuntian Zhu Committee Member

DEDICATION

I dedicate this dissertation to my beloved parents.

BIOGRAPHY

Narendiran Vitchuli Gangadharan was born to his parents Mr. Gangadharan Vitchuli and Mrs. Dhanabhagyam Vitchuli in a small town Nagari, Andhra Pradesh State, India. He earned his bachelor degree in Textile Technology at A C College of Technology, Anna University, Chennai, India in 2006. He received his master degree in Fiber and Polymer Science at Indian Institute of Technology Delhi, New Delhi, India in 2008. He joined North Carolina State University in 2008 to pursue his PhD program in Fiber and Polymer Science under the guidance of Dr Xiangwu Zhang and Dr Marian McCord. His research work focused on fabrication of functional electrospun nanofibers for protective application and atmospheric plasma application to improve adhesion of nanofibers on fabric surface.

ACKNOWLEDGMENTS

I would like to express my sincere gratitude to Professor Xiangwu Zhang for all his support and encouragement throughout my PhD program. I deeply appreciate his efforts, to provide me feedbacks at appropriate moments and advocate pursuing independent research. It was great learning experience and I absolutely enjoyed working with him for the past three years. I would also like to express my deep praise to Professor Marian McCord for providing me excellent feedback and encouragement on my research and for her continues support which motivated me to do things better. I express my special thanks to Professor Mohamed Bourham for his guidance and providing outstanding clues at critical junctures, which helped to solve the difficult problems. I express my sincere gratitude to Professor Yuntian Zhu for serving in my research dissertation committee. I also thank Professor Stoyan Smoukov for accepting to be graduate school representative of my dissertation committee. My sincere acknowledgements to colleagues Dr Quan Shi and Josh Nowak for providing amazing support, without whom I could not have done this PhD work. I also thank Rupesh Nawalakhe and Michael Sieber for their constant help. I would like to express my big acknowledgement to Defense Threat Reduction Agency for providing financial support to this research work. I also thank College of Textiles, NC State University for providing excellent facilities for me to carry out experiments and tests.

I am very grateful to Dr Xiangwu Zhang's research group members. I sincerely thank Birgit Andersen, Prof Keith Beck, Jane Caldwell, Danielle Lehman, Chuck Mooney, Teresa White,

and Dr Bong-Yeol Yeom for assisting me to use the testing instruments. I also thank Dr Russell Gorga and his student Nagarajan Thoppey for allowing me to use their lab facility.

I want to thank my companions Avinav, Bhargava, Rupesh and Vidya for their support and tasty food. I want to thank my senior researchers Loganathan, Pruthesh, Jaspreet, Vamsi, Nagarajan, and Mei for their help and support. I also like to express my gratitude to all student friends at the College of Textiles for their support and wishes. Big thanks to all friends!

Finally I would like to thank my sister's family and brother for their love and support.

TABLE OF CONTENTS

LIST OF TABLES

LIST OF FIGURES

CHAPTER 1

Background, Hypothesis and Objectives

1.1 Background

Chemical and Biological (C-B) Warfare Agents are considered to be the most lethal weapon of mass destruction next to nuclear weapons. The C-B agents include nerve agents such as Sarin, Soman and VX, blistering agents like sulfur mustard, and biological agent like anthrax *(Bacillus anthracis)*.[1] These C-B warfare agents are generally dispersed into atmospheric air, in the form of submicron size aerosol particles.[2] C-B agents attack body vital organs either by inhalation or diffusion through skin in the form of aerosol. This could lead to unconsciousness, permanent impairment of brain and body function, paralysis, severe illness or even death in case of lethal exposure.[3-6] For example, the nerve agent attacks the central nerve system by inhibiting cholinesterase enzymes throughout the body. This results in excessive amount of acetylcholine in all vital body organs causing impairment of brain function, loss of muscle control, respiratory arrest, and even death. Similarly, the HD sulfur mustard diffuses through skin and causes severe skin burns. The biological agent anthrax, deadly bacteria, takes the body as host and multiplies at fast rates, causing respiratory collapse, leading to fatality. Apart from physical casualty, C-B agents may also cause psychological problems such as depression, anxiety, fear, and stress disorder.[7] In addition to these most threatening C-B warfare agents, other toxic warfare agents like irritants, incapacitant, and blood gases including phosgene, hydrogen cyanide have relatively low toxicological risk because of their high volatility.[8] Plague (*Yersinia pestis*), tularemia (*Francisella tularensis*), hemorrhagic fevers (*arena* viruses) and smallpox (*variola* virus) are other biological agents.[9-10]

1.1.1 Chemical-Biological Warfare Protective Clothing

Military and rescue team personnel use Chemical and Biological Protective Clothing (CBPC) materials for protection against C-B threat agents.[7] The CBPC ensemble provides maximum protection when it is worn with all components (Figure 1.1). Usually the protective suit is made of air tight thermoplastic clothing material with laminated charcoal or activated carbon. To improve chemical and thermal resistances, CBPCs are often made using fiberglass/Teflon or Teflon/Kevlar blend fibers. These suits are highly diffusion resistant against C-B agents.[11-13]

These conventional CBPC materials are heavy weight, air tight, poor wearing comfort, high cost, and they require repeated maintenance. In addition, the cumbersomeness caused by conventional CBPC leads to increase in thermal burden, resistance to breathing, and decrease in manual dexterity, speech quality, eye vision, hearing and olfactory senses. It also affects the performance level of the wearer and leads to psychological problems such as stress and fatigue.[7, 11] These limitations hinder CBPC from bieng used by untrained military personnel and civilians.

Recently, there has been growing interest to prepare advanced protective clothing material using lightweight and functional fibers such as micro and nanofibers not only for military but also for civilians. The protective clothing made from these functional fibers and their

composites gives better comfort and protection for the wearer without sacrificing any performance level and with possibility of lower cost.

Figure 1.1 Chemical and Biological Protective Clothing and supporting gears.[12]

1.2.2 Recent Advances in CBPC Related Research Work

In 1993, US army designed a new protective clothing system, *Joint Service Lightweight Integrated Suit Technology* (JSLIST), which is much lighter than previous heavier protective clothing uniform.[12] The JSLIST clothing weighs 6 pounds, which is about half the weight of conventional CBPC. The JSLIST clothing (Figure 1.2) includes a light weight C-B protective garment with integrated hood, bellows-type sockets, high waist trousers, adjustable

suspenders, waist bands, multipurpose over-boots and gloves. To improve the comfort of wearer, JSLIST used a modified version of previous design of CBPC containing polyurethane foam-nylon laminate, impregnated with bulky charcoal.

Figure 1.2 JSLIST protective suits.[14]

JSLIST clothing was made lighter by using nonwoven liner consisting of laminated activated carbon particles, bonded to knitted back to adsorb chemical warfare agents. The nonwoven layer with activated carbon particles is not completely air tight compared to the previous design of fully laminated foam. JSLIST clothing provides passive protection to the wearer from environment contaminated with high level warfare agents for less than 24 hours. After 24 hours, the suit is considered to be a hazard and has to be safely disposed or has to be

subjected to rigorous decontamination procedure for reuse. The US army officially introduced JSLIST clothing into service in 1997. Though the JSLIST clothing provides only passive protection to wearer and has several limitations, it is the best C-B protective suit available till to date. Table 1.1 highlights the properties of conventional protective suits and JSLIST.

Table 1.1 Distinguish properties of protective suits.[15]

	Conventional protective clothing	JSLIST
Material	Polymer based material with bulky charcoal laminate; safeguard against chemical, biological and radiological agents	Charcoal impregnated non- woven layer
Protection	Equipped with self containing breathing apparatus	Charcoal based breathing mask
Advantages	Good protection against C-B agents	Good protection against majority of chemical agents; light in weight
Limitations	Poor moisture vapor transmission, buildup of heat stress, zero comfort	Poor comfort and poor moisture vapor transmission; after use, suit has to safely decontaminated and disposed

In the recent decades, extensive research work on advanced protective clothing system has been carried out by bridging interdisciplinary fields of science and engineering. Efforts are being made to prepare protective clothing materials including advanced smart textiles with self detection and self detoxifying ability against warfare threats, with in-built microelectronics for real time network communication and medical applications.[13,14,16]

1.2.3 Chemical Warfare Agents and their Decontamination

Chemical warfare agents can be broadly classified into four categories as follows i) nerve agent ii) Blister agent iii) Choking agent iv) Asphyxiants.[2, 17, 18, 19] Table1.2 shows the major list of chemical warfare agents.

Table 1.2 List of chemical warfare agents. [2,18]

Nerve agent		Blister agent	Choking agent	Asphyxiants
G series	V series			
Tabun	VE	Sulfur mustard	Chlorine	Cyanogen chloride
Sarin	VX	Nitrogen mustard	Chloropicrin	Hydrogen cyanide
Soman	VG	Lewisite	Phosgene	Arsine

Nerve agents are considered to be most deadly chemical warfare agent. They are class of organophosphate compound that react with acetylcholinesterase enzyme, which is responsible for muscle relaxation. The strong chemical bond between acetylcholinesterase

and organophosphate compound results in inhibition of muscle relaxation and neurotransmission signals, leading to loss of muscle control and difficulty in breathing.

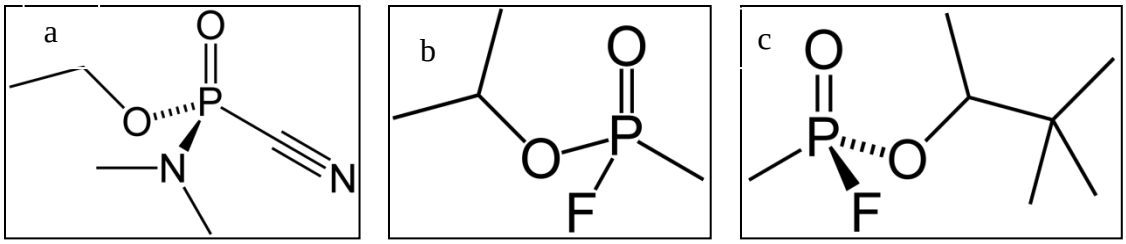

Figure 1.3 The chemical structures of a) Tabun, b) Sarin and c) Soman. [17,18]

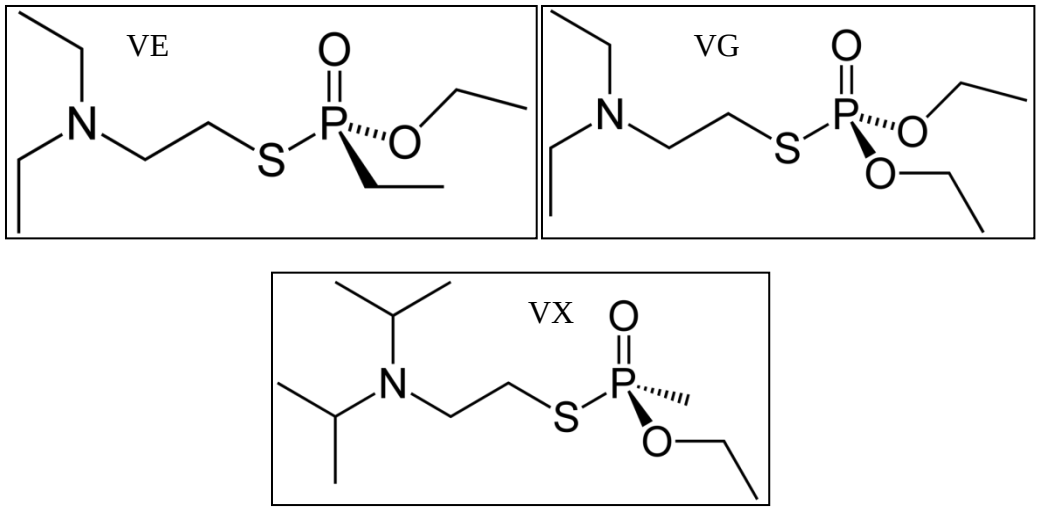

Figure 1.4 The chemical structures of nerve agents VE, VG and VX.[17, 18]

Nerve agents are categorized into G agents (Tabun, Sarin and Soman) and V agents (VE, VG, VX). The letter G represents the country of origin Germany and letter V represents venomous nature. Figure 1.3 and 1.4 shows the chemical structures of G and V agents respectively. The nerve agents are generally liquid at standard temperature and pressure. They can be vaporized 10 times faster than blistering agent, making it deadliest weapon of

mass destruction. Among nerve agents, VX is least volatile and can present in ground for 24 hours. It has high lipo-philicity which makes it 100 times deadlier than G type agents.[2]

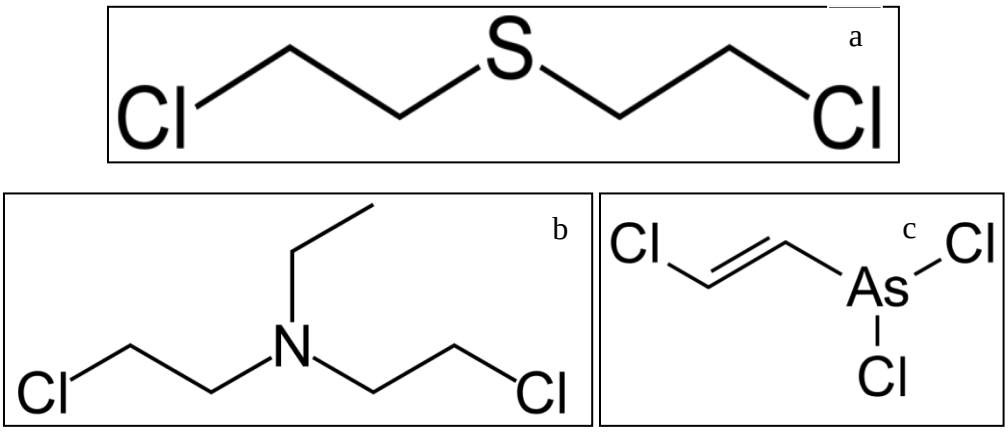

Figure 1.5 The chemical structure of a) Sulfur mustard b) Nitrogen mustard and c) Lewisite.[17, 18]

Blister agents are class of chemical compounds that causes severe chemical burns and fluid blisters when come in contact with skin. Blister agents are not as lethal as nerve agents; however they could severely affect and incapacitate the person.[2] Blister agents can be categorized as Sulfur mustard, Nitrogen mustard and Lewisite. Figure 1.5 shows the chemical structures of blistering agents. Sulfur and Nitrogen mustard agents are usually in liquid form at cold and damp environments and could be readily vaporized into gaseous form in dry and warm temperature conditions. The vapor form mustard agents are 5-6 times heavier than air and could penetrate clothing material easily. The mustard agent dissolves in aqueous medium of human sweat and lead to alkylation reactions forming cyclic ethylene sulfonium ions. These ions react with deoxyribonucleic acid (DNA) and cause cellular death. The effects of mustard agent generally appear within 2-24 hour depending upon the exposure

dosage. Lewisites are organoarsenic chemical compounds and they are classified as blistering agents. These chemical compounds can easily penetrate ordinary clothing material and even rubberized protective clothing. It causes severe damage to the surfaces come in contact.[17]

Choking agents are class of chemical compounds that attack human lungs, cause fluid buildup in pulmonary tract leading to breathing difficulty, nausea, eye and skin irritation. Choking or pulmonary agents include chlorine, chloropicrin, phosgene and diphosgene nitrogen oxides. These chemical agents are usually pressurized and stored as liquid at cold temperature. These liquid forms of chemical agents become gaseous form after release into atmosphere. When these toxic agents come in contact with moist tissue they form hydrochloric acid and nascent oxygen and they lead to tissue damage and pulmonary choking. Depend upon the concentration and dosage these agents can cause mild to severe lung injury and breathing difficulties.[2,17,19]

Asphyxiants are group of chemical compounds that are non lethal in nature and can incapacitate a person. The incapicitant chemicals include lysergic acid diethylamide, ketamine and glycolate anticholinergics. 3-quinuclidinyl benzilate an anticholinergic, can arrest the neurotransmitter acetylcholine enzymes and cause paralysis by attacking central nervous system. Depending upon the concentration and exposure period these agents can cause mild to severe hallucinations, impairment of near vision, nausea, hyperthermia and coma.[17, 19]

Decontamination of chemical warfare agents can be classified into physical and chemical processes. Physical processes include but are not limited to: adsorption using activated carbon, silica gels, zeolites, swell-able layer mineral-tetra calcium aluminates hydrate.[8] The complete detoxification by chemical method includes: i) nucleophilic reaction such as hydrolysis, ii) electrophilic reactions, such as oxidation and chlorination, iii) thermal destruction such as pyrolysis, iv) degradation by plasma flame, photo or radio chemical reactions, and v) combination of these mechanisms.[8,20,21]

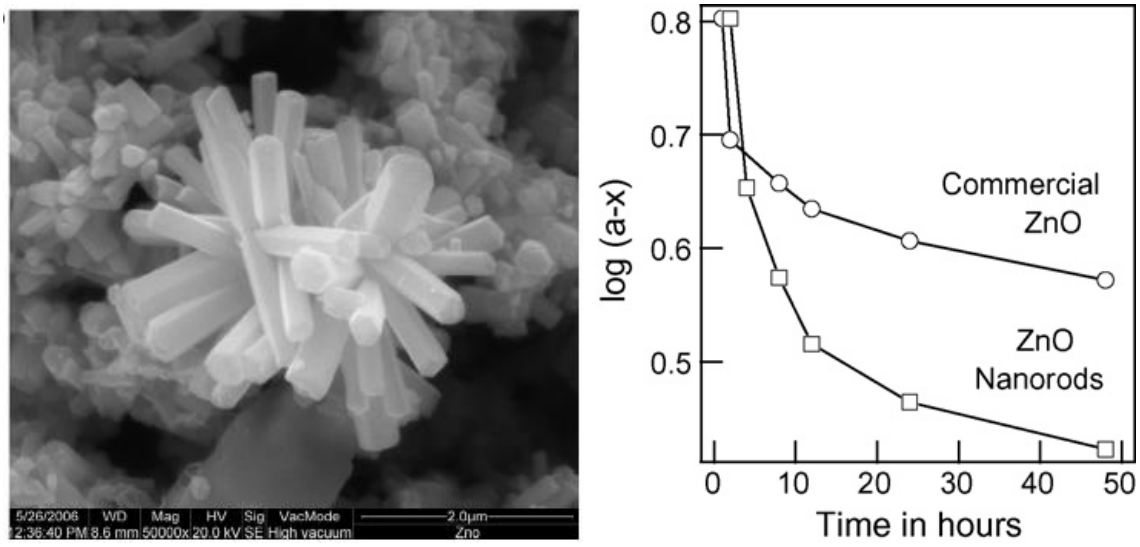

Figure 1.6 SEM image of ZnO nano rods and degradation kinetics of Sulfur Mustard (HD) on zinc oxide nano rods and bulk zinc oxide.[22]

Decontamination of nerve agents O-ethyl S-[2-(diisopropylamino) ethyl] methyl-phosphonothioate (VX), Soman (GD) and HD-Sulfur Mustard, on the surface of nano-sized metal oxide particles such as ZnO, MnO_2, MgO, TiO_2, and AlO_3 have been reported (Figure 1.3).[22-27] The metal oxides can also catalytically break down the phosphorous linkage and convert the organophosphate nerve agent into harmless products. Similarly, cyclodextrin

(CD) in combination with ortho-iodobenzoic acid (IBA) is also capable of detoxifying nerve agents.[28,29] Prasad et.al[22] reported that ZnO and MnO nano structures can catalytically break sulfur mustard into thiodiglycol and hydroxyvinyl ethyl sulphide compounds through dehydro halogenation and hydrolysis reactions.

Detoxification of nerve agent and sulfur mustard agents by enzymatic hydrolysis reactions were reported by several researchers.[30-35] The organophosphorus hydrolase (OPH) and organophosphorous acid anhydrolase (OPAA) enzymes have proven to exhibit hydrolytic reaction against nerve agent VX.[33,34] These enzymes cleave the P-S bonds and convert VX nerve agent into non toxic products. The *LinB* enzyme or haloalkane dehalogenase can catalytic cleave the C-Cl bond in sulfur mustard resulting in harmless products and prevents formation of toxic sulfone/sulfonium intermediates, unlike as in oxidative degradation method. It is reported that the enzyme can be immobilized on polymer surface with assistance of cyclodextrin inclusion compound and the resultant functional polymer surface can act as detoxifying material.[30] In addition, liquid phase decontamination of warfare agents can be carried out with chemicals, such as electrolyzed ozone water, hydrogen peroxide, aqueous sodium carbonate, sodium or potassium hydroxide and calcium and sodium hypo-chloride, have also been reported.[20, 36, 37]

1.1.4 Biological Warfare Agents and their decontamination

Biological warfare refers to use of deadly pathogens such as bacteria, virus or biological toxins to kill or incapacitate humans, animals and plants.[1,9,10,38] In general the biological agent attack human body, take it as host to multiply and cause severe diseases or even death depending on the toxicity. Table 1.3 shows the list of toxic biological agents that can be potentially used in warfare. Bio warfare agents are usually dispersed into atmosphere; in the form of aerosols. They are difficult to detect because of invisible, odorless and tasteless nature. Biological warfare agents are very cheap to produce. For similar mass destruction, it takes less than 1% of cost for bio weapons preparation compare to other form of weapons.

Table 1.3 List of harmful biological warfare agents.[38]

Biological disease	Biological Agents
Anthrax	*B. anthracis*
Botulism	*C.botulinum toxin*
Plague	*Y. pestis*
Smallpox	*V. major*
Tularemia	*F. tularensis*
Viral hemorrhagic fevers	*Filoviruses and Arenaviruses*

The Centers for Disease Control and Prevention, US government has classified Critical Biological Agents that are lethal in nature and could cause severe harm to human lives by

intentional usage, listed in table 1.2. These biological agents are characterized as toxins that have capability to cause high mortality and severe health damage, and highly contagious.

Anthrax is a severe disease caused by certain type of gram-positive, spore forming bacteria called *B.anthracis.* The infection begins after exposed to aerosols of *B.anthracis* endospores, having particle size ranging between 1-5μm. The incubation time is usually couple of days to a week. After exposure, the *B.anthracis* spores attacks the prime targets like subcutaneous skin layer, lungs and gastrointestinal mucosa. Anthrax bacilli grow and proliferate to spread through the lymph and vascular regions. When the amount of endotoxins release reaches the peak stage, it results in severe health deterioration and eventually may lead to death. The person exposed to this biological agent has to be given medical attention within 48 hours; the delay beyond that period may lead to mortality in 95% cases. The anthrax spores do not have definite metabolism rate, they are highly resistant to elevated temperature conditions, UV light, gamma radiation and several disinfectants. Anthrax spores are hard to kill and can persist in dormant state in some variety of soils for few decades; they are considered to most lethal biological warfare agent.[10,39]

Botulinum toxin refers to a type of spore forming bacterium *C.botulinum* which is anaerobic in nature. The bacteria is a powerful neurotoxin known to mankind. It attacks the central nervous system by inhibiting release of acetylcholine a neurotransmitter which causes loss of muscle control and respiratory collapse.[9,38]

Plague is highly contagious and deadly disease caused by bacterium *Y.pestis*. Usually the disease occurs through infectious parasites transmitted by mites or bugs bite. This cause bacterial growth in human body host resulting in plague disease. Intentional spreading of plague bacteria could also cause transmission of disease; after exposure the disease symptoms appear within couple of days. Once symptoms detected, failure to give medical treatment beyond 24 hours may result in critical health deterioration conditions.[9,38]

Small pox is another highly contagious disease spread within humans through *variola* virus by close contact of infected person. After initial exposure, followed by incubation period of two weeks the symptoms appear as fever, headache and inflammations on upper body portion skin. The infected person incapacitated for approximately 2-3 weeks. The inflammation reduces after two weeks leaving behind skin scars. So far, no treatments exist for small pox disease; the disease can be prevented only through prior vaccination.[38,40,41]

Exposure to *Francisella tularenis*, a non spore forming bacteria results in Tularemia disease. After 3-5 days with initial symptoms of fever, headache and pneumonia the disease could continue to impair the body function, respiratory failure, shock and may lead to eventual mortality if not proper treatment provide. The bacterial *Francisella tularenis*, can persist in land, water and vegetations for several weeks and they are considered to be one of the dangerous biological agent.[9,38]

Viral hemorrhagic fevers caused by few Ribonucleic acid (RNA) types of viruses. These viruses attack visceral organs and lead to necrosis. The disease disseminates through infected persons' blood, fluid and other contaminated items. In some case it transmits through air borne particles. This disease does not have a specific vaccine so far and could be prevented only through strict protective measures of using gloves, impermeable clothing, gas mask etc.[9,38]

In general, decontamination of above mentioned biological warfare agents can be carried out using several common disinfectants or sterilizing chemicals such as alcohols, halogens, and quaternary ammonium compounds.[9] These common decontaminants are regularly used to clean surfaces of materials, clothing, laboratory or living room work space, etc. However, these common disinfectants do not kill all types of microorganisms. In addition to these common decontaminants, powerful antibacterial agents, including silver compounds and chemicals having strong oxidizing properties, such as hydrogen peroxide and metal oxides like ZnO, MgO and CaO, can also be used.[42] Application of plasma flame to decontaminate biological agents that present in interior air and electrolyzed ozone water to sterilize contaminated material surface have also been reported.[43,44]

1.1.5 Electrospun Nanofibers

Electrospinning is a simple, yet versatile process to prepare fine polymer fibers with diameters in the range between tens of nanometer and few hundreds of nanometer.[45,46] The

resultant fiber mats have found various applications including tissue engineering, catalytic reaction materials, electrochemical electrodes, affinity membranes, and nano-composites.[47-52]

A typical electrospinning set-up (Figure 1.7) consists of a syringe fitted in a metered pump, a high voltage (10-60 kV) power supply to charge the polymer solution, and a grounded collector plate to deposit the fiber web.[53-55] When the polymer solution droplet comes out of the needle tip, it is influenced by two simultaneous forces, i.e., surface tension force associated with the polymer solution liquid and the electric field created by the high voltage power supply. Taylor cone theory explains the mechanism of droplet motion as follows.[56, 57]

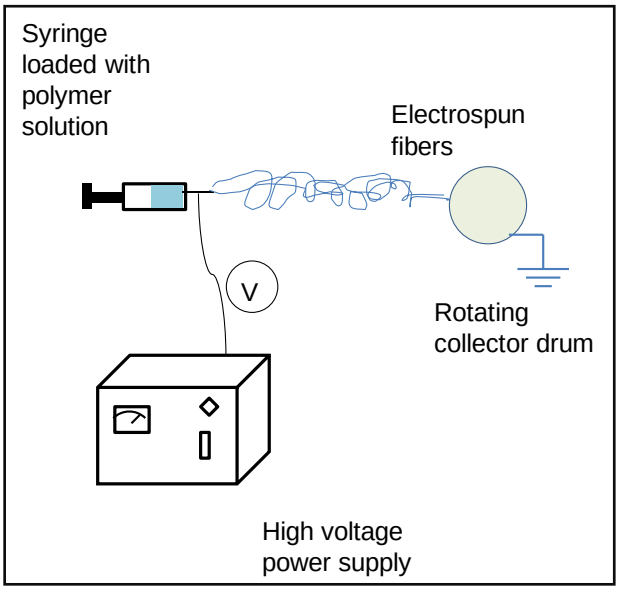

Figure 1.7 Schematic of an electrospinning setup.

As long as the electrical and surface tension forces are balanced, the droplet remains stable in the form of Taylor cone. When the electric field force overcomes the surface tension force, the droplet is deformed into very thin charged polymer solution jet. The charged polymer jet subjected to bending instabilities (Figure 1.8) by the electric field and undergoes whipping motion and gets attracted towards the grounded collector plate.[58-60] During the process of deposition the solvent gets evaporated leaving behind dry fibers.

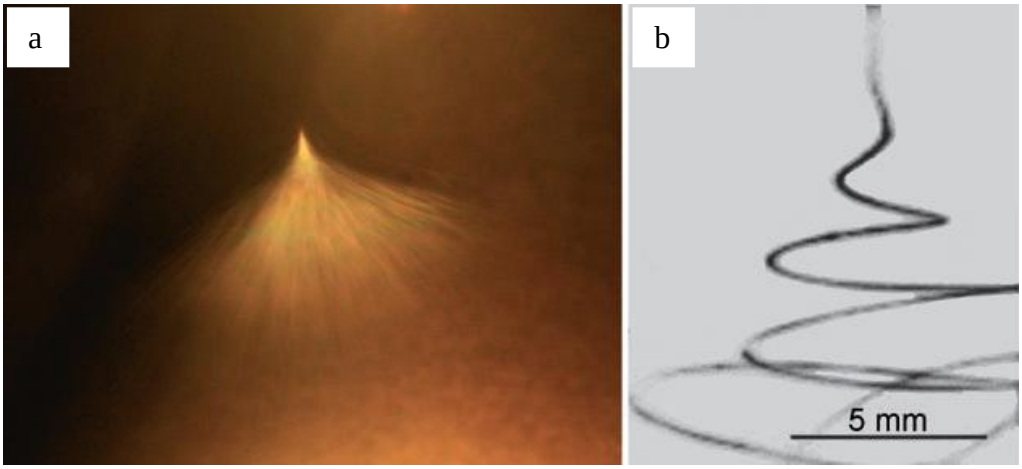

Figure 1.8 a) Photograph of electrospinning jet b) High-speed photograph of jet instabilities.[53,58]

Electrospinning of various polymers including Chitosan,[61] PA 6,[62] PAN,[63,64] PEO,[65] PET,[66,67] PVA,[68] polyaniline,[69] polyurethane,[70] and other materials[55] has been reported. The polymer molecular weight, solvent used, solution conductivity and solution viscosity influences the electrospinning process.[71] The fiber morphology, surface topography, fiber diameter and mat structure can be controlled by varying the parameters such as solvent type, relative humidity, applied voltage, polymer solution concentration, flow rate and needle tip to

collector distance.[54,71] For example, by choosing particular solvent or mixture of solvents, polymer rich and polymer poor region or phase separation in fibers matrix can be created.[53] Figure 1.9 shows the porous PLA nanofibers obtained by phase separation method.

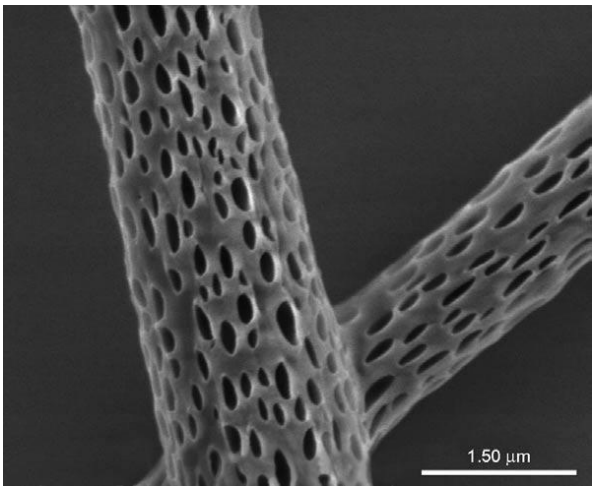

Figure 1.9 SEM image of electrospun porous PLA fibers.[53]

1.1.6 Nanofibers of C-B Protective Applications

Electrospun fiber mats have small fiber diameters, small pore size, high porosity, and large surface areas, and they are considered to be promising material for aerosol filtration applications.[72-75] Figure 1.10 shows the surface area comparison graph for different categories of fibers. It can be observed that the electrospun fibers have surface area 2 orders higher than conventional synthetic fibers. Figure 1.11 shows a) typical image of nanofiber nonwoven mat and b) the pore size and pore area distributions for electrospun fiber mat prepared using different polymer solution concentration. The term 'aerosol' refers to suspended solid and liquid particles in air; and aerosol filtration is selective removal of these

solid and liquid particles through a filter media, allowing the air pass through. The aerosol filtration through a filter media occurs by mainly four mechanisms that include (Figure 1.12) interception, inertial impaction, Brownian diffusion, and gravitational settling. [76,77] The aerosol filtration efficiency of a filter can be defined as the fraction of aerosol particles

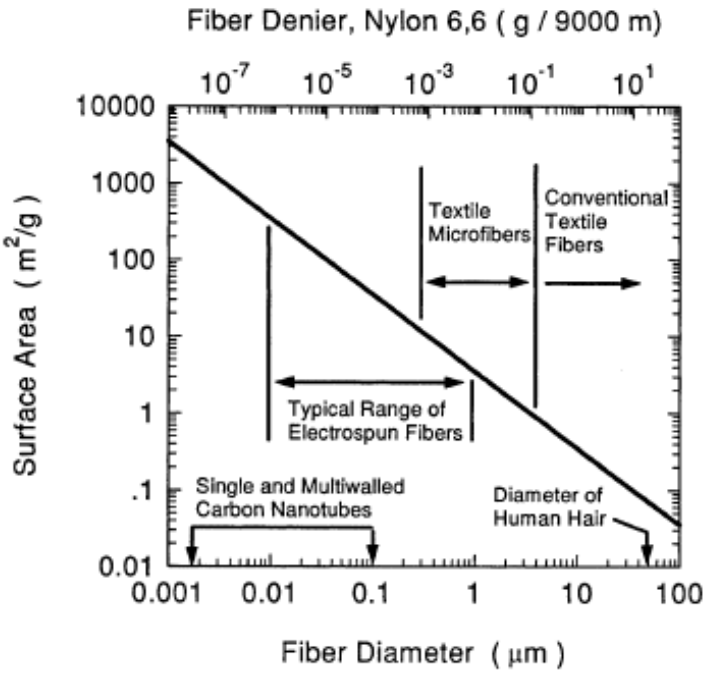

Figure 1.10 Electrospun nanofibers have high surface area.[74]

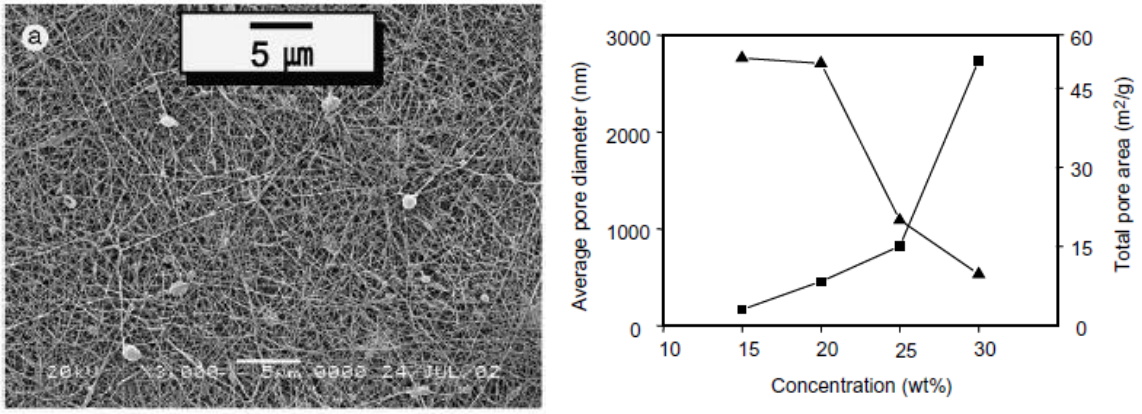

Figure 1.11 a) SEM image of electrospun Nylon 6 nonwoven mat; b) Average pore diameters and total pore areas of mats obtained from different concentration of polymer solutions.[73]

collected by the media. Nonwoven fibrous filters reported to exhibit good filtration efficiency and low pressure drop.[78] Maze et.al [79] reported a simulation study on filtration efficiency of nanofiber web against submicron size aerosols. In the study it was found that the filtration efficiency of nanofiber web increases with smaller fiber diameter and higher temperature of aerosol air results in increase the filtration efficiency due to random Brownian diffusion of particles. The study also revealed that the nanofiber web model offered least pressure drop and high air permeability, unlike traditional filtration media which cannot simultaneously achieve high filtration efficiency and low pressure drop or high air permeability. However, electrospun nanofibers typically do not have good mechanical properties and they are often deposited on fabric substrates to achieve advantages of both materials.[72, 80]

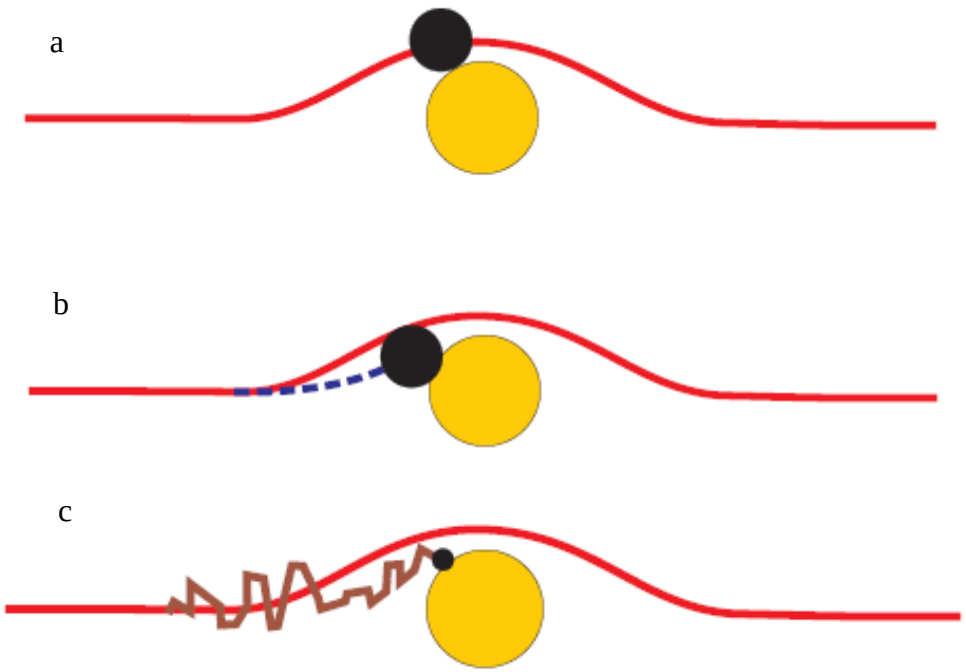

Figure 1.12 a) Interception b) Inertial impaction c) Brownian diffusion mechanisms in air filter media.[77]

In this research, protective clothing material was prepared using electrospun fiber mats deposited onto fabric surfaces. The electrospun nanofiber mats provide the barrier properties that are necessary to filter aerosol particulate form of C-B threat agents. In addition, electrospinning process provides the opportunity to functionalize and carry out surface modification of nanofibers during pre, post or *in-situ* electrospinning. Electrospun nanofibers could also be functionalized with active chemical groups that can detoxify C-B agents into harmless products.

1.1.7 Electrospun Functional Composite Nanofibers

Active chemicals and metal oxide nanoparticles are reported to have very good detoxifying ability against chemical warfare agents. However, the limitation lies in using these active chemicals and micro or nano particles for practical application. These active chemicals or nanoparticles need a high surface area medium, where they can be dispersed uniformly and made available for detoxifying reaction. Electrospun polymer nanofibers having very high surface area, and they can act as a medium to hold these active chemicals or nanoparticles on their surface. They can be incorporated onto nanofibers electrospinning process and the resultant functional nanofibers are capable of detoxifying C-B warfare agents.[81] Zinc-Titanate ($ZnO\text{-}TiO_2$) is an interesting metal oxide material, which is being used in making semiconductors, dielectrics, catalyst, adsorbents of toxic gases in chemical industries and in manufacturing sensors for detecting nerve agents. It is reported that precursor $ZnO\text{-}TiO_2$ can be electrospun into ceramic nanofibers (Figure 1.13) by blending with polyvinylpyrrolidone

polymer through sol-gel process. The precursor nanofiber subjected to annealing process at different temperature (300-700°C) to arrive ZnO-TiO_2 ceramic fibers. The resultant composite fibers were able to chemically detoxify the p-nitrophenyl diethyl phosphate (paraxon) and 2-chloroethyl ethyl sulfide (CEES), simulants of nerve agent and sulfur mustard, respectively.[82]

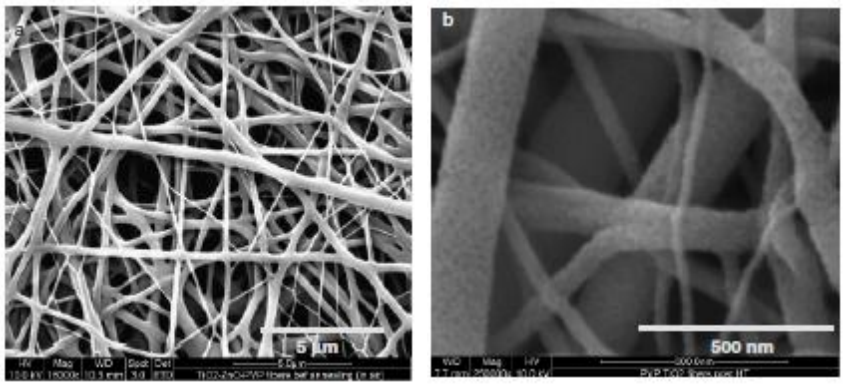

Figure 1.13 SEM images of electrospun 40%zinc titanate nanofibers (a) before heat treatment, (b) heat treated at 700°C.[82]

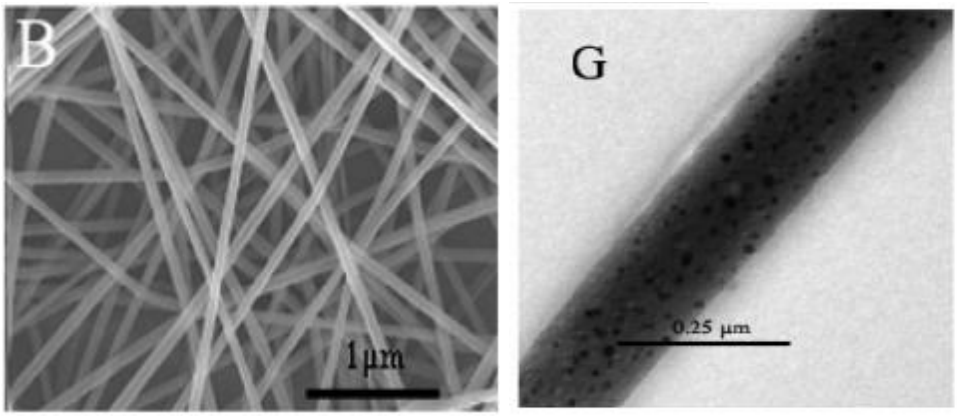

Figure 1 14 SEM images of silver nano particle containing porous silica nanofibers.[50]

The fabrication of silver particles incorporated polymer nanofibers (Figure1.14) by electrospinning process were reported.[50] In general $AgNO_3$ dispersed in polymer solution and electrospun into precursor composite nanofibers. The precursor fibers were subjected to heat treatment to reduce $AgNO_3$ into silver particles. These kinds of catalytic nanofibers containing silver nanoparticles can be used to detoxify biological warfare agents.

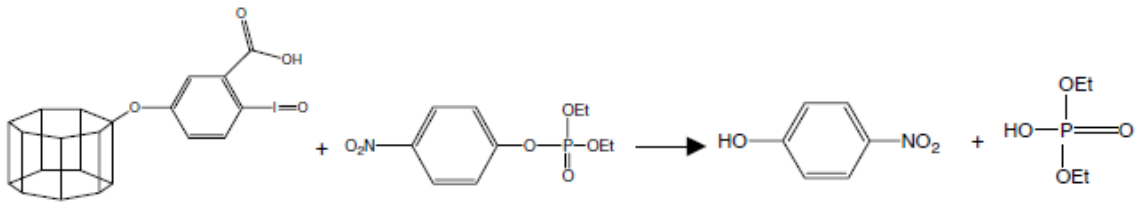

Figure 1.15 Catalytic cleavage of paraoxon by IBA-CD compound.[83]

In another literature [83] it was reported about active chemical ortho-iodobenzoic acid (IBA) in combination with Cyclodextrin (CD) can be incorporated into nanofibers. These functional nanofibers have shown to have good detoxifying ability against nerve agents. CD and IBA were mixed at certain stoichiometry ratio and then blended with PVA polymer. This precursor solution electrospun into functional nanofibers and its detoxifying properties against nerve agent were tested. Figure 1.15 shows the detoxification reaction of nerve agent simulant paraoxon by CD-IBA functionalized PVA nanofibers.

Sundarrajan et.al reported that poly (ethylene imine) (PEI), which has secondary amine structure, has been proven to have antibacterial activity.[84] It was reported by the author that PEI fibers exhibited detoxification reaction against simulant of sarin. PEI polymer has

limitation in fiber forming tendency and hence it is typically blended with a polymer to overcome this shortcoming. PEI blended with Nylon 6 polymer and electrospun into nanofibers. The functional nanofiber was subjected to detoxification reaction against Dimethyl chlorophosphate (DMCP) a simulant of sarin. It was proposed that composite Nylon/PEI fibers break the P-Cl bond by de-halogenation process and convert DMCP into harmless product. Figure 1.16 shows the P-Cl bond breaking reaction PEI fibers and DMPC.

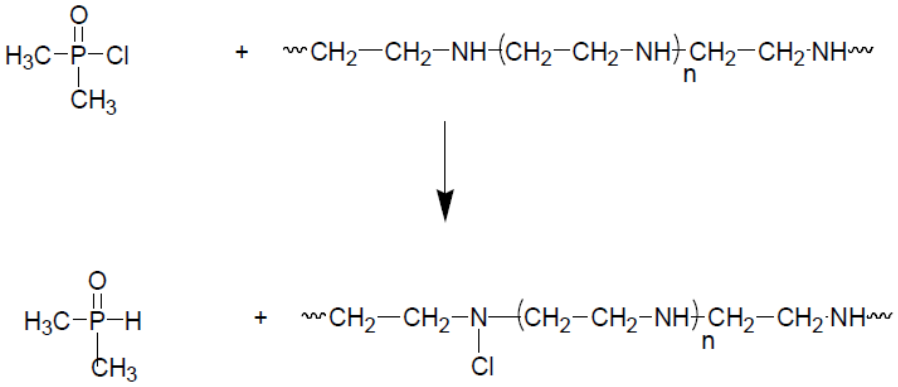

Figure 1.16 Chemical reaction of DMCP on Nylon/PEI nanofiber membrane.[84]

1.1.8 Plasma Treatment of Polymer Surfaces

Functional nanofiber deposited woven fabrics can serve as smart protective clothing with self detoxifying ability against C-B warfare agents. However, the adhesion between electrospun nanofiber mat layer and deposited fabric substrate is often poor due to lack of chemical bonds at the interface. The nanofiber layer can be easily removed due to repeated flex, twist and abrasive actions during practical usage of this fabric. To improve the adhesive force between electrospun fiber mat and the fabric substrate, the polymer nanofiber and fabric

substrate can be plasma treated. Plasma treatment of polymer surface to improve its adhesive ability onto other polymer material has been reported.[85, 86]

Plasma processing of polymer materials is used to modify the surface properties and introduce surface functionalities without affecting the bulk properties. It is a simple, clean and green process as compared to many chemical processes.[87] Plasma treatment of polymers results in their surface modification for various applications through surface etching, chain scission, functionalization, and cross linking.[88-95] Figure 1.17 shows the plasma etched aramid fiber surface.

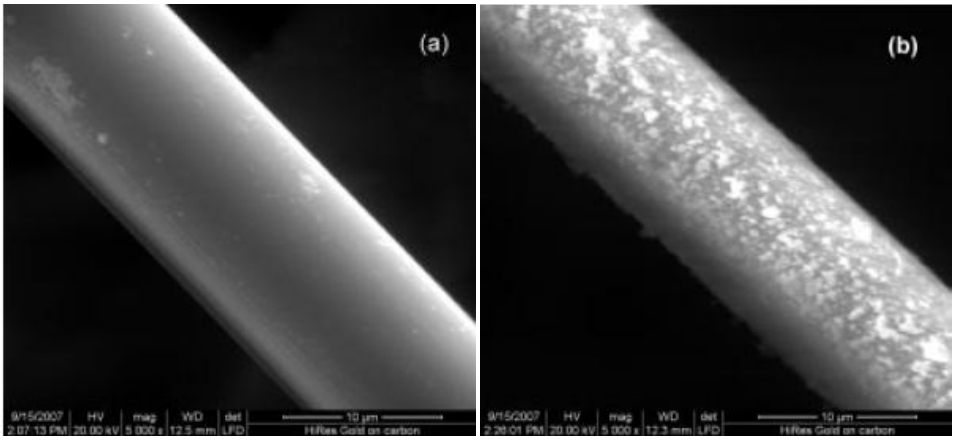

Figure 1.17 SEM photographs of aramid fiber (a) untreated; (b) plasma-treated.[88]

Plasma can be characterized by its dissociative interactions in which the gaseous molecules first dissociate into ions at break down voltage of gas, and the resulting plasma consists of highly active charged species, electrons, ions and radicals.[87, 96] These charged species of plasma create highly unusual environment and can be used in interacting with surfaces of

materials to modify them. Plasma treatment has been used for the surface hydrophobicity or hydrophilicity modification of polymers,[97] polymer surface etching and nano texturing treatments,[98-103] and the improvement of the mechanical properties depending on treatment conditions.[98, 104]

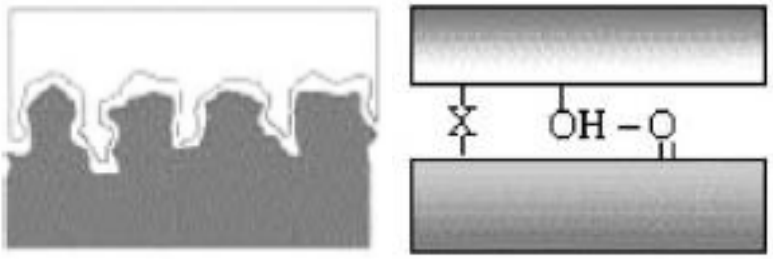

Figure 1.18 The factors controlling adhesion strength between polymeric surfaces: (a) physical forces, (b) chemical forces.[85]

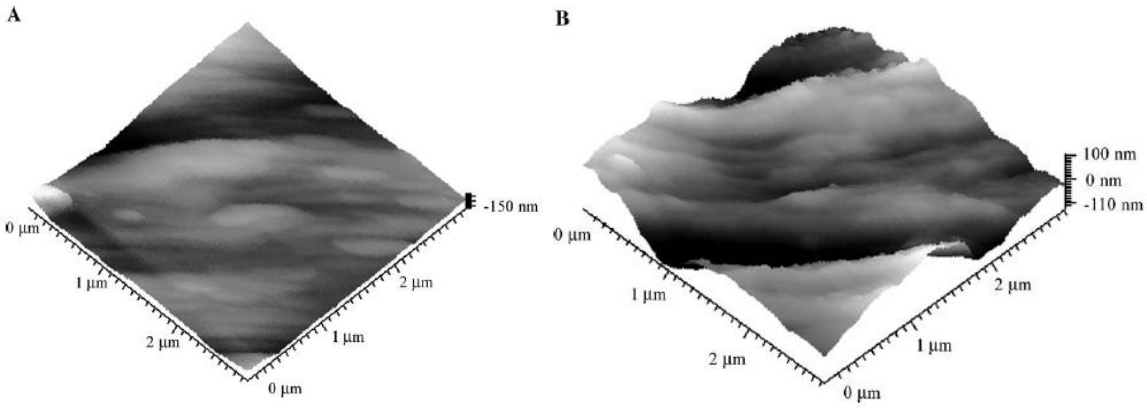

Figure 1.19 AFM images of the PA-6 fibres before and after plasma treatment.[86]

Krump et.al reported improvement of adhesion between plasma treated polyester fiber and rubber matrix.[85] The atmospheric pressure plasma treatment cause surface roughness, increase surface functional groups (Figure1.18) that can assist in adhesion improvement through physical and chemical forces.[85]

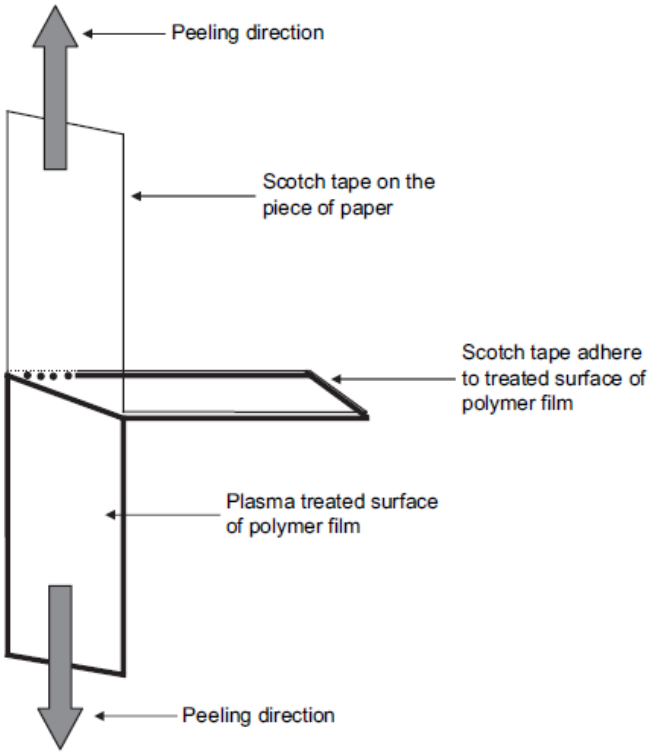

Figure 1.20 Schematic of peel test to estimate adhesion strength.[105]

Dumitrascu et.al has reported improved wet ability and surface roughness (Figure1.19) are the prime reasons for subsequent increase in adhesion energy of polyamide 6 fibers treated in atmospheric pressure plasma.[86] Pandiyaraj et.al reported improved adhesion strength between polymeric films due to plasma treatment and the adhesion energy estimated by peel test as shown in Figure1.20.[105] It was pointed out that the plasma treatment on polymer surface caused significant morphological, chemical changes and introduced high polar groups functional groups. These functional groups increased the surface energy and reduced the water contact angle. The change in polymer surface energy and surface topography are the important reasons for increase in adhesion strength.

1.1.9 Atmospheric Pressure Plasma

In general, plasma treatment is carried out in low pressure, and is a high-energy batch process, that involves time and space limitation, and is expensive against the requirement of continuous industrial process. Sometimes, the temperature of low pressure plasma is high enough to melt the polymer fiber materials that have low glass transition temperature. Additionally, in low pressure plasma, the density of active charged species is relatively low due to the vacuum condition, which makes it unsuitable for current research work. However, the atmospheric pressure plasma, which does not involve low pressure condition, can be safely utilized to treat polymer fiber material. The atmospheric pressure plasma is an economical process which can be obtained on the dielectric barrier discharge principle.[87,106] Atmospheric pressure plasma is a low temperature process and is suitable for continuous treatment with higher density of active charged species and temperature less than 40°C. Additionally, plasma carrier gas, such as helium (He), argon (Ar) along with active gas like oxygen (O_2), can be used.

Figure 1.21 shows the photographs of the atmospheric pressure plasma system designed and fabricated at NC State University. The system is a capacitive-coupled dielectric barrier discharge (DBD), operated by audio frequency power supply. The device has an active exposure area of approximately 60 × 60 cm^2 between two copper electrodes with an adjustable 5 cm gap separation. The dielectric-barrier non-equilibrium discharge generates a low-temperature (1-2eV), low electron number density (10^{14}-10^{16} $/m^3$) pseudo-glow discharge

plasma, which is typical for dielectric-barrier discharges at atmospheric pressure. The discharge generates electrons, ions, excited atoms and molecules, as well as UV radiation. This atmospheric pressure plasma system is capable of batch treatment of substrates using a test cell, as well as continuous operation using the roller feed system for large fabric rolls or continuous films.

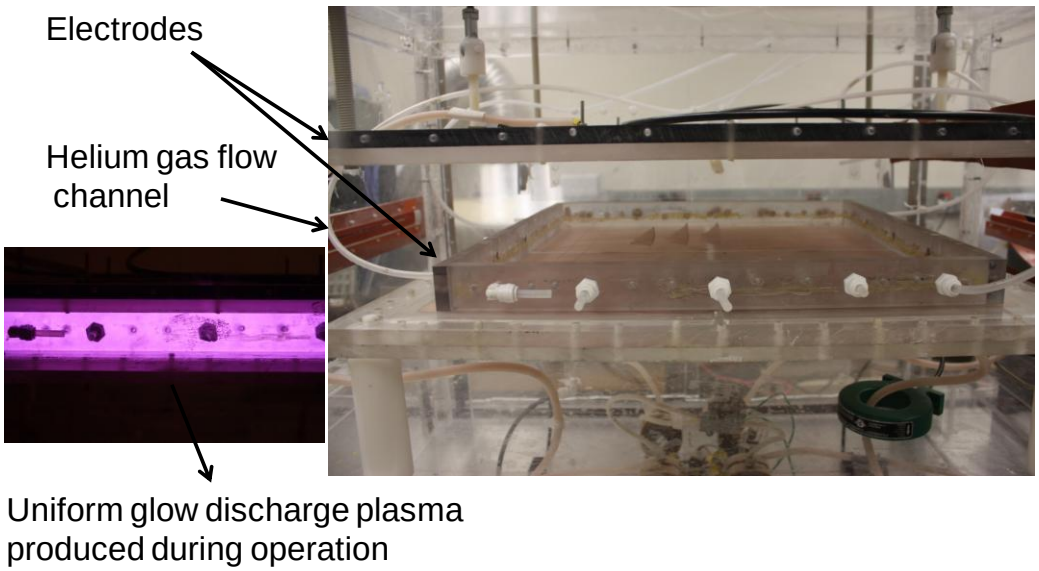

Figure 1.21 Atmospheric pressure plasma treatment system.

This atmospheric pressure plasma system can be used to modify the structures and properties of polymer materials to *i*) improve surface bonding or adhesive ability,[107,108] *ii*) increase mechanical strength depending on materials and treatment conditions,[107-109] *iii*) change fiber surface hydrophobicity,[107] *iv*) roughen fiber surfaces,[110] *v*) increase crystallinity,[110] *vi*) attach adsorbents to fiber surface,[111] and *vii*) introduce biocidal functionality (such as the

capability to kill or inhibit the growth of microorganisms such as bacteria, molds, and fungi, and insect and tick repelling action) to fiber materials.[112, 113]

1.2 Hypothesis of the Dissertation

The basic requirements for advanced C-B warfare protective clothing are listed as follows.

The basic requirements for advanced C-B warfare protective clothing are listed as follows. Protective clothing should: i) be able to filter and stop diffusion of submicron level C-B threat aerosol particles; ii) have the capability to chemically detoxify C-B agents into harmless product; and iii) provide comfort to the wearer. Functional nanofibers with active detoxifying chemicals on their surface can be used for protective clothing application. Theoretically, electrospun functional nanofiber mats deposited onto woven fabric surface could provide both barrier property and detoxifying ability with possible good air permeability. However, it is important to make sure a sufficient adhesion between nanofiber mat and fabric substrate during practical usage. The adhesion between nanofiber mat and fabric substrate can be improved through plasma treatment.

Plasma is considered to be the fourth state of matter and is characterized by its dissociative interactions, in which molecules first dissociate and then ionize, with either positive or negative charges. Plasma can create a highly unusual and reactive chemical environment, which can be used to modify substrates with any kind of geometry. Plasma modifies the polymer surface by etching, functionalization, and leads to cross-linking between active chemical groups. Hence, it was anticipated that the plasma treatment of nanofibers and fabric surfaces during the deposition process would create active sites by etching and

functionalization on them. These functional groups could assist to improve the adhesion by forming cross-linking bond between nanofibers and fabric surfaces.

In this research, as a novel approach, the electrospun nanofibers are subjected to *in-situ* plasma treatment through a plasma-electrospinning hybrid process. The plasma may have a greater impact if the treatment occurs during the electrospinning process and before the solidification of the polymer jets. Due to the large surface area of electrospun nanofibers, a large amount of active species can be generated *in-situ* during the electrospinning process, and hence the resultant plasma-treated nanofibers can have enhanced adhesion onto the fabric substrates.

1.3 References

1. L. Szinicz, History of Chemical and Biological Warfare Agents, *Toxicology,* 2005, **214,** 167.
2. S. Chauhan, R. D'Cruz, Chemical Warfare Agents *Environ. Toxicol. Pharmacol,* 2008, **26,** 113.
3. R.T. Delfino, T.S. Ribeiro, J.D. Figueroa-Villar, Organophosphorus Compounds as Chemical Warfare Agents: A Review, *Journal of the Brazilian Chemical Society,* 2009, **20,** 407.
4. M. J. Geraci, Mustard Gas: Imminent Danger Or Eminent Threat? *Ann. Pharmacother* 2008, **42,** 237.
5. R. Pita, Toxin Weapons: From World War I to Jihadi Terrorism, *Toxin Reviews,* 2009, **28,** 219.
6. H.Salem, Issues in Chemical and Biological Terrorism, *Int.J.Toxicol,* 2003, **22,** 465.
7. G. P. Krueger, Effects of Chemical Protective Clothing on Military Performance: A Review of the Issues,*Milit Psychol,* 1997, **9,** 255.
8. R. Trapp, The Detoxification and Natural Degradation of Chemical Warfare Agents, *Taylor & Francis, London*, 1985.
9. R.J. Hawley, E.M. Eitzen, Biological weapons-a primer for microbiologists Annu. Rev. Microbiol. 2001, **55,** 235.
10. J.C. Pile, J.D. Malone, E.M. Eitzen, A.M. Friedlander, Anthrax as a Potential Biological Warfare Agent, Arch Intern Med. 1998, **158**, 429.

11. C.K. Bensel., Soldier Performance and Functionality: Impact of Chemical Protective Clothing, *Mil.Psychol.,* 1997, **9,** 287.
12. Retrieved from http://www.globalsecurity.org/military/systems/ground/jslist.htm.
13. G. Thilagavathi, A.S.M. Raja, T. Kannaian, Nanotechnology and Protective Clothing for Defence Personnel, *Def. Sci. J.,* 2008, **58,** 451.
14. H.L. Schreuder-Gibson, Q. Truong, J.E. Walker, J.R. Owens, J.D. Wander, W.E. Jones, Chemical and Biological Protection and Detection in Fabrics for Protective Clothing, *MRS Bull,* 2003, **28,** 574.
15. S. Sundarrajan, A.R. Chandrasekaran, S. Ramakrishna, An Update on Nanomaterials-Based Textiles for Protection and Decontamination, *J Am Ceram Soc*, 2010, **93**, 3955.
16. C. A. Winterhalter, J. Teverovsky, P. Wilson, J. Slade, W. Horowitz, E. Tierney, V. Sharma, Development of Electronic Textiles to Support Networks, Communications, and Medical Applications in Future US Military Protective Clothing Systems, *IEEE Transactions on Information Technology in Biomedicine,* 2005, **9,** 402.
17. Ellison, D. Hank. Handbook of Chemical and Biological Agents, CRC Press, New York: 2007, p. 47.
18. S.L. Bartelt-Hunt, D.R.U. Knappe, M.A. Barlaz, A Review of Chemical Warfare Agent Simulants for the Study of Environmental Behavior, *Critical Reviews in Environmental Science and Technology*, 2008, **38**, 112.
19. N.B. Munro, K.R. Ambrose, A.P. Watson,Toxicity of the Organophosphate Chemical Warfare Agents GA, GB, and VX: Implications for Public Protection, *Environmental Health Perspectives*, 1994, **102** (1), 8.

20. H.S. Uhm, H.Y. Lee, Y.C. Hong, D.H. Shin, Y.H. Park, Y.F. Hong, A decontamination study of simulated chemical and biological agents, *Journal of Applied Physics*, 2007, **102**, 013303.
21. B.M. Smith, Catalytic Methods for the Destruction of Chemical Warfare Agents Under Ambient Conditions, *Chem. Soc. Rev.*, 2008, **37,** 470.
22. G. K. Prasad, T. H. Mahato, Beer Singh, K. Ganesan, P. Pandey, K. Sekhar, Detoxification Reactions of Sulphur Mustard on the Surface of Zinc Oxide Nanosized Rods, *J. Hazard. Mater.*, 2007, **149,** 460.
23. G.K. Prasad, T.H. Mahato, B. Singh, P. Pandey, A.N. Rao, K. Ganesan, R. Vijayraghavan, Decontamination of Sulfur Mustard on Manganese Oxide Nanostructures, *AICHE J.*, 2007, **53,** 1562.
24. R.M. Narske, K.J. Klabunde, S. Fultz, Solvent Effects on the Heterogeneous Adsorption and Reactions of (2-Chloroethyl) Ethyl Sulfide on Nanocrystalline Magnesium Oxide, *Langmuir*, 2002, **18,** 4819.
25. S.T. Han, G.Y. Zhang, H.L. Xi, D.N. Xu, X.Z. Fu, X.X. Wang, Sulfated TiO_2 Decontaminate 2-CEES and DMMP in Vapor Phase, *Catalysis Letters*, 2008, **122,** 106.
26. D.B. Mawhinney, J.A. Rossin, K. Gerhart, J.T. Yates, Adsorption and Reaction of 2-Chloroethylethyl Sulfide with Al_2O_3 Surfaces, *Langmuir*, 1999, **15,** 4789.
27. G.W. Wagner, O.B. Koper, E. Lucas, S. Decker, K.J. Klabunde, Reactions of VX, GD, and HD with Nanosize CaO: Autocatalytic Dehydrohalogenation of HD, *J Phys Chem B*, 2000, **104,** 5118.

28. R.A. Moss, P.K. Gong, Cyclodextrin-Mediated Hydrolyses of Novel Phosphotriesters, *Langmuir*, 2000, **16,** 8551.
29. R.A. Moss, H. Morales-Rojas, H.M. Zhang, B.D. Park, Cleavage of VX Simulants by Micellar Iodoso- and Iodoxybenzoate, *Langmuir*, 1999, **15,** 2738.
30. R. Helburn, M. F. Vitha, Interfaces and Interphases in Analytical Chemistry, *ACS Symposium Series*, Washington, DC, 2011, 1062, 249.
31. V.K. Rastogi, J.J. DeFrank, T. Cheng, J.R. Wild, Enzymatic Hydrolysis of Russian-VX by Organophosphorus Hydrolase, *Biochemical and Biophysical Research Communications*, 1997, **241,** 294.
32. F.M Raushel, Bacterial detoxification of organophosphate nerve agents, *Current Opinion in Microbiology*, 2002, **5**, 288.
33. C.M. Hill, W. Li, J.B. Thoden, H.M. Holden, F.M. Raushel, Enhanced Degradation of Chemical Warfare Agents through Molecular Engineering of the Phosphotriesterase Active Site, *J Am Chem Soc*, 2003, **125**, 8990.
34. B.K. Singh, A. Walker, Microbial degradation of organophosphorus compounds, *FEMS Microbiol Rev*, 2006, **30**, 428.
35. A.J. Russell, J.A. Berberich, G.F. Drevon, Richard R. Koepsel, Biomaterials for Mediation of Chemical and Biological Warfare Agents, *Annu Rev Biomed Eng*, 2003, **5,** 1.
36. Y. Yu-Chu, B. James, W. J. Richard, Decontamination of Chemical Warfare Agents, *Chem. Rev.*, 1992, **92,** 1729.

37. S.S. Talmage, A.P. Watson, V. Hauschild, N.B. Munro, J. King, Chemical Warfare Agent Degradation and Decontamination, *Current Organic Chemistry*, 2007, **11,** 285.
38. D.K. Bhalla, D.B. Warheit, Biological agents with potential for misuse: a historical perspective and defensive measures, *Toxicology and Applied Pharmacology*, 2004, **199**, 71.
39. R C Spencer, Bacillus anthracis, *J Clin Pathol*, 2003, **56**,182.
40. B.W.J. Mahy, An overview on the use of a viral pathogen as a bioterrorism agent: why smallpox, *Antiviral Research*, 2003, **57**, 1.
41. R.J. Whitley, Smallpox: a potential agent of bioterrorism, *Antiviral Research*, 2003, **57**, 7.
42. J. Sawai, T. Yoshikawa, Quantitative Evaluation of Antifungal Activity of Metallic Oxide Powders (MgO, CaO and ZnO) by an Indirect Conductimetric Assay, *J. Appl. Microbiol.*, 2004, **96,** 803.
43. H.W. Herrmann, G.S. Selwyn, I. Henins, J. Park, M. Jeffery, J.M. Williams, Chemical Warfare Agent Decontamination Studies in the Plasma Decon Chamber, IEEE Transactions on Plasma Science, 2002, **30**, 4.
44. Y.C. Hong, J.H. Kim, H.S. Uhm, Simulated experiment for elimination of chemical and biological warfare agents by making use of microwave plasma torch, *Phys Plasmas*, 2004, **11**, 2.
45. D.H. Reneker, I. Chun, Nanometre diameter fibres of polymer, produced by electrospinning, Nanotechnology, 1996, **7**(3), 216.

46. D. Li, Y.N. Xia, Electrospinning of nanofibers: Reinventing the wheel?, *Adv. Mater.* 2004, **16**, 1151.

47. C. Xu, R. Inai, M. Kotaki, S. Ramakrishna, Electrospun Nanofiber Fabrication as Synthetic Extracellular Matrix and its Potential for Vascular Tissue Engineering, *Tissue Eng.*, 2004, **10,** 1160.

48. H.W. Kim, H.H. Lee, J.C. Knowles, Electrospinning Biomedical Nanocomposite Fibers of hydroxyapaite/poly(Lactic Acid) for Bone Regeneration, *Journal of Biomedical Materials Research. Part A,* 2006, **79a,** 643.

49. H. Jia, G. Zhu, B. Vugrinovich, W. Kataphinan, D.H. Reneker, P. Wang, Enzyme-Carrying Polymeric Nanofibers Prepared Via Electrospinning for use as Unique Biocatalysts, *Biotechnol. Prog.,* 2002, **18,** 1027.

50. A.C. Patel, S. Li, C. Wang, W. Zhang, Y. Wei, Electrospinning of Porous Silica Nanofibers Containing Silver Nanoparticles for Catalytic Applications, *Chemistry of Materials,* 2007, **19,** 1231.

51. Y.W. Ju, G.R. Choi, H.R. Jung, C. Kim, K.S. Yang, W.J. Lee, A Hydrous Ruthenium Oxide-Carbon Nanofibers Composite Electrodes Prepared by Electrospinning, *J.Electrochem.Soc.,* 2007, **154,** A192.

52. Z. Ma, M. Kotaki, S. Ramakrishna, Electrospun Cellulose Nanofiber as Affinity Membrane, *J. Membr. Sci.,* 2005, **265,** 115.

53. Greiner, J.H. Wendorff, Electrospinning: A Fascinating Method for the Preparation of Ultrathin Fibers, Angew Chem Int Ed, 2007, 46, 5670.

54. W.E. Teo, S. Ramakrishna, A review on electrospinning design and nanofibre assemblies, Nanotechnology, 2006, **17**, R89.

55. Z. Huang, Y.Z. Zhang, M. Kotaki, S. Ramakrishna, A review on polymer nanofibers by electrospinning and their applications in nanocomposites, *Composites Science and Technology*, 2003, **63**, 2223.

56. G. Taylor, Disintegration of Water Drops in an Electric Field, *Proceedings - Royal Society. Mathematical, Physical and Engineering Sciences,* 1964, **280,** 383.

57. A.L. Yarin, S. Koombhongse, D.H. Reneker, Taylor cone and jetting from liquid droplets in electrospinning of nanofibers, *Journal of Applied Physics*, 2001, **90**, 4836.

58. A.L. Yarin, S. Koombhongse, D.H. Reneker, Bending instability in electrospinning of nanofibers, *Journal of Applied Physics*, 2001, **89**, 3018.

59. M.M. Hohman, M. Shin, G. Rutledge, M.P. Brenner, Electrospinning and electrically forced jets. I. Stability theory, *Physics of Fluids*, 2001, **13**, 2201.

60. M.M. Hohman, M. Shin, G. Rutledge, M.P. Brenner, Electrospinning and electrically forced jets. II. Applications, *Physics of Fluids*, 2001, **13**, 2221.

61. N. Bhattarai, D. Edmondson, O. Veiseh, F.A. Matsen, M. Zhang, Electrospun chitosan-based nanofibers and their cellular compatibility, Biomaterials, 2005, **26**, 6176.

62. H. Fong, W. Liu, C. Wang, R.A. Vaia, Generation of electrospun fibers of nylon 6 and nylon 6-montmorillonite nanocomposite, *Polymer*, 2002,**43**, 775.

63. S.Y. Gu, J. Ren, G.J. Vancso, Process optimization and empirical modeling for electrospun polyacrylonitrile (PAN) nanofiber precursor of carbon nanofibers, *European Polymer Journal*, 2005, **41**, 2559.

64. S.F. Fennessey, R.J. Farris, Fabrication of aligned and molecularly oriented electrospun polyacrylonitrile nanofibers and the mechanical behavior of their twisted yarns, *Polymer*, 2004, **45**, 4217.
65. J. M. Deitzel, J.D. Kleinmeyer, J.K. Hirvonen, N.C. Beck Tan, Controlled deposition of electrospun poly(ethylene oxide) fibers, Polymer, 2001,**42**, 8163.
66. Z. Ma, M. Kotaki, T. Yong, W. He, S Ramakrishna, Surface engineering of electrospun polyethylene terephthalate (PET) nanofibers towards development of a new material for blood vessel engineering, *Biomaterials*, 2005, **26**, 2527.
67. M.G. McKee, G.L. Wilkes, R.H. Colby, T.E. Long, Correlations of Solution Rheology with Electrospun Fiber Formation of Linear and Branched Polyesters Macromolecules 2004, **37**, 1760.
68. Koski, K. Yim, S. Shivkumar, Effect of molecular weight on fibrous PVA produced by electrospinning, *Materials Letters*, 2004, **58**, 493.
69. I.D. Norris, M.M. Shaker, F.K. Ko, A.G. MacDiarmid, Electrostatic fabrication of ultrafine conducting fibers: polyaniline/polyethylene oxide blends, *Synthetic Metals*, 2000, **114**, 109.
70. M. M. Demir, I. Yilgor, E. Yilgor, B. Erman, Electrospinning of polyurethane fibers, *Polymer*, 2002, **43**, 3303.
71. J. M. Deitzel, J. Kleinmeyer, D. Harris and N. C. Beck Tan, The effect of processing variables on the morphology of electrospun nanofibers and textiles, *Polymer*, 2001,**42**, 261.

72. S. Thandavamoorthy, G.S. Bhat, R.W. Tock, S. Parameswaran, S.S. Ramkumar, Electrospinning of Nanofibers, *J. Appl. Polym. Sci.,* 2005, **96,** 557.

73. Y.J. Ryu, H.Y. Kim, K.H. Lee, H.C. Park, D.R. Lee, Transport properties of electrospun nylon 6 nonwoven mats, *European Polymer Journal*, 2003, **39**,1883.

74. P. Gibson, H. Schreuder-Gibson, D. Rivin, Transport properties of porous membranes based on electrospun nanofibers, *Colloids and Surfaces A: Physicochemical and Engineering Aspects*, 2001, **187–188**, 469.

75. P. W. Gibson, H. L. Schreuder-Gibson, D. Rivin, Electrospun Fiber Mats: Transport Properties AIChE J. 1999, **45**, 190.

76. W.C. Hinds, Aerosol technology: properties, behavior, and measurement of airborne particles, 2nd edn. Wiley, New York, 1999.

77. Q. Wang, An Investigation of Aerosol Filtration via Fibrous Filters, PhD Dissertation, 2008, NC State University, USA.

78. Q. Wang, B. Maze, H.V. Tafreshi, B. Pourdeyhimi, Acase study of simulating submicron aerosol filtration via lightweight spun-bonded filter media, *Chemical Engineering Science*, 2006, **61**, 4871.

79. B. Maze, H. V. Tafreshi, Q. Wang, B. Pourdeyhimi, A simulation of unsteady-state filtration via nanofiber media at reduced operating pressures, Aerosol Science, 2007, 38, 550.

80. F. Dotti, A. Varesano, A. Montarsolo, A. Aluigi, C. Tonin, G. Mazzuchetti, Electrospun Porous Mats for High Efficiency Filtration, *Journal of Industrial Textiles*, 2007, **37,** 151.

81. S. Ramakrishna, K. Fujihara, W. Teo, T. Yong, Z. Ma, R. Ramaseshan, Electrospun Nanofibers: Solving Global Issues, *Materials Today,* 2006, **9,** 40.
82. R. Ramaseshan, S. Ramakrishna, Zinc Titanate Nanofibers for the Detoxification of Chemical Warfare Simulants, *J Am Ceram Soc,* 2007, **90,** 1836.
83. R. Ramaseshan, S. Sundarrajan, Y.J. Liu, R.S. Barhate, N.L. Lala, S. Ramakrishna, Functionalized Polymer Nanofibre Membranes for Protection from Chemical Warfare Stimulants, *Nanotechnology,* 2006, **17,** 2947.
84. S. Sundarrajan, A. Venkatesan, S. Ramakrishna, Fabrication of Nanostructured Self-Detoxifying Nanofiber Membranes that Contain Active Polymeric Functional Groups, *Macromolecular Rapid Communications,* 2009, **30,** 1769.
85. H. Krump, M. Simor, I. Hudec, M. Jasso, A. S. Luyt, Adhesion Strength Study between Plasma Treated Polyester Fibres and a Rubber Matrix, *Appl. Surf. Sci.,* 2005, **240,** 268.
86. N. Dumitrascu, C. Borcia, Adhesion Properties of Polyamide-6 Fibres Treated by Dielectric Barrier Discharge, *Surf. Coat. Technol.,* 2006, **201,** 1117.
87. F. S. Denes, S. Manolache, Macromolecular Plasma-Chemistry: An Emerging Field of Polymer Science, *Progress in Polymer Science,* 2004, **29,** 815.
88. P. Chen, J. Wang, B. Wang, W. Li, C. Zhang, H. Li, B. Sun, Improvement of interfacial adhesion for plasma-treated aramid fiber-reinforced poly(phthalazinone ether sulfone ketone) composite and fiber surface aging effects, *Surf. Interface Anal.* 2009, **41**, 38.
89. Chun Huang, Ya-Chi Chang, Shin-Yi Wu, Contact Angle Analysis of Low Temperature Cyclonic Atmospheric Pressure Plasma Modified Polyethylene Terephthalate, *Thin Solid Films*, 2010, **518,** 3575.

90. Ita Junkar, Alenka Vesel, Uros Cvelbar, Miran Mozetic, Simona Strnad, Influence of Oxygen and Nitrogen Plasma Treatment on Polyethylene Terephthalate (PET) Polymers, *Vacuum*, 2009, **84,** 83.
91. Jun Young Kim, Yongbeom Lee, Dae Young Lim, Plasma-Modified Polyethylene Membrane as a Separator for Lithium-Ion Polymer Battery, *Electrochim.Acta*, 2009, **54,** 3714.
92. L. I. Kravets, S. N. Dmitriev, A. B. Gil'man, Modification of Properties of Polymer Membranes by Low-Temperature Plasma Treatment, *High Energy Chemistry*, 2009, **43,** 181.
93. Dixon T. K. Kwok, Liping Tong, Che Yan Yeung, C. G. dos Remedios, Paul K. Chu, Hybrid Plasma Surface Modification and Ion Implantation of Biopolymers, *Surf.Coat.Technol.*, 2010, **204,** 2892.
94. M. G. McCord, Y. J. Hwang, P. J. Hauser, et al., Modifying Nylon and Polypropylene Fabrics with Atmospheric Pressure Plasmas, *Textile Research Journal*, 2002, **72,** 491.
95. Y. J. Hwang, Y. Qiu, C. Zhang, M. G. McCord, et. al., Effects of atmospheric pressure helium/ air plasma treatment on adhesion and mechanical properties of aramid fibers, *J. Adhes. Sci. Technol.* 2003, **17**, 751.
96. B. Eliasson, and U. Kogelschatz, Nonequilibrium Volume Plasma Chemical Processing, *IEEE Trans. Plasma Sci.* 1991, **19**, 1063.
97. Antonella Milella, Rosa Di Mundo, Fabio Palumbo, Pietro Favia, Francesco Fracassi, Riccardo d'Agostino, Plasma Nanostructuring of Polymers: Different Routes to Superhydrophoblicity, *Plasma Processes and Polymers*, 2009, **6,** 460.

98. M. G. McCord, Y. Qiu, C. Zhang, Y. J. Hwang, and B. L. Bures, Atmospheric pressure helium + oxygen plasma treatment of ultrahigh modulus polyethylene fibers, J. Adhes. Sci. Technol. 2002, **16**, 449.

99. Zhiqiang Gao, Jie Sun, Shujing Peng, Lan YaoYiping Qiu, Surface Modification of a Polyamide 6 Film by He/CF4 Plasma using Atmospheric Pressure Plasma Jet, *Appl.Surf.Sci.,* 2009, **256,** 1496.

100. Irmina Wendling, Peter Munzert, Ulrike Schulz, Norbert Kaiser, Andreas Tuennermann, Creating Anti-Reflective Nanostructures on Polymers by Initial Layer Deposition before Plasma Etching, *Plasma Processes and Polymers*, 2009, **6,** S716.

101. Juana Abenojar, Rafael Torregrosa-Coque, Miguel Angel Martinez, Jose Miguel Martin-Martinez, Surface Modifications of Polycarbonate (PC) and Acrylonitrile Butadiene Styrene (ABS) Copolymer by Treatment with Atmospheric Plasma, *Surf.Coat.Technol.,* 2009, **203,** 2173.

102. K. Tsougeni, N. Vourdas, A. Tserepi, E. Gogolides, C. Cardinaud, Mechanisms of Oxygen Plasma Nanotexturing of Organic Polymer Surfaces: From Stable Super Hydrophilic to Super Hydrophobic Surfaces, *Langmuir,* 2009, **25,** 11748.

103. K. Navaneetha, Pandiyaraj, V. Selvarajan, Young Ha Rhee, Hyoung Woo Kim, Matteo Pavese, Effect of Dc Glow Discharge Plasma Treatment on PET/TiO2 Thin Film Surfaces for Enhancement of Bioactivity, *Colloids and Surfaces B-Biointerfaces,* 2010, **79,** 53.

104. L. Volynskii, D. A. Panchuk, Zh K. Sadakbaeva, A. V. Bol'shakova, L. M. Yaryshevam N. F. Bakeev, Evaluation of the Stress-Strain Properties of Surface Layers in Plasma-Treated Polymers, *High Energy Chemistry,* 2010, **44,** 341.

105. K.N. Pandiyaraj, V. Selvarajan, R.R. Deshmukh, C. Gao, Adhesive properties of polypropylene (PP) and polyethylene terephthalate (PET) film surfaces treated by DC glow discharge plasma, *Vacuum*, 2009, **83**, 332.

106. Schutze, J. Y. Jeong, S. E. Babayan, R. F. Hicks, et. al., The Atmospheric-Pressure Plasma Jet: A Review and Comparison to Other Plasma Sources *IEEE Trans. Plasma Sci. 1998,* **26**, 1685.

107. Y. J. Hwang, J. S. An, M. G. McCord, S. W. Park, and B. C. Kang, Effects of Helium Atmospheric Pressure Plasma Treatment on Low-Stress Mechanical Properties of Polypropylene Nonwoven Fabrics, *Text. Res. J.* 2005, **75**, 771.

108. M. G. McCord, Y. Qiu, C. Zhang, Y. J. Hwang, B. Bures, The effect of atmospheric pressure helium plasma treatment on the surface and mechanical properties of ultrahigh-modulus polyethylene fibers, *Adhes. Sci. Technol.* 2002, **16**, 99.

109. Zaisheng Cai, Yiping Qiu, Yoon Joong Hwang, Chuyang Zhang, Marian McCord, The use of Atmospheric Pressure Plasma Treatment in Desizing PVA on Viscose Fabrics, *Journal of Industrial Textiles,* 2003, **32,** 223.

110. M. G. McCord, Y. J. Hwang, Y. Qiu, L. K. Hughes, M. A. Bourham, Surface Analysis of Cotton Fabrics Fluorinated in Radio-Frequency Plasma, *J Appl Polym Sci,* 2003, **88,** 2038.

111. S. R. Matthews, Y. J. Hwang, M. G. McCord, M. A. Bourham, Investigation into Etching Mechanism of Polyethylene Terephthalate (PET) Films Treated in Helium and Oxygenated-Helium Atmospheric Plasmas, *J Appl Polym Sci,* 2004, **94,** 2383.

112. S. M. Gawish, S. R. Matthews, D. M. Wafa, F. Breidt, M. A. Bourham, Atmospheric Plasma-Aided Biocidal Finishes for Nonwoven Polypropylene Fabrics. I. Synthesis and Characterization, *J Appl Polym Sci,* 2007, **103,** 1900.

113. D.M.Wafa, F.Breidt, S.M.Gawish, S. R. Matthews, K. V. Donohue, R. M. Roe, M. A. Bourham, et. al., Atmospheric Plasma-Aided Biocidal Finishes for Nonwoven Polypropylene Fabrics. II. Functionality of Synthesized Fabrics, *J Appl Polym Sci,* 2007, **103,** 1911.

CHAPTER 2

Objectives

2.1 Research Objectives

Electrospun nanofiber mats are promising material to be used in advanced protective clothing as an excellent barrier against submicron-sized aerosol particulates of C-B threats agents. In addition, functional electrospun nanofiber could be used as self detoxifying material against C-B agents. However, few works has been done on the fabrication of multi-functional nanofiber mats and use these nanofiber mats to prepare C-B warfare protective clothing materials.

The barrier performance of nanofiber mats against sub micron particulates has not been optimized and their high performances under required standard conditions of Agency for Toxic Substances and Disease Registry (ATSDR) Minimal Risk Levels have not been studied. Processing parameters, such as solution concentration, syringe-tip-to-collector distance, applied voltage, conductivity nature of polymer solution, may affect the nanofiber mat structure and porosity. Since nanofiber diameter, mat structure and porosity significantly affect the ability to stop the diffusion of submicron particulates and CB agents, it is very important to control them. So the **first objective** of this research work is controlled deposition of electrospun nanofiber mats onto woven fabric substrate to improve barrier properties; and to optimize the parameters, including polymer solution concentration, applied voltage, areal density of nanofiber mats deposited, to get better barrier efficiency with minimum loss of fabric comfort properties.

In addition to prevent the diffusion of C-B agents through protective clothing, it is important to detoxify them into harmless products and ensure the safety of the wearer. For this purpose, electrospun nanofiber mats can be functionalized with active chemicals on their fiber surfaces to make them self detoxifying material. Metal oxide nanoparticles of ZnO have been reported to have good detoxifying ability against chemical warfare agents such as Sarin and Sulfur mustard. It has been reported that ZnO nanoparticles also posses the antibacterial capability against variety of pathogens. However, no studies have been done about how to effectively use ZnO nanoparticles in electrospun fibers as multifunctional detoxifying material against C-B threat agents. So, the **second objective** of this research is to fabricate ZnO/Nylon 6 functional electrospun nanofiber mats by electrospinning and electrospraying hybrid process and characterize their detoxifying ability against simulants of C-B warfare agents.

Deposition of functional electrospun fibers on textile fabric surface may provide barrier properties and self detoxifying ability against C-B agents. In addition, it is critical to establish the adhesion and durability of nanofiber mat on fabric surface to counter the forces of repeated twist, flex and abrasive actions during practical usage of the protective clothing. Modifying polymer surface property is one way to improve its adhesive behavior. For this purpose, the surface modification of polymers using plasma has been widely studied. Plasma process to improve the adhesive property of polymer material is simple, clean and green. However, literature study does not shed any light on plasma treatment of textile fabric and electrospun fibers to improve adhesion between their surfaces. So the **third objective** of this

research is to plasma treat the surfaces of fabric substrate and electrospun nanofibers to improve the adhesion and durability properties.

2.2 Organization of Dissertation

Chapter 3 deals with the deposition of electrospun nanofibers on fabric surface, and effects of polymer solution concentration, nanofiber areal density and applied voltage on fabric barrier and comfort related properties. The fabrication of multifunctional ZnO/Nylon 6 nanofibers by hybrid electrospinning and electrospraying process and characterization of their ability to detoxify simulants of warfare agents are discussed in Chapter 4. The plasma pretreatment of fabric and the deposition of electrospun nanofibers on it to improve the adhesion and durability, are explained in Chapter 5. Chapter 6 describes the plasma-electrospinning hybrid process to improve the adhesion and durability of nanofiber mat on fabric surface and also discusses the characterization of plasma effect on plasma polymers. Chapter 7 summarizes the key findings of this research work and identifies the future scope of research.

CHAPTER 3

Electrospun Nylon Nanofibers for Protective Applications

Electrospun Nylon Nanofibers for Protective Applications

Abstract

Electrospun Nylon 6 nanofiber mats were deposited on woven 50:50 Nylon:Cotton fabric with the motive of making them into protective material against submicron-level aerosol chemical and biological threats. Polymer solution concentration, electrospinning voltage and deposition areal densities were varied to establish the relationships of processing-structure-filtration efficiency of electrospun nanofiber mats. A high barrier efficiency of greater than 99.5 % was achieved on electrospun nanofiber mats without sacrificing air permeability and pressure drop.

Keywords: Electrospinning; Nylon 6; Nanofiber; Protection; Aerosol

3.1Introduction

Electrospinning technique is being widely used to produce nanofibrous mat structures from many different materials and the resultant nanofiber mats have found various applications including tissue engineering, catalytic reaction materials, electrochemical electrodes, affinity membranes, and nano-composites.[1-11]

Electrospun nanofiber mats are promising barrier material for aerosol filtration.[12] Unlike traditional filtration media that cannot *simultaneously* achieve high filtration efficiency and low pressure drop or high air permeability, electrospun nanofiber mats have small fiber diameters and large surface areas, and hence they can significantly increase the filtration efficiency without sacrificing the air permeability. Usually the electrospun nanofiber mats are deposited on fabric substrates to combine advantages of both materials.[12,13] In this work, electrospun Nylon 6 nanofiber mats were deposited onto Nylon:Cotton fabric to prepare a protective clothing material against chemical and biological warfare agents. Nylon 6 was chosen for the electrospinning of nanofibers because it has good toughness, high abrasion resistance, and easy process ability. The effects of solution concentration, electrospinning voltage and deposition areal density on the structure and performance of electrospun nanofiber mats were investigated to establish processing-structure-filtration efficiency relationships for these new materials. The focus of this paper is on the protective performance of electrospun nanofiber-deposited fabrics.

3.2 Experimental

3.2.1. Electrospinning of Nylon 6 nanofibers

Nylon 6 and 2, 2, 2-tri-fluoro ethanol were purchased from Aldrich and used without further purification. Nylon 6 solutions with different concentration were prepared under constant stirring at room temperature. Figure 3.1 shows the electrospinning setup used in experiments. A 10 ml plastic syringe fitted with a needle tip (inner diameter = 0.4 mm) was used for electrospinning. For all experiments, the feed rate was fixed at 0.3 ml/hr, electrospinning voltage ranged from 8 to 20 kV, and the collector distance from the syringe tip was about 15 cm. Electrospun Nylon 6 nanofiber mats (Figure 3.2) were collected on 50/50 Nylon/Cotton woven fabric placed on a rotating drum type collector. The areal density of nanofiber mats were controlled by varying the deposition time.

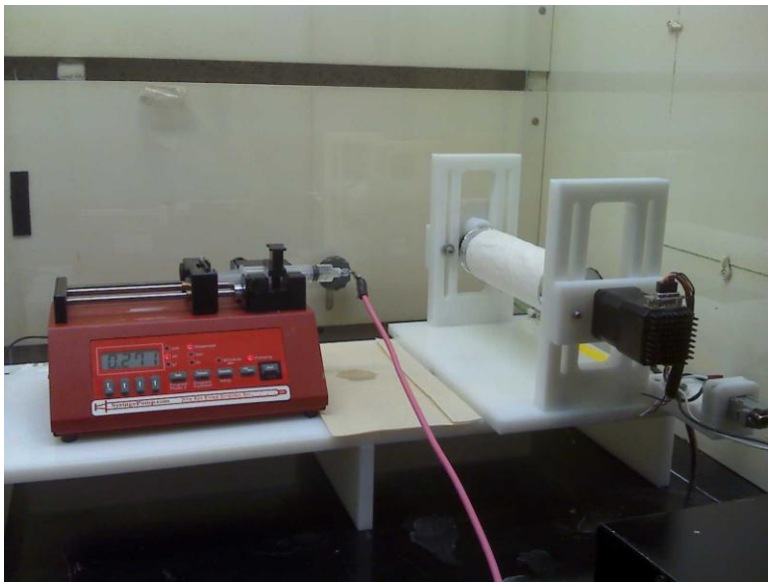

Figure 3.1 Photograph of electrospinning setup.

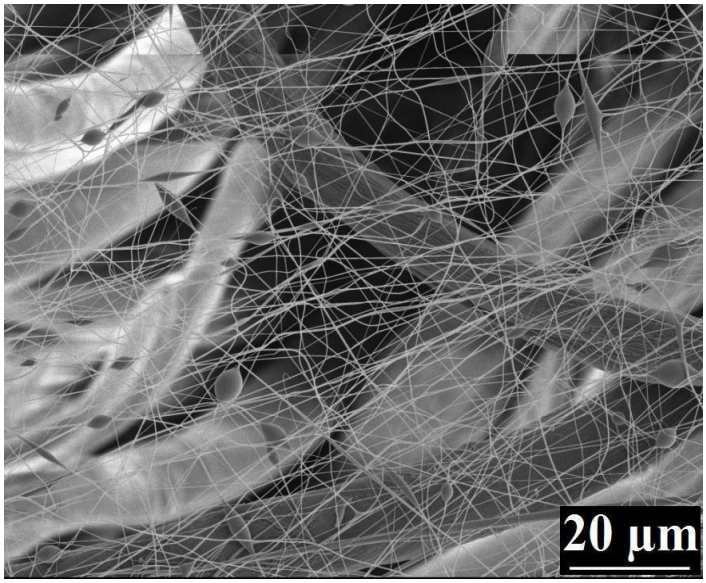

Figure 3.2 SEM image of a typical Nylon 6 nanofiber-deposited Nylon/Cotton woven fabric.

3.2.2. Fiber structure characterization

The morphology of nanofiber mats was examined using scanning electron microscopy JEOL JSM-6400F at an accelerated voltage of 5 kV. The images were acquired and fiber diameters were obtained by measuring 100 nanofibers using the Revolution software provided by 4pi Analysis.

3.2.3. Filtration performance evaluation

The filtration performance and pressure drop value of the nanofiber mats deposited on Nylon:Cotton fabric was *simultaneously* evaluated using TSI 3160 advanced automated tester. During the evaluation, the TSI 3160 instrument used a bank of atomizers and an electrostatic classifier to challenge the nanofiber mats with 300 nm NaCl particles at a face

velocity of 5.332 cm/s and an air flow rate of 32 l/min. Two condensation particle counters were used to simultaneously count the upstream and downstream particles and the penetration values were calculated.

3.2.4. Air permeability testing

The air permeability of nanofiber-deposited fabrics was measured separately using Frazier air permeability testing instrument. The measurement was carried out according to the ASTM D737-04 standard, with 1.4 mm orifice, 2.75 square inch test area, at 30 inch mercury pressure, 21 ^{o}C, 65 % RH.

3.3 Results and Discussion

3.3.1. Filtration efficiency, pressure drop, and air permeability of Nylon 6 nanofiber mats

One of the most important factors that affect the filtration efficiency of nanofiber-deposited fabrics is the areal density or basis weight of nanofiber mats. In this work, Nylon 6 nanofibers were deposited onto 50:50 Nylon/Cotton woven fabrics from 12 % wt/vol. Nylon solution at 10 kV spinning voltage. Deposited Nylon 6 fibers have an average diameter of around 150 nm. The areal density of nanofiber mats was controlled by adjusting the fiber deposition time. Figure 3.3 shows the filtration efficiencies of Nylon 6 nanofiber mat-deposited fabrics. Before fiber deposition (*i.e.*, nanofiber areal density = 0), the filtration efficiency of the 50/50 Nylon/Cotton fabric is only 38%, indicating most of the challenging

particles penetrate through the fabric. Depositing a small amount of electrospin Nylon 6 nanofibers significantly increases the filtration efficiency. For example, when the nanofiber areal density is 1.2 g/m^2, the filtration efficiency increases to 72 %, *i.e.*, a 90 % increase in efficiency. Considering that the areal density of the unmodified substrate Nylon/Cotton is 250 g/m^2, the deposition of 1.2 g/m^2 of nanofibers leads to a weight increase of only 0.5 %.

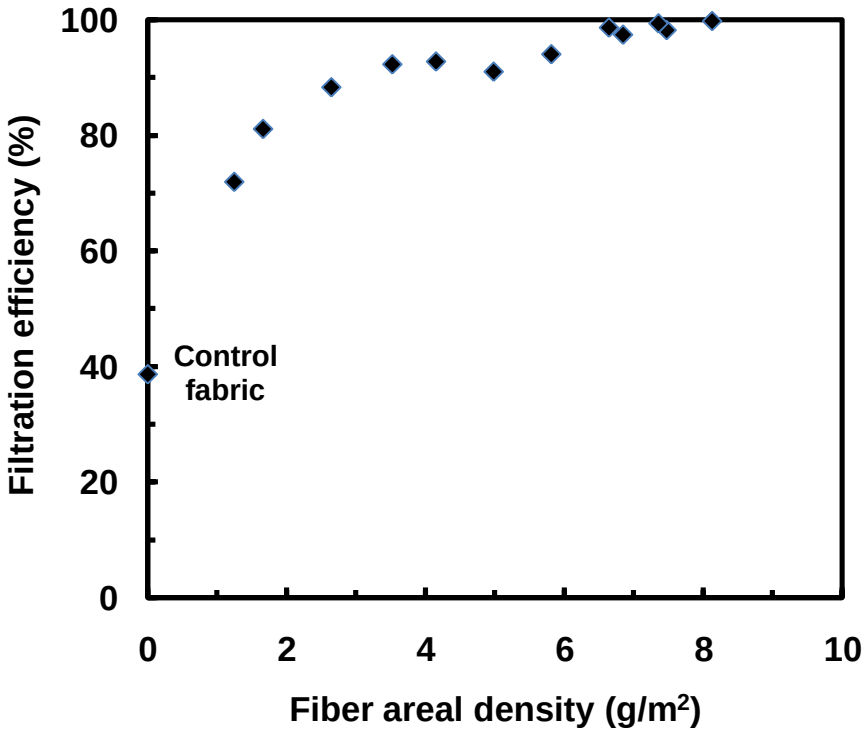

Figure 3.3 Filtration efficiencies of Nylon 6 nanofiber mats on 50/50 Nylon/Cotton fabric with different nanofiber areal densities.

With further increase in nanofiber areal density, the filtration efficiency continues to increase and an efficiency greater than 99.5 % can be obtained when the areal density is between 6.5 and 8.5 g/m^2, corresponding to a weight increase of less than 3.4 %. The filtration efficiency

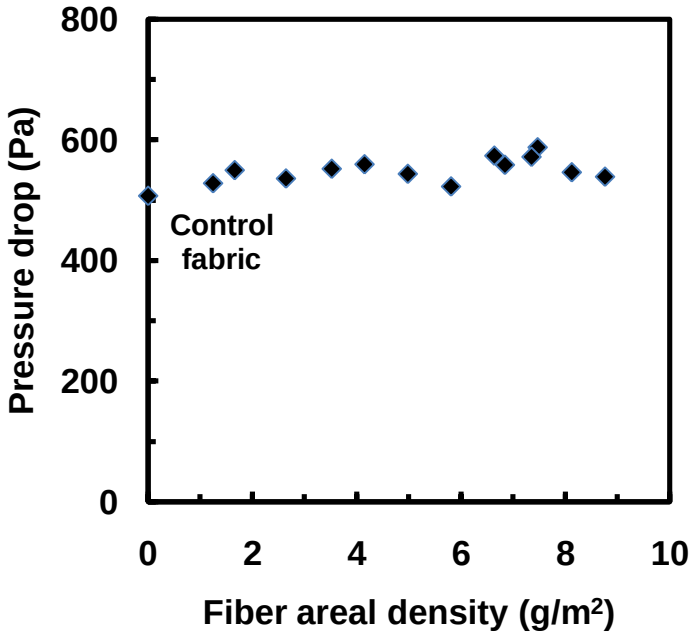

Figure 3.4 Pressure drop of Nylon 6 nanofiber mats on 50/50 Nylon/Cotton fabric with different nanofiber areal density.

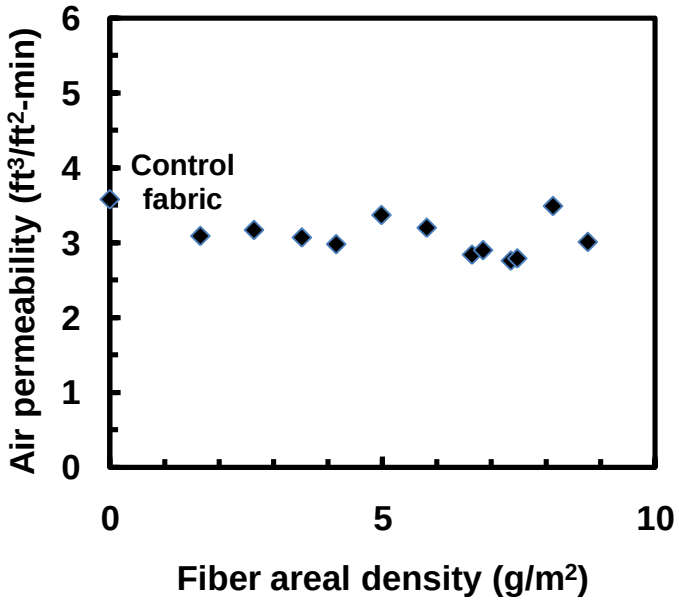

Figure 3.5 Air permeability of Nylon 6 nanofiber mats on 50/50 Nylon/Cotton fabric with different nanofiber areal density.

can be further improved by optimizing the structure of nanofiber mats, as discussed in the following sections.

One major challenge in developing protective materials is to maintain low pressure drop and high air permeability while increasing the filtration efficiency. Many filtration media provide high efficiency by sacrificing pressure drop or air permeability. Figure 3.4 and 3.5 shows that the pressure drop and air permeability of Nylon 6 nanofiber-deposited fabrics with different areal densities are not significantly decreased as compared with the unmodified substrate fabric. Therefore, electrospun nanofiber mats can provide high filtration efficiency without sacrificing pressure drop and air permeability.

In the following sections, the effects of solution concentration and electrospinning voltage on the structure and filtration efficiency of Nylon 6-deposited fabrics are discussed using fabrics with a small areal density (such as 1.2 or 1.7 g/m^2) since the filtration efficiency is sensitive to electrospun nanofiber mat structure at this low deposition amount.

3.3.2. Effect of solution concentration on electrospun nanofiber mat morphology and filtration performance

Electrospun Nylon 6 nanofiber mats were deposited on 50/50 Nylon/Cotton fabric from solutions with different concentrations under an electrospinning voltage of 10 kV. Figure 3.6 shows SEM images of these nanofiber mats, and their fiber distributions are shown in Figure

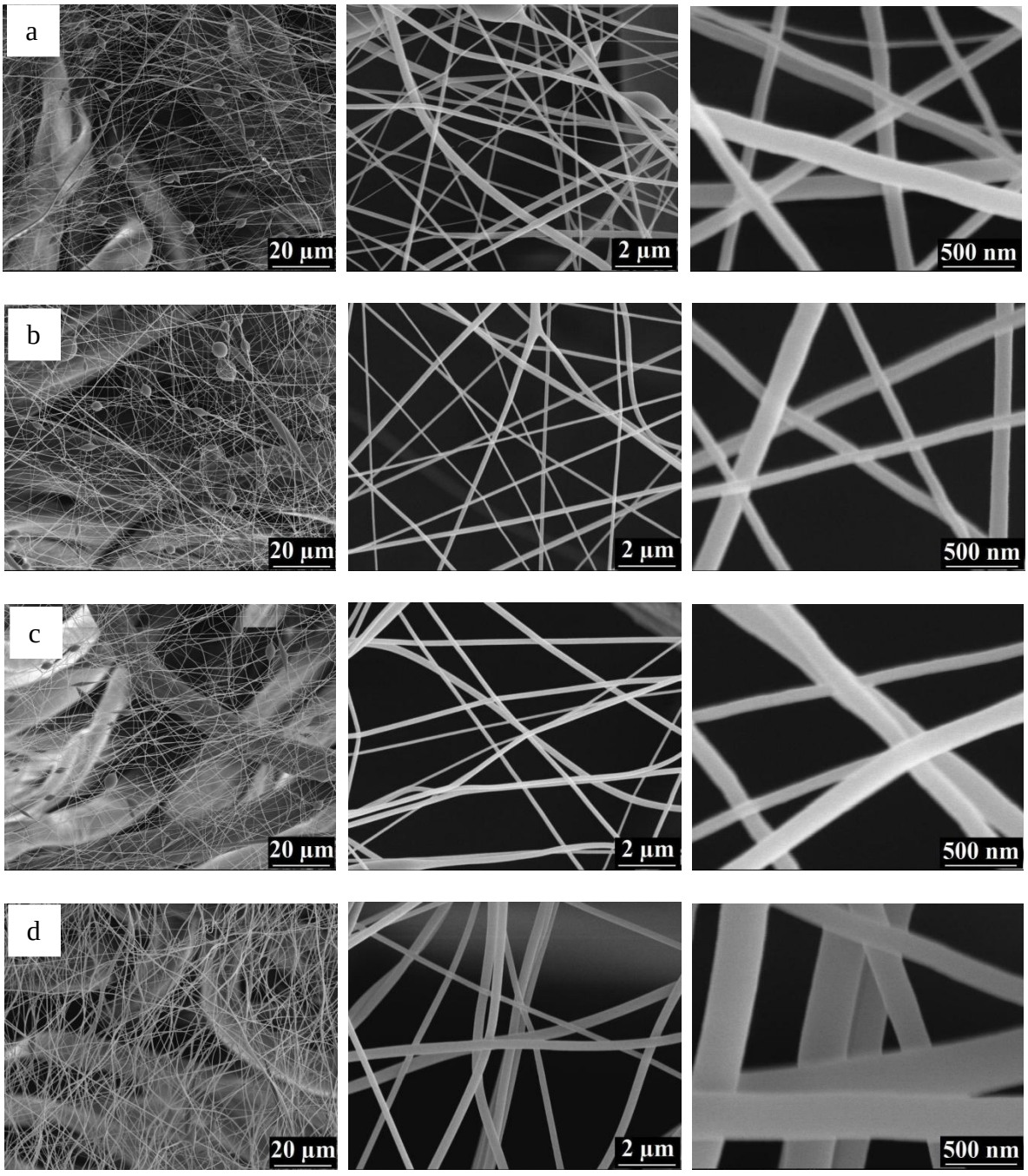

Figure 3.6 SEM images of Nylon 6 nanofiber mats produced with different solution concentration: (a) 10; (b) 11; (c) 12; and (d) 13 % wt/vol.

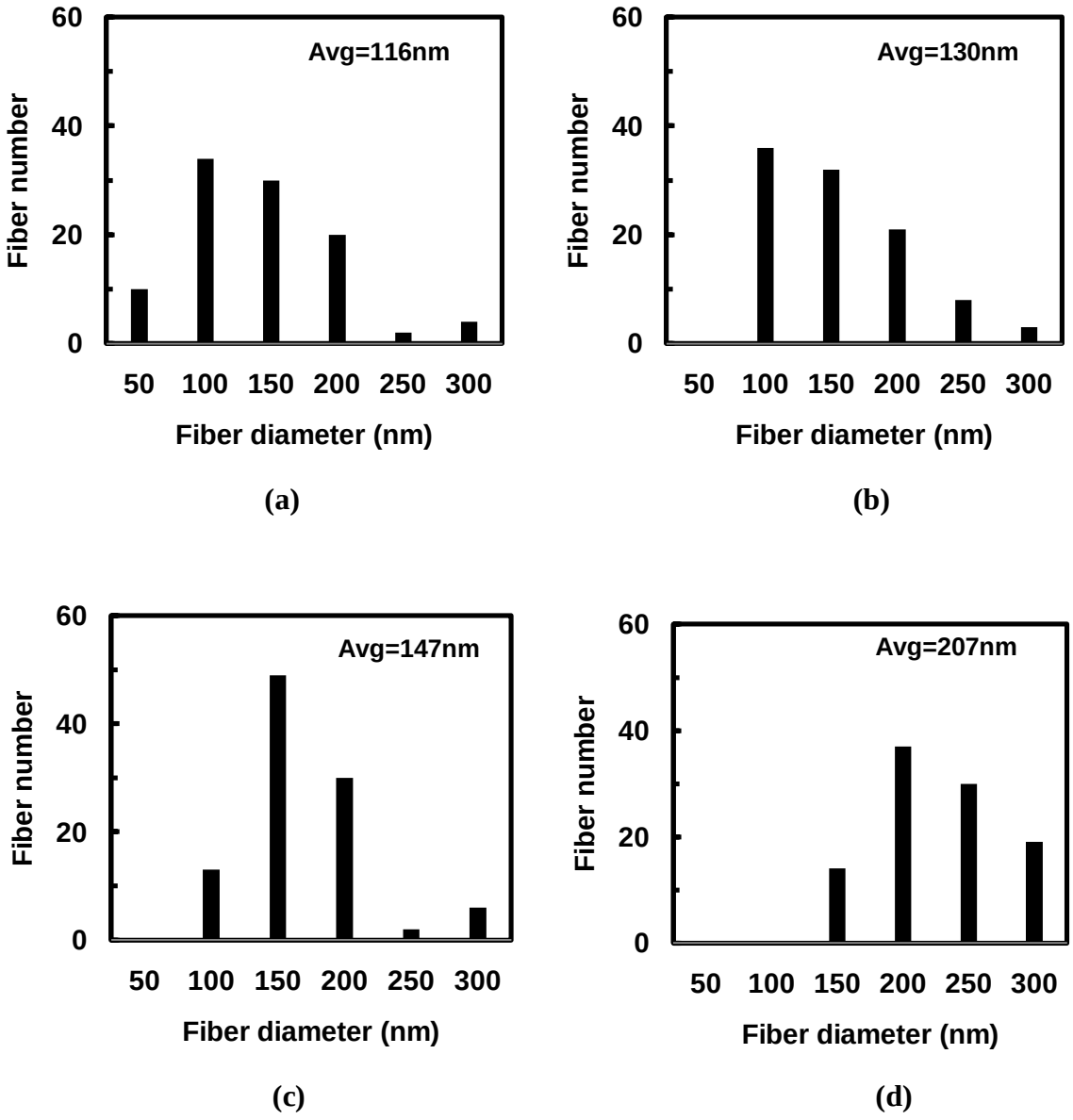

Figure 3.7 Fiber diameter distributions of Nylon nanofiber mats produced with different solution concentration: (a) 10; (b) 11; (c) 12; and (d) 13% wt/vol.

3.7. It is seen that with increase in solution concentration, fiber diameter increases. This is a result of increased solution concentration, which in turn leads to increased solution viscosity and resistance to jet stretching during whipping, thereby resulting in thicker fiber diameter.[14-16] From Figure 3.6, it was seen that beads are formed at lower solution concentrations of 10 and 11% wt/vol., although these solutions produce nanofibers with smaller diameters. The formation of beads might be caused by insufficient chain entanglements at low concentrations. [17-19] When the solution concentration increases to 12 and 13% wt/vol., the solution viscosity and chain entanglement density increase and favor the formation of smooth nanofibers without beads.

Figure 3.8 shows the effect of solution concentration on the filtration efficiency of Nylon 6 nanofiber mats deposited on Nylon/Cotton fabric. These mats have the same areal density, *i.e.*, 1.2 g/m^2. In general, as fiber diameter increases, the filtration efficiency decreases.[13, 20] The filtration efficiencies of nanofiber mats produced from 10, 11, and 12 % wt/vol solutions are greater than 75 % due to their smaller diameters, but the mat efficiency is lower than 70 % when the solution concentration is 13 %.

3.3.3. Effect of electrospinning voltage on nanofiber morphology and filtration performance

Another crucial parameter in fiber diameter control is the voltage between the spinneret and collector. In general, a voltage higher than 6 kV is able to cause the polymer solution drop at

the tip of the needle to distort into the shape of a Taylor Cone during the initiation of electrospinning.[21]

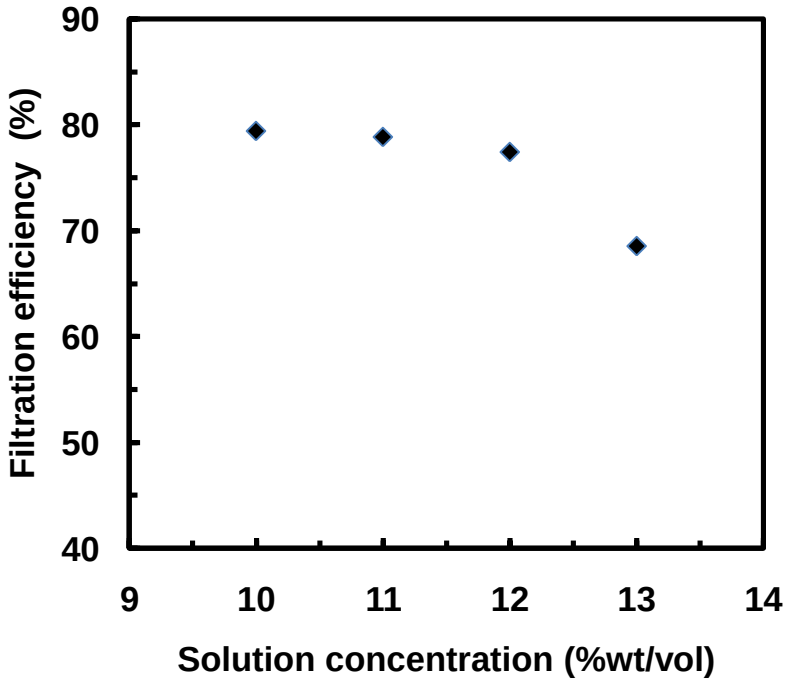

Figure 3.8 Filtration efficiency of Nylon 6 nanofiber mats prepared using different solution concentration.

Previous studies of the effect of voltage on electrospun fiber morphology have reported interesting results. Some researchers reported that a higher voltage leads to enhanced stretching of the solution due to the greater columbic forces in the jet as well as the stronger electric field.[22-26] As a result, the fiber diameter becomes smaller at higher voltages. In addition, when a solution of lower viscosity is used, a higher voltage favors the formation of secondary jets, which in turn also causes reduced diameter. However, some other reports show that larger fiber diameters are obtained at higher voltages.[27]

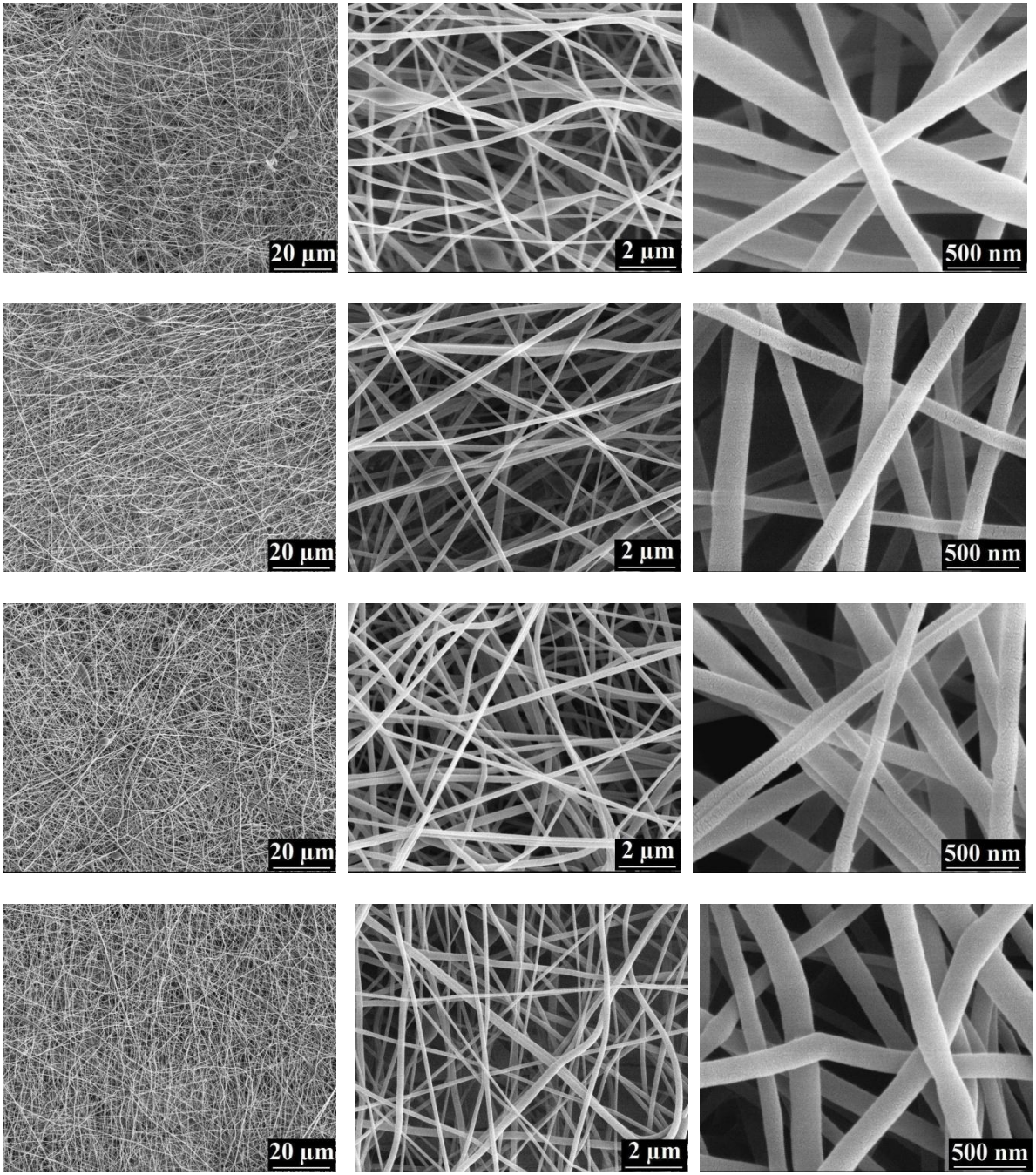

Figure 3.9 SEM images of Nylon 6 nanofiber mats prepared at different electrospinning voltage: (a) 8; (b) 12: (c) 16; and (d) 20kV.

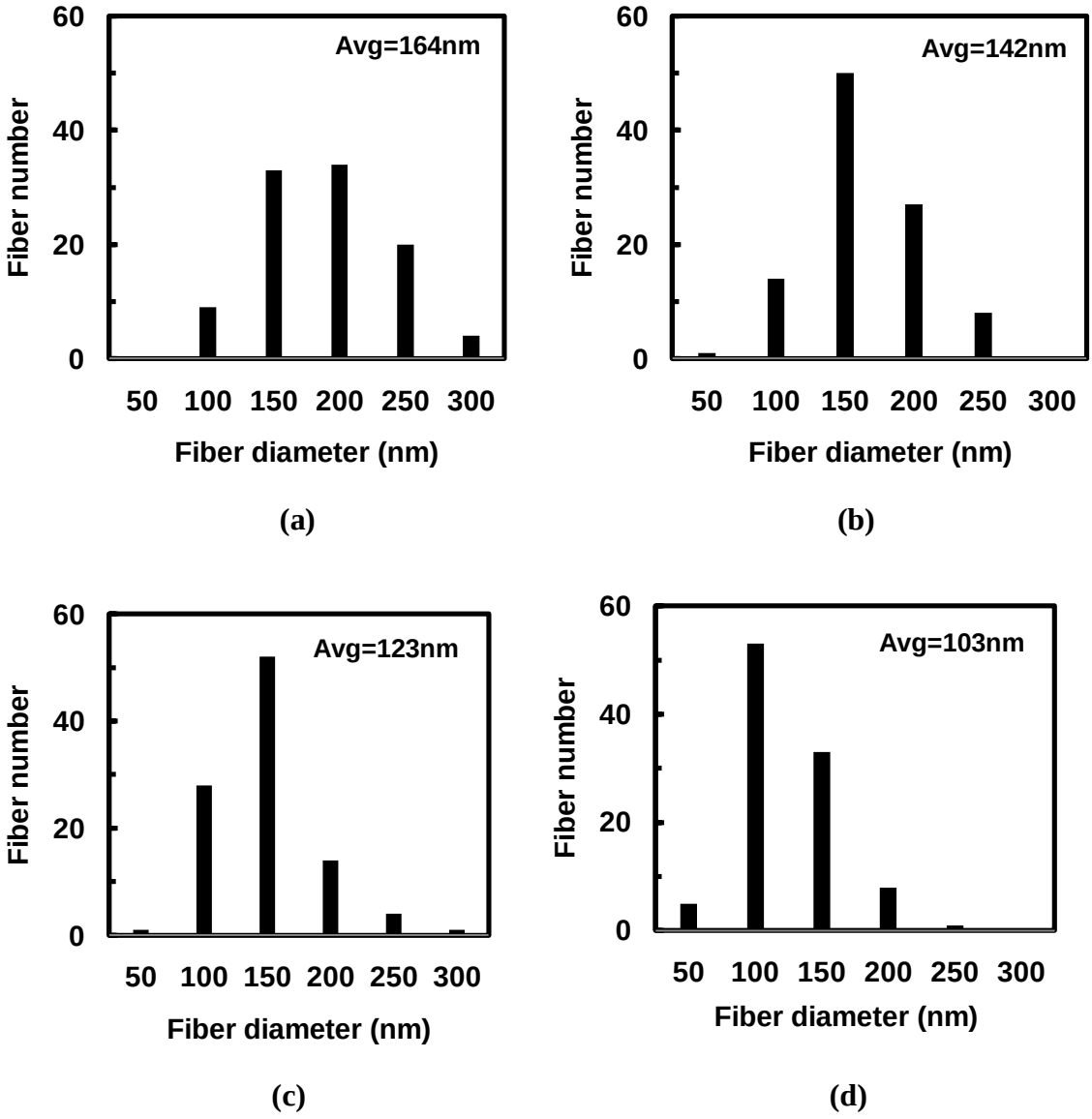

Figure 3.10 Fiber diameter distributions of Nylon 6 nanofiber mats prepared at different electrospinning voltage: (a) 8; (b) 12; (c); and (d) 20 kV.

This is probably because the flight time for the fibers to stretch and elongate is reduced at high voltages. There are also reports showing that fiber diameter does not change significantly when the electrospinning voltage changes.[28-30] Therefore, in order to obtain nanofiber mats with desired diameter and performance, electrospinning voltage must be carefully controlled to obtain a proper balance among electric field strength, jet flight time, and jet stability, etc.

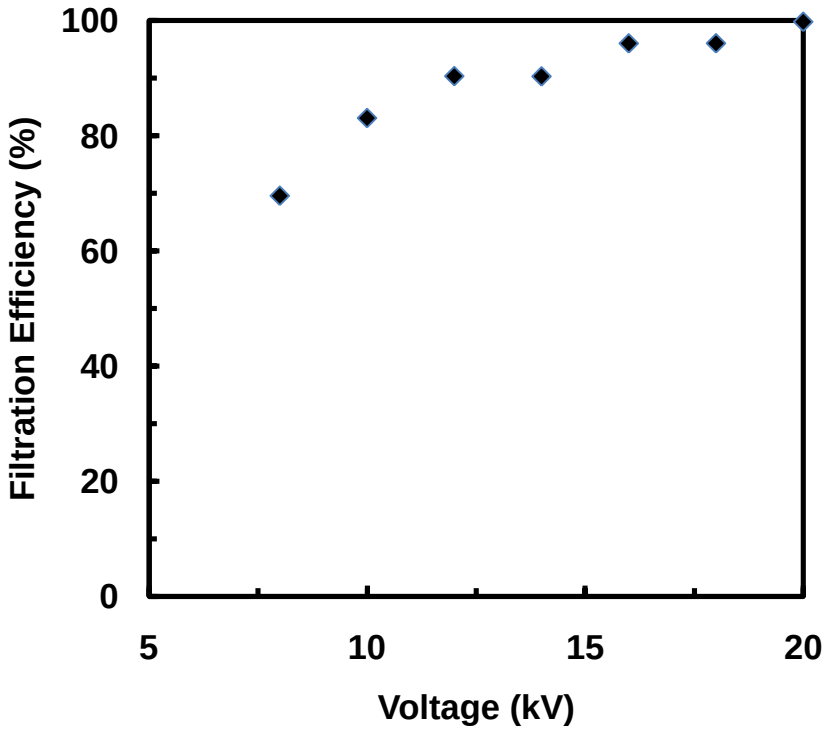

Figure 3.11 Filtration efficiency of Nylon6 nanofiber mats prepared at different electrospinning voltage.

Figure 3.9 and 3.10 shows SEM images and fiber diameter distributions of Nylon 6 nanofiber mats deposited on Nylon/Cotton fabric from 12% wt/vol solution using different voltages.

The deposition areal density is 1.7 g/m^2. It is seen that with increase in electrospinning voltage, the fiber diameter decreases gradually. Therefore, in this work, higher applied voltage enhances polymer jet extension, resulting in finer fiber diameter.

Figure 3.11 shows the effect of electrospinning voltage on the filtration efficiency of Nylon 6 nanofibers on 50/50 Nylon/Cotton fabric. When the spinning voltage was increased from 8kV to 20kV, the filtration efficiency of nanofiber mats increased continuously. Hence, increasing spinning voltage yields a corresponding enhancement in filtration efficiency.

3.4 Summary

Electrospun Nylon 6 nanofiber mats were deposited on 50:50 Nylon:Cotton woven fabrics with varying processing parameters such as solution concentration, electrospinning voltage, and deposition time or areal density. It was found that depositing Nylon 6 nanofiber mats can significantly improve the filtration efficiencies without sacrificing pressure drop and air permeability. The effect of electrospinning conditions, such as applied voltage and solution concentration, on the filtration efficiency was studied. It was observed that the filtration efficiency increased with decreasing solution concentration and increasing applied voltage. Filtration efficiency of the fabric was increased by a maximum of more than 250% after the deposition of nanofiber mats. Electrospun nanofiber mats promise to be highly effective components of high performance barrier fabric materials.

3.5 References

1.C. Xu, R. Inai, M. Kotaki, S. Ramakrishna, Electrospun Nanofiber Fabrication as Synthetic Extracellular Matrix and Its Potential for Vascular Tissue Engineering, *Tissue Eng* 2004, **10**, 1160.

2.H. Kim, H. Lee, J.C. Knowles, Electrospinning biomedical nanocomposite fibers of hydroxyapaite/poly(lactic acid) for bone regeneration, *Journal of biomedical materials research Part A* 2006, **79a**, 643.

3.H. Jia, G. Zhu, B. Vugrinovich, W. Kataphinan, D.H. Reneker, P. Wang, Enzyme-carrying polymeric nanofibers prepared via electrospinning for use as unique biocatalysts, *Biotechnol Prog.*, 2002, **18**, 1027.

4.A.C. Patel, S. Li, C. Wang, W. Zhang, Y. Wei, Electrospinning of Porous Silica Nanofibers Containing Silver Nanoparticles for Catalytic Applications, *Chemistry of Materials* 2007, **19**, 1231.

5.Y. Ju, G. Choi, H. Jung, C. Kim, K. Yang, W. Lee, A Hydrous Ruthenium Oxide-Carbon Nanofibers Composite Electrodes Prepared by Electrospinning, *J. Electrochem. Soc*, 2007, **154**, A192.

6.Z. Ma, M. Kotaki, S. Ramakrishna, Electrospun cellulose nanofiber as affinity membrane, *J Membr. Sci.,* 2005, **265**, 115.

7.Z. Ma, M. Kotaki, S. Ramakrishna, Surface modified nonwoven polysulphone (PSU) fiber mesh by electrospinning : A novel affinity membrane, *J. Membr. Sci*. 2006, **272**, 179.

8.W. Salalha, Y. Dror, R. L. Khalfin, Y. Cohen, A.L. Yarin, E. Zussman, Single-walled carbon nanotubes embedded in oriented polymeric nanofibers by electrospinning, *Langmuir*, 2004, **20**, 9852.

9.S. Kedem, J. Schmidt, Y. Paz, Y. Cohen, Composite Polymer Nanofibers with Carbon Nanotubes and Titanium Dioxide Particles, *Langmuir*, 2005, **21**, 5600.

10.K. Fujihara, M. Kotaki, S. Ramakrishna, Guided bone regeneration membrane made of polycaprolactone/calcium carbonate composite nano –fibers, *Biomaterials*, 2005, **26**, 4139.

11.I. Uslu, B. Baser, A. Yayli, M.L. Aksu, Preparation and characterization of PVA/zinc acetate/boron composite fibers, *E-Polymers* 2007, No. **145**

12.S. Thandavamoorthy, G.S. Bhat, R.W. Tock, S. Parameswaran, S.S. Ramkumar, Electrospinning of Nanofibers, *J Appl Polym Sci* 2005, **96**, 557.

13.F. Dotti, A. Varesano, A. Montarsolo, A. Aluigi, C. Tonin, G. Mazzuchetti, Electrospun porous mats for high efficiency filtration, *Journal of Industrial Textiles* 2007, **37**, 151.

14.J. Kameoka, R. Orth, Y. Yang, D. Czaplewski, R. Mathers, G.W Coates, H.G. Craighead, A scanning tip electrospinning source for deposition of oriented nanofibers, *Nanotechnology*, 2003, **14**, 1124.

15.S. S. OJha, M. Afshari, R. Kotek, R. E. Gorga, Morphology of Electrospun Nylon-6 Nanofibers as a Function of Molecular Weight and Processing Parameters, *J Appl Polym Sci* 2008, **108**, 308.

16.A. Frenot, I. Chronakis, Polymer nanofibers assembled by electrospinning, *Current Opinion in Colloid Interface Science* 2003, **8**, 64.

17.S.L. Shenoy, W.D. Bates, H.L. Frisch, G.E. Wnek, Role of chain entanglements on fiber formation during electrospinning of polymer solutions: good solvent, non-specific polymer–polymer interaction limit, *Polymer*, 2005, **46**, 3372.

18.H. Fong, I. Chun, D.H. Reneker, Beaded nanofibers formed during electrospinning, *Polymer*, 1999, **40**, 4585.

19.K.H. Lee, H.Y. Kim, H.J. Bang, Y.H. Jung, S.G. Lee, The change of bead morphology formed on electrospun polystyrene fibers, *Polymer* 2003, **44**, 4029.

20.Y. Lee, L.C. Wadsworth, Structure and filtration properties of melt-blown polypropylene webs, *Polym Eng Sci* 1990, **30**, 1413.

21.G. Taylor, Disintegration of Water Drops in an Electric Field, *Proceedings - Royal Society.Mathematical, Physical and Engineering Sciences*, 1964, **280**, 383.

22.Y. M. Shin, M. M. Hohman, M. P. Brenner, G. C. Rutledge, Experimental characterization of electrospinning: the electrically forced jet and instabilities, *Polymer* 2001, **42**, 09955.

23.S. Megelski, J.S. Stephens, D.B. Chase, J.F. Rabolt, Micro and Nanostructured Surface Morphology on Electrospun Polymer Fibers, *Macromolecules*, 2002, **35**, 8456.

24.R. Jalili, S.A. Hosseini, M. Morshed, The Effects of Operating Parameters on the Morphology of Electrospun Polyacrilonitrile Nanofibres, *Iranian Polymer Journal* 2005, **14**, 1074.

25.J.S. Lee, K.H. Choi, H. D. Ghim, S.S. Kim, D. H. Chun, H.Y. Kim, W.S. Lyoo, Role of molecular weight of atactic poly(vinyl alcohol) (PVA) in the structure and properties of PVA nanofabric prepared by electrospinning, *J Appl Polym Sci* 2004, 93, 1638.

26.M. Spasova, N. Manolova, D. Paneva, I. Rashkov, Preparation of chitosan-containing nanofibres by electrospinning of chitosan/poly(ethylene oxide) blend solutions, *E-Polymers* 2004, No 056.

27.S.C. Baker, N. Atkin, P.A. Gunning, N. Granville, K. Wilson, D. Wilson, J. Southgate, Characterisation of electrospun polystyrene scaffolds for three-dimensional in vitro biological studies, *Biomaterials*, 2006, **27**, 3136.

28.X. Yuan, Y. Zhang, C. Dong, J. Sheng, Morphology of ultrafine polysulfone fibers prepared by electrospinning, *Polym Int*, 2004, **53**, 1704.

29.S. H. Tan, R. Inai, M. Kotaki, S. Ramakrishna, Systematic parameter study for ultra-fine fiber fabrication via electrospinning process, *Polymer,* 2005, **46**, 6128.

30.S. Kidoaki, I.K. Kwon, T. Matsuda, Structural features and mechanical properties of *in situ*–bonded meshes of segmented polyurethane electrospun from mixed solvents, *Journal of biomedical materials research. Part B, Applied biomaterials***,** 2006, 76b, 219.

CHAPTER 4

Multifunctional Zinc Oxide/Nylon 6 Nanofiber Mats by Electrospinning-Electrospraying Hybrid Process for Use in Protective Applications

Multifunctional Zinc Oxide/Nylon 6 Nanofiber Mats by Electrospinning-Electrospraying Hybrid Process for Use in Protective Applications

Abstract

ZnO/Nylon 6 nanofiber mats were prepared by an electrospinning-electrospraying hybrid process in which ZnO nanoparticles were dispersed on the surface of Nylon 6 nanofibers without becoming completely embedded. The prepared ZnO/Nylon 6 nanofiber mats were evaluated for their abilities to kill bacteria or inhibit their growth and to catalytically detoxify chemicals. Results showed that these ZnO/Nylon 6 nanofiber mats had excellent antibacterial efficiency (99.99%) against both the gram-negative *E. coli* and gram positive *B. cereus* bacteria. In addition, they exhibited good detoxifying efficiency (95%) against paraoxon, a simulant of highly toxic chemicals. ZnO/Nylon 6 nanofiber mats were also deposited onto Nylon/Cotton woven fabrics and the nanofiber mats did not significantly affect the moisture vapor transmission rates and air permeability values of the fabrics. Therefore, ZnO/Nylon 6 nanofiber mats prepared by the electrospinning-electrospraying hybrid process are promising material candidates for protective applications.

Keywords: Electrospinning; Electrospraying; Nylon 6; Zinc Oxide; Antibacterial; Detoxification.

4.1 Introduction

Electrospun nanofiber mats are characterized by their small fiber diameters, controllable pore sizes, and high porosities.[1] These aforementioned properties could be utilized to attain protective clothing materials to efficiently adsorb submicron aerosols such as pathogens and toxic chemicals. By introducing functional materials into nanofibers, it is also possible to provide electrospun nanofibers with antibacterial and detoxifying properties.

Extensive research on zinc oxide (ZnO) reveals a gamut of functionalities such as antifungal properties,[2] photo-catalysis,[3] and UV light absorption.[4] J. Sawai et al.[5] reported antibacterial properties of ZnO particles against *E.coli* bacteria. Recently, Prasad et al.[6] demonstrated that ZnO in the form of nanorods or nanoparticles can detoxify highly toxic chemicals. Therefore, incorporating ZnO into electrospun nanofibers can lead to composite nanofiber mats that have the ability to effectively kill bacteria and detoxify poisonous chemicals. In general, the active particles could be dispersed directly in polymer solution to be electrospun into functional composite nanofibers.[7] However, this process has the limitation of particle aggregation in the polymer solution and related fiber spinning difficulties. In addition, in the resultant composite nanofibers, most nanoparticles are encapsulated in the polymer matrix and thus are not available for providing active antibacterial and detoxifying functions.

This paper presents the preparation of novel ZnO/Nylon 6 nanofiber mats by an electrospinning-electrospraying hybrid process. During that process, Nylon 6 nanofibers were electrospun from a Nylon solution, and *simultaneously* ZnO nanoparticles were electrosprayed using a ZnO suspension. The ZnO nanoparticles in the resultant nanofiber mats are dispersed on the fiber surface and are exposed to the environment; therefore, these functional nanofibers are readily available for active reactions against pathogens and toxic chemicals. This manuscript discusses about chemical detoxification and antibacterial activities of functional ZnO/Nylon 6 nanofiber mats. Paraoxon was chosen as a simulant of toxic chemicals,[8] and *B.cereus* and *E.coli* were for antibacterial property tests.[9]

4.2Experimental

4.2.1 Materials

Nylon 6 pellets, zinc oxide (ZnO, particle size = 50 nm), 2, 2, 2-tri-fluoro ethanol (TFE), methanol, acetone and diethyl *p*-nitro phenyl phosphate (paraoxon) were purchased from Sigma-Aldrich. All reagents were used without further purification.

4.2.2 Preparation of ZnO/Nylon 6 nanofiber mats

The ZnO/Nylon 6 functional nanofibers were prepared by an electrospinning-electrospraying hybrid process as illustrated in Figure 4.1 Nylon 6 was dissolved in TFE solvent at a concentration of 10 wt %. ZnO nanoparticles (10 wt %) were dispersed in methanol and subjected to ultra-sonication for 15 minutes to obtain a homogeneous ZnO suspension. Nylon

6 polymer solution and ZnO nanoparticle dispersion were loaded into two separate syringes and placed side-by-side on a two-syringe pump. The feed rate was maintained at 1.0 ml/hr for both syringes. The distance between the syringe needle tips and the collector plate was 15 cm. The syringe needles were positively charged with 20 kV using a high-voltage power supply (Gamma ES40P-20W/DAM) to electrospin Nylon 6 nanofibers and *simultaneously* electrospray ZnO nanoparticles. The prepared ZnO/Nylon 6 nanofiber mats were vacuum dried overnight to remove residual TFE and methanol. For comparison, Nylon 6 nanofibers were also prepared by electrospinning the Nylon 6 solution under similar conditions.

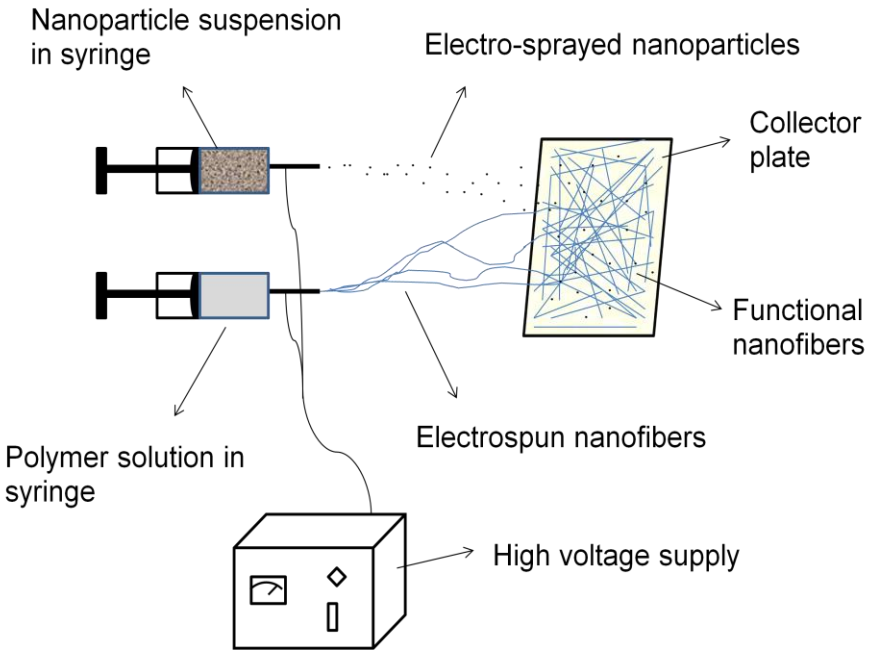

Figure 4.1 Schematic of the electrospinning-electrospraying hybrid process.

4.2.3 Characterizations of solution and dispersion properties and nanofiber mat structure

The viscosity of Nylon 6 solution was measured using a rheometer (StressTech HR, Rheologica Instruments AB) at 25 °C with assistance of rheoExploer V5 software. The ionic conductivities of Nylon 6 solution and ZnO suspension were measured using Orion model 164 conductivity measuring instrument (Orion Research Inc., Boston, MA). The morphology of ZnO/Nylon 6 nanofiber mats was examined using JEOL JSM-6400F Field Emission Scanning Electron Microscopy (FESEM) at an accelerated voltage of 5 kV.

4.2.4 Evaluation of antibacterial activity of ZnO/Nylon 6 nanofiber mats

The antibacterial activity of ZnO/Nylon 6 nanofiber mats was first evaluated qualitatively using the Antibacterial Activity Assessment of Textile Materials AATCC Test Method 147-2004. The *E. coli* O157:H7 (FSRU-B387) harboring plasmid pSM433 encoding green fluorescent protein (GFP) was prepared by inoculating 5 ml of Luria-Bertani (LB) broth with a bacterial colony and incubated for 18 hours at 37^{o}C. Using a 4-mm inoculating loop, 5 parallel streaks of bacterial culture were spread across a LB agar plate without refilling the loop between streaks. An aseptically-cut, rectangular ZnO/Nylon 6 nanofiber mat specimen was gently pressed transversely face-down across the streak area on the agar plate. Plates were evaluated for clearing and interruption of growth along the streak lines. Since the *E. coli* contained GFP, ultraviolet light (370 nm) was employed to improve visualization. To get consistent results, four replicate plates were used for the streak method for each nanofiber mat sample.

For quantitative analysis of the bactericidal effects of the nanofiber mats, *E. coli* O157:H7 (B179), a Gram negative enteric pathogen, and *Bacillus cereus* (B002), a spore-forming Gram positive pathogen, were used. The pathogens *E. coli* B179 and *B. cereus* B002 were grown in LB agar or broth and Tryptic Soy Agar (TSA) agar, respectively. The bacterial cells were taken from randomly chosen colonies on an agar plates and cultured by inoculating into 5 ml LB broth or TSA broth, then incubated for 18 hours at 37 ^{o}C on a shaker platform at 200 rpm. The independent replications of each culture were prepared. After the incubation period, the cells were harvested by centrifugation (5000 rpm, 10 min, 4 ^{o}C, Sorvall RB-5C centrifuge) and re-suspended in 5 ml of physiological saline (0.85% NaCl). Cells were diluted to 10^7 CFU (colony forming units)/mL and used immediately for testing. During testing, the ZnO/Nylon 6 nanofiber mat specimens (5 - 8 mg) were aseptically prepared and placed in a 1.5 ml micro-centrifuge tube. The saline cell suspension (200 µL) containing approximately 10^7 CFU/ml of the test organism was injected into the tube, completely covering the nanofiber mat. Appropriate positive (cell suspension in saline without nanofiber mat) and negative controls (saline without cells, saline plus nanofiber mat, cells plus a Nylon 6 nanofiber mat), were also included in the experimental design. Samples were incubated for 24 hr at 37 °C with gentle agitation at 300 rpm on a shaker platform. After 24 hr, cells were enumerated on LB agar (*E. coli*) or TSA (*B. cereus*) plates using a spiral plater (Spiral Biotech Model 4000). After 24 hr incubation at 37°C, bacterial colonies on plates were counted by an automated plate reader (Qcount, Spiral Biotech). The lowest level of detection using this method was approximately 10^2 CFU/ml. All antibacterial measurements were

conducted in a Bio-safety Level 2 laboratory in the USDA Agricultural Research Service laboratory, Department of Food Science, NC State University, Raleigh, North Carolina.

4.2.5 Evaluation of detoxification properties of ZnO/Nylon 6 nanofiber mats

For detoxification test, a piece of ZnO/Nylon 6 nanofiber mat (~300 mg) was placed in a glass vial, which was then filled with 8 ml solution of ~20 µM concentration paraoxon in acetone. For comparison, Nylon 6 nanofiber mat (~150 mg) and pure ZnO particles (~150 mg) were also loaded in separate vials and filled with 8 ml of the above mentioned paraoxon solution. All the vials were stored at room temperature for the detoxifying reaction. After specific time intervals, the solutions were extracted and tested by Gas Chromatography-Mass Spectrometry (Agilent 5975B GC-MS, Agilent Technologies, USA) to determine the residual concentration of paraoxon. In the GS-MS spectra, concentration of paraoxon was represented by the area under the peak.

4.2.6 Air permeability and moisture vapor transmission rate measurements

To evaluate air permeability and moisture vapor transmission rate (MVTR), ZnO/Nylon 6 nanofibers were deposited onto a 50:50 Nylon/Cotton blend fabric by the electrospinning-electrospraying hybrid process. The fabric deposited with pure Nylon 6 electrospun nanofibers and control fabrics without any nanofibers were included in the test. The areal density of ZnO/Nylon 6 and Nylon 6 nanofiber mats were measured by weighing the sample fabric substrate before and after nanofiber deposition at 20 °C and 65% relative humidity.

The air permeability values of ZnO/Nylon 6 and Nylon 6 nanofiber mats deposited on fabric substrate were measured using Frazier air permeability testing instrument. The measurement was carried out according to the Standard Test Method for Air Permeability of Textile Fabrics ASTM D737-04 standard, with 1.4 mm orifice, 2.75 square inch test area, at 30 inch mercury pressure, 20^{o} C, and 65 % relative humidity.

The MVTRs of ZnO/Nylon 6 and Nylon 6 nanofiber mats deposited onto fabric substrate were measured using the ASTM E96-80 standard. Prior to the test, the samples were conditioned at 20 °C and 65% relative humidity for 24 hours. The MVTR values were calculated in units of g/m^2-24 hours.

4.3 Results and Discussion

4.3.1 Preparation and characterization of ZnO/Nylon 6 nanofiber mats

Table 4.1 shows the viscosity of ZnO suspension and the ionic conductivities of both Nylon 6 solution and ZnO suspension. The measured ionic conductivity and viscosity values were found to be in the ranges that can produce a stable electrospinning or electrospraying process.[10, 11] During the hybrid process, the positively-charged Nylon 6 solution was ejected and underwent a stretching-and-whipping process resulting in the formation of a long, thin thread. This stretching-and-whipping process is accompanied by the rapid evaporation of the solvent that reduces the jet diameter from hundreds of micrometers to as small as tens of nanometers.

The dry fibers are accumulated on the surface of the grounded collector forming a non-woven mat of Nylon 6 nanofibers. At the same time, the positively-charged ZnO suspension was also sprayed onto the collector and ZnO nanoparticles were captured by Nylon 6 nanofibers.

Table 4.1 Properties of Nylon 6 solution and ZnO suspension.

Measurement	**Nylon 6 in TFE (10 wt %)**	**ZnO in Methanol (10 wt %)**
Zero shear viscosity (cP)	110 ± 5	-
Ionic conductivity (μS/cm)	3.7 ± 0.1	175 ± 3

Figure 4.2 shows photographs and FESEM images of ZnO/Nylon 6 nanofibers prepared by the electrospinning-electrospraying hybrid process and Nylon 6 nanofibers obtained solely by electrospinning. It is seen that electrospun Nylon 6 nanofibers have an average fiber diameter of 210 ± 30 nm and they are randomly deposited to form a nonwoven mat. For ZnO/Nylon 6 nanofibers, the average fiber diameter decreases to 190 ± 40 nm, and at the same time, ZnO particles were attached on the nanofiber surface and were distributed throughout the entire mat. More important, ZnO nanoparticles are not encapsulated by the fiber matrix and are exposed to the environment. This is important for utilizing the functionalities of ZnO and achieving the high antibacterial and detoxifying activities.

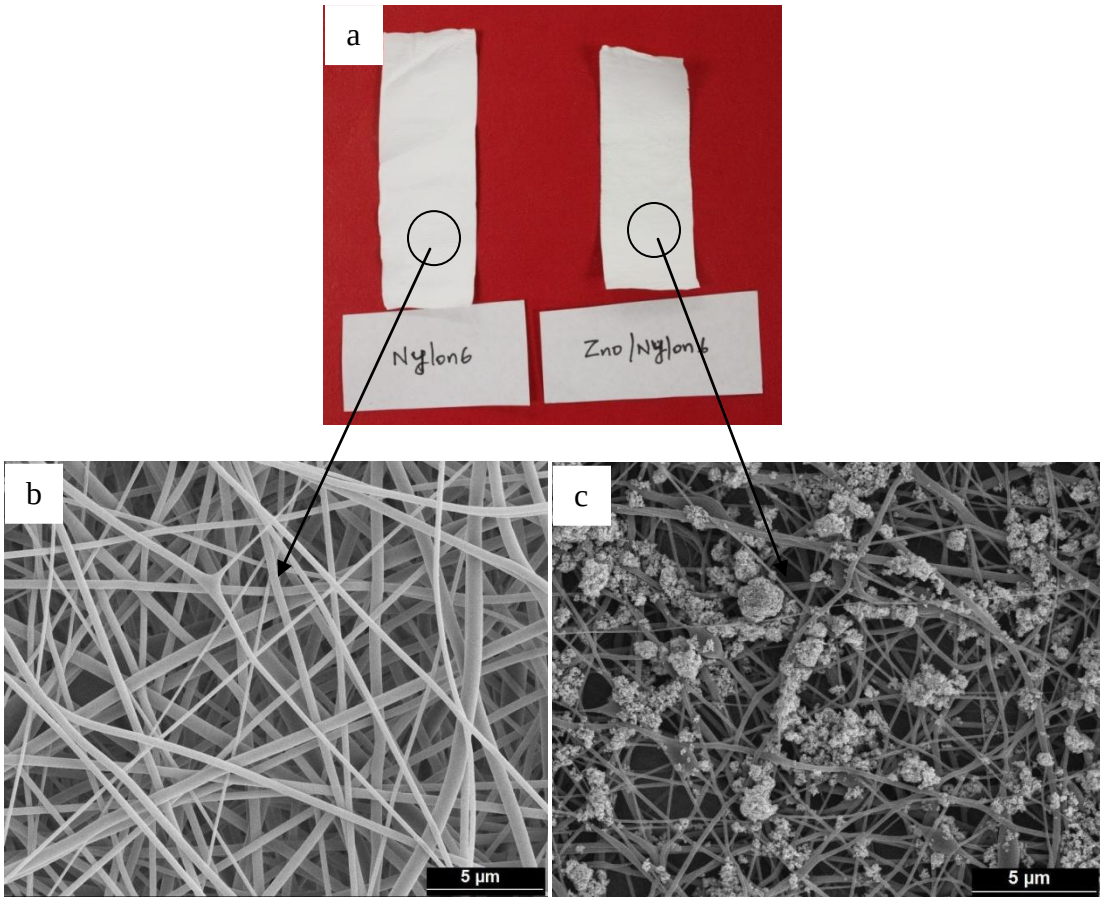

Figure 4.2 a) Photographs of Nylon 6 and ZnO/Nylon 6 nanofiber mats, and FESEM image of b) Nylon 6, and c) ZnO/Nylon 6 nanofiber mats.

4.3.2 Antibacterial activity of ZnO/Nylon 6 nanofiber mats

Figure 4.3 shows the qualitative AATCC 147 antibacterial testing results of Nylon 6 and ZnO/Nylon 6 nanofiber mats against E. *coli*. It is seen that the Nylon 6 nanofiber mat does not have antibacterial function and the bacterial streaks grow across the entire nanofiber mat from underneath. In contrast, the ZnO/Nylon 6 nanofiber mat inhibits the growth of E. *coli* and there are no bacterial streaks under and near the mat.

Table 4.2 Antibacterial activities of Nylon 6 and ZnO/Nylon 6 nanofiber coated fabrics.

Sample	**E. *coli* [log(CFU/ml)]**	**B. *cereus* [log(CFU/ml)]**
Nylon 6 nanofiber mat	7.18	7.08
ZnO/Nylon 6 nanofiber mat	0.0	0.0

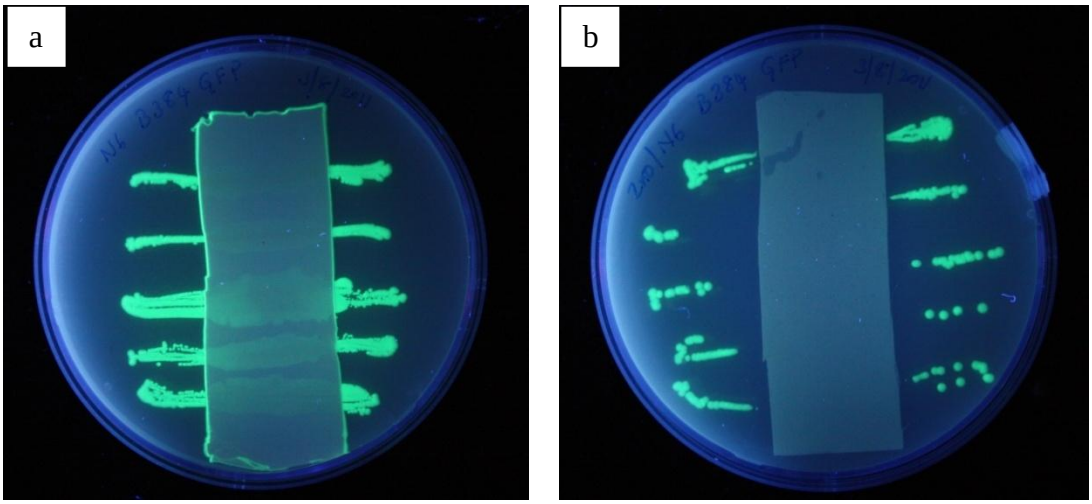

Figure 4.3 Agar plates with parallel streaks of green fluorescent protein (GFP) E.*coli* on: a) Nylon 6, and b) ZnO/Nylon 6 nanofiber mats.

Quantitative antibacterial assessments were carried out using both gram negative *E. coli* and gram positive *B. cereus* bacteria. Table 4.2 shows the concentrations (CFU/ml) of bacterial suspensions after being treated with Nylon 6 and ZnO/Nylon 6 nanofiber mats for 24 hours. The initial bacterial concentrations were 10^7 CFU/ml. It is seen that with Nylon 6 nanofiber mats, the concentrations of both *E. coli* and *B. cereus* bacteria are not significantly different from the control populations. However, for the ZnO/Nylon 6 nanofiber mats, the number of

colony forming unit drops below the detection level, indicating that the ZnO/Nylon 6 nanofiber mats can effectively kill both gram negative and gram positive bacteria in 24 hours. The observed reduction in bacterial cell was greater than 4 log CFU/ml, which indicates that the ZnO/Nylon 6 nanofiber mats have an antibacterial efficiency of at least 99.99%.

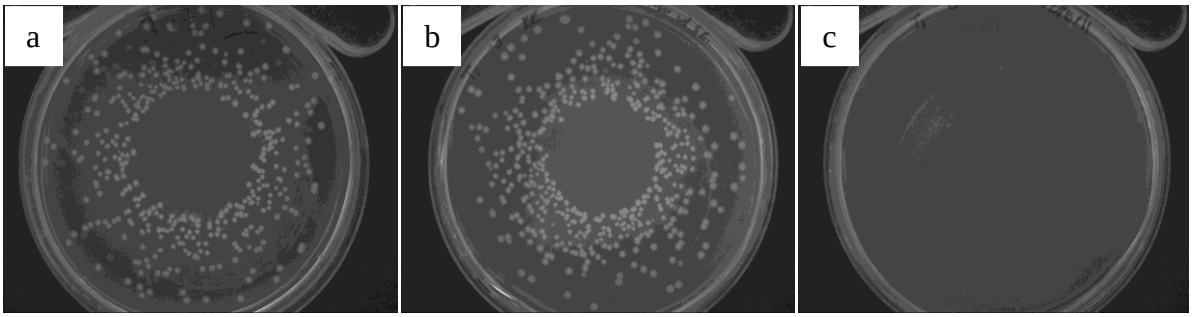

Figure 4.4 Agar plates of E.*coli* bacterial suspensions incubated for 24 hr: a) without nanofiber treatment, b) treated with Nylon 6 nanofiber mat, and c) treated with ZnO/Nylon 6 nanofiber mat.

Figure 4.4 shows the photographs of agar plates of *E. coli* bacterial suspensions exposed to Nylon 6 and ZnO/Nylon 6 nanofiber mats for 24 hrs. For comparison, the photograph of the control, which was not exposed to any nanofiber mat, is also shown. It is seen that *E. coli* bacterial colonies have spread throughout the control plate and the plate with Nylon 6 nanofiber mat, and the Q count reading showed 10^7 CFU/ml. However, for the plate containing ZnO/Nylon 6 nanofiber mat-treated bacterial suspension, the bacterial growth was less than the minimum detectable range by the Q count instrument. Similar results are can be seen from *B. cereus* testing plates, as shown in Figure 4.5.

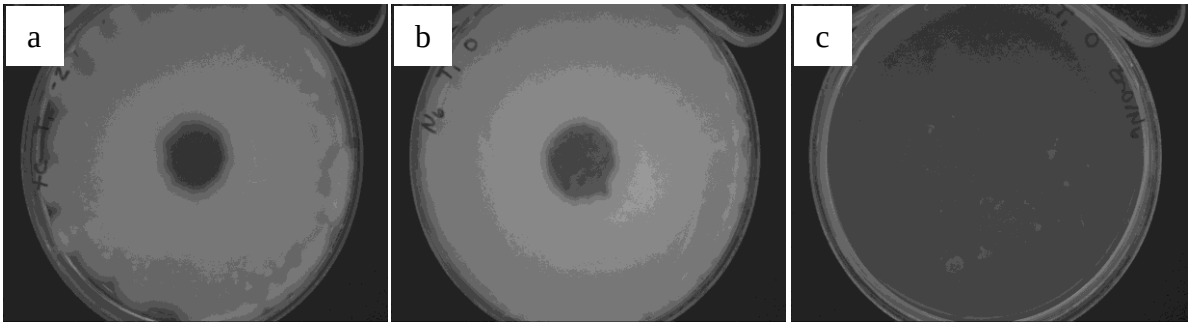

Figure 4.5 Agar plates of B.*cereus* bacterial suspensions incubated for 24 hr: a) without nanofiber treatment, b) treated with Nylon 6 nanofiber mat, and c) treated with ZnO/Nylon 6 nanofiber mat.

The antibacterial activity of ZnO/Nylon 6 nanofiber mats is due to the uniform presence of ZnO particles on the nanofiber surface. The antibacterial mechanism of ZnO particles has been studied and reported in literature.[12] J. Sawai et al.[13] reported that in atmospheric environment, the ZnO particles could release active oxygen species which lead to the generation of hydrogen peroxide (H_2O_2) in aqueous media. The H_2O_2 is capable of penetrating the bacterial cells, causing damage to the cell membranes and inhibiting the growth of or killing the bacteria. Other proposed mechanisms include release of Zn^{2+}, radical oxygen of superoxide or superoxide anions ($^{\bullet}O_2^-$), and hydroxyl radicals ($^{\bullet}OH$) by the ZnO slurry.[14-18] Of these, the most likely explanation for the antibacterial activity of ZnO/Nylon 6 nanofiber mats is the presence of active radical oxygen species of superoxide anion ($^{\bullet}O_2^-$) and their strong oxidizing interactions with bacterial cells.

4.3.3 Detoxification of toxic chemical agent

Figure 4.6 shows the area counts under the peaks of GC-MS spectra obtained for the paraoxon solutions exposed to Nylon 6 and ZnO/Nylon 6 nanofiber mats. Without any nanofiber mats, the GC-MS area count of the paraoxon solution is approximately 2 million units. That area count decreases slightly for solutions exposed to Nylon 6 nanofiber mat for 15 min, indicating a small decrease in the paraoxon concentration. This concentration decrease is mainly caused by the absorption of paraoxon into the high-surface area nanofiber mat. From Figure 4.6, it is also seen that exposing the solution to ZnO/Nylon 6 nanofiber mat can significantly reduce the paraoxon concentration. In 15 min, the GC-MS area count decreases from ~2 million to ~0.1 million, indicating a detoxification efficiency of approximately 95%. After 15 min, the paraoxon concentration does not change significantly. For comparison, the GC-MS area count of paraoxon solution exposed to pure ZnO powder for 60 min is also shown in Figure 4.6. It is seen that the paraoxon solution exposed to ZnO powder for 60 min shows a concentration reduction that is similar to solutions exposed to ZnO/Nylon 6 nanofiber mats. Therefore, it can be concluded that the exposure of ZnO nanoparticles on the nanofiber surfaces takes full advantage of their detoxifying capabilities.

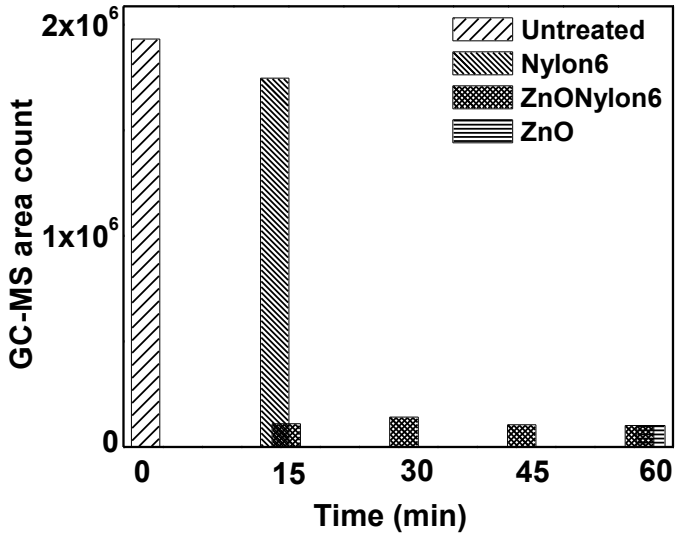

Figure 4.6 GC-MS area counts for paraoxon solutions treated with Nylon 6 nanofiber mat, ZnO/Nylon 6 nanofiber mat, and ZnO powder. For comparison, area count of the paraoxon solution without any treatment is shown at t = 0 min.

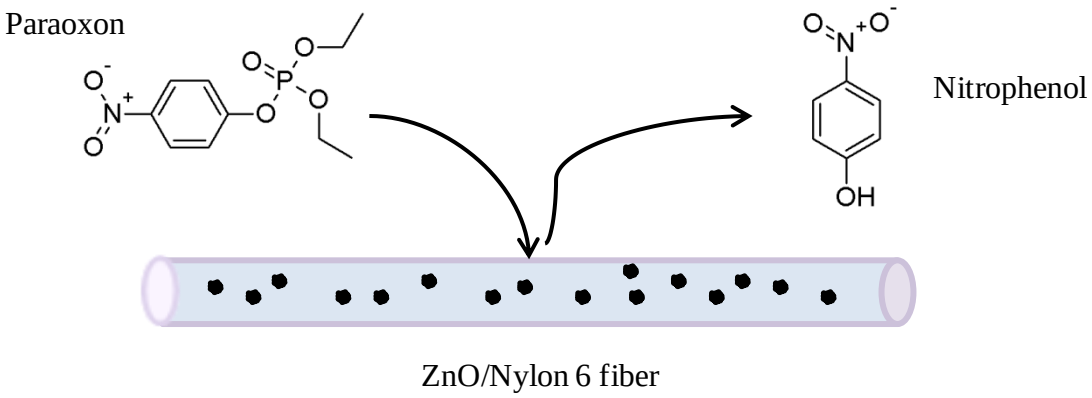

Figure 4.7 Possible detoxifying mechanism of paraoxon by ZnO/Nylon 6 nanofibers.

The detoxification reaction mechanism could be explained by dissociative chemisorptions of paraoxon by ZnO particles. Shyamala Rajagopalan et al.[19] proposed a destructive adsorption mechanism in which paraoxon is catalyzed by a metal oxide, which leads to the breakage of

P-O bonds. Figure 4.7 shows the possible detoxification reaction of paraoxon by a ZnO/Nylon nanofiber. Since ZnO particles are exposed on the fiber surface, they can access the paraoxon molecules and detoxify them by breaking the P-O bonds to form less harmful nitro-phenol.

4.3.4 Air permeability and MVTR

The air permeability and MVTR values are considered to be important parameters of electrospun nanofiber mats for many applications.[20, 21]

Table 4.3 Moisture vapor transmission rate (MVTR) and air permeability values of Nylon 6 and ZnO/Nylon 6 nanofiber mats.

Sample	Nanofiber mat areal density (g/m^2)	MVTR (g/m^2/24hrs)	Air permeability (ft^3air/ft^2-min)
Control substrate fabric	0	647 ± 17	3.55 ± 0.02
Nylon 6 nanofiber mat	3.59 ± 0.06	649 ± 34	2.97 ± 0.02
ZnO/Nylon 6 nanofiber mat	3.80 ± 0.21	654 ± 28	2.78 ± 0.02

For example, in protective clothing, electrospun nanofiber mats are typically deposited onto traditional textile fabrics to provide antibacterial and/or detoxifying functions. In this case, high air permeability and good moisture vapor transmission behavior are necessary for keeping the wearers comfortable and healthy. To further examine the feasibility of using ZnO/Nylon 6 nanofiber mats in protective applications, they were deposited onto woven

Nylon/Cotton fabrics and the air permeability and MVTR values of the deposited fabrics were evaluated. Table 4.3 compares the air permeability and MVTR values obtained for the control fabric substrate and fabrics deposited with Nylon 6 and ZnO/Nylon 6 nanofiber mats. It is seen that the control fabric and the fabric coated with Nylon 6 nanofiber mat have comparable MVTR values, which indicates that the deposition of Nylon 6 nanofiber mats does not alter the moisture vapor transmission through the fabric structure. This may be due to the small fiber diameter and high porosity of the electrospun nanofiber mat. In addition, depositing a ZnO/Nylon nanofiber mat onto the fabric leads to insignificant increase in MVTR. Therefore, the presence of ZnO particles on electrospun fiber surface does not significantly affect the transmission of water vapor across the mat. From Table 4.3, it is also seen that depositing Nylon 6 and ZnO/Nylon 6 nanofiber mats onto the fabric only slightly reduces the air permeability. However, the resultant total air permeability is still in acceptable range for practical applications.[22]

4.4 Summary

ZnO/Nylon 6 nanofiber mats were prepared by the electrospinning-electrospraying hybrid process. The nanofiber mat structure characterization suggests that ZnO particles are distributed on the nanofiber surfaces. The capabilities of ZnO/Nylon 6 nanofiber mats to kill bacteria and detoxify chemical agents were evaluated. It was found that these ZnO/Nylon 6 nanofiber mats showed powerful antibacterial activity against gram negative E.*coli* and gram

positive B.*cereus* pathogens with efficiencies over 99.99%. They also exhibited good detoxifying ability against paraoxon, a simulant of toxic chemicals, with detoxification efficiency over 95%. To further examine the feasibility of using ZnO/Nylon 6 nanofiber mats in protective applications, they were deposited onto woven Nylon/Cotton fabrics, and it was found that the air permeability and MVTR values of nanofiber mat-deposited fabrics are acceptable for practical uses. Therefore, ZnO/Nylon 6 nanofiber mats prepared by the electrospinning-electrospraying hybrid process have effective antibacterial and detoxifying functions without sacrificing air permeability and MVTR values, which are highly desirable in protective applications.

4.5 References

1. N. Vitchuli, Q. Shi, J. Nowak, M. McCord, M. Bourham, X. Zhang, Electrospun ultrathin nylon fibers for protective applications, *J Appl Polym Sci* 2010, **116,** 2181.
2. M. Eskandari, N. Haghighi, V. Ahmadi, F. Haghighi, SH.R Mohammadi, Growth and Investigation of Antifungal Properties of ZnO Nanorod Arrays on the Glass, *Physica B*, 2011 **406**, 112.
3. J. Rodriguez, F. Paraguay-Delgado, A. López, J. Alarcón, W. Estrada, Synthesis and Characterization of ZnO Nanorod Films for Photocatalytic Disinfection of Contaminated Water, *Thin Solid Films,* 2010, **519,** 729.
4. Y. Liu, C.R. Gorla, S. Liang, N. Emanetoglu, Y. Lu, H. Shen, M. Wraback, Ultraviolet Detectors Based on Epitaxial ZnO Films Grown by MOCVD, *J Electron Mater* 2000, **29,** 69.
5. J. Sawai, S. Shoji, H. Igarashi, A. Hashimoto, T. Kokugan, M. Shimizu, H.Kojima, Hydrogen Peroxide as an Antibacterial Factor in Zinc Oxide Powder Slurry, *J Ferment Bioeng,* 1998, **86,** 521.
6. G. K. Prasad, T. H. Mahato, Beer Singh, K. Ganesan, P. Pandey, K. Sekhar, Detoxification Reactions of Sulphur Mustard on the Surface of Zinc Oxide Nanosized Rods, *J.Hazard.Mater.,* 2007, **149,** 460.
7. Shu-Cai Li, Bang LiZong-Jie Qin, The Effect of the Nano-ZnO Concentration on the Mechanical, Antibacterial and Melt Rheological Properties of LLDPE/Modified Nano-ZnO Composite Films, *Polym.Plast.Technol.Eng.*, 2010, **49,** 1334.

8. F.M. Menger, M.J.Rourk, Deactivation of Mustard and Nerve Agent Models via Low-Temperature Microemulsions, *Langmuir*, 1999, **15** (2) 309.
9. M. Ehling-Schulz, M. Fricker, H. Grallert, P. Rieck, M. Wagner, S. Scherer, Cereulide synthetase gene cluster from emetic *Bacillus cereus*: Structure and location on a mega virulence plasmid related to *Bacillus anthracis* toxin plasmid pXO1, *BMC Microbiol*, 2006, **6**:20
10. E. Marsano, L. Francis, F. Giunco, Polyamide 6 Nanofibrous Nonwovens via Electrospinning, *J Appl Polym Sci*, 2010, **117,** 1754.
11. S.S. Ojha, M. Afshari, R. Kotek, R.E. Gorga, Morphology of electrospun nylon-6 nanofibers as a function of molecular weight and processing parameters, Journal of Applied Polymer Science, 2008, **108**, 308.
12. J. Sawai, E. Kawada, F. Kanou, H. Igarashi, A. Hashimoto, T. Kokugan, M. Shimizu, Detection of Active Oxygen Generated from Ceramic Powders having Antibacterial Activity, *J.Chem.Eng.Japan,* 1996, **29,** 627.
13. J. Sawai, Quantitative Evaluation of Antibacterial Activities of Metallic Oxide Powders (ZnO, MgO and CaO) by Conductimetric Assay, *J.Microbiol.Methods,* 2003, **54,** 177.
14. T. Ohira, O. Yamamoto, Y. Iida, Z. Nakagawa, Antibacterial Activity of ZnO Powder with Crystallographic Orientation, *Journal of Materials Science-Materials in Medicine,* 2008, **19,** 1407.
15. L. Zhang, Y. Jiang, Y. Ding, N. Daskalakis, L. Jeuken, M. Povey, A.J. O'Neill, D.W.York, Mechanistic Investigation into Antibacterial Behaviour of Suspensions of ZnO Nanoparticles Against E. Coli, *Journal of Nanoparticle Research*, 2010, **12,** 1625.

16. G. Applerot, A. Lipovsky, R. Dror, N. Perkas, Y. Nitzan, R. Lubart, A. Gedanken, Enhanced Antibacterial Activity of Nanocrystalline ZnO due to Increased ROS-Mediated Cell Injury, *Advanced Functional Materials,* 2009, **19,** 842.
17. L.K. Adams, D.Y. Lyon, P. J. Alvarez, Comparative Eco-Toxicity of Nanoscale TiO2, SiO2, and ZnO Water Suspensions, *Water Res.,* 2006, **40,** 3527.
18. Y. Liu, L. He, A. Mustapha, H. Li, Z.Q. Hu, M.Lin Antibacterial Activities of Zinc Oxide Nanoparticles Against Escherichia Coli O157:H7, *J. Appl.Microbiol.,* 2009, **107,** 1193.
19. S. Rajagopalan, O. Koper, S. Decker, K.J. Klabunde, Nanocrystalline Metal Oxides as Destructive Adsorbents for Organophosphorus Compounds at Ambient Temperatures, *Chem. Eur. J.* 2002, **8** (11), 2602.
20. P. W. Gibson. , Factors Influencing Steady-State Heat and Water-Vapor Transfer Measurements for Clothing Materials, *Text.Res.J.,* 1993, **63,** 749.
21. J. C. Gretton, D. B. Brook, H. M. Dyson, S. C. Harlock. , Moisture Vapor Transport through Waterproof Breathable Fabrics and Clothing Systems Under a Temperature Gradient, *Text. Res. J.,* 1998, **68,** 936.
22. S. Mavruz, R.T. Ogulata Investigation of air permeability of single jersey fabrics with different relaxation states, Journal of the Textile Institute, 2011, **102** (1), 57.

CHAPTER 5

Atmospheric Plasma Application to Improve Adhesion of Electrospun Nanofibers onto Protective Fabric

Atmospheric Plasma Application to Improve Adhesion of Electrospun Nanofibers onto Protective Fabric

Abstract

Nylon 6 electrospun nanofibers were deposited on plasma-pretreated woven fabric substrates with the objective of improving adhesion between them. The prepared samples were evaluated for adhesion strength and durability of nanofiber mats by carrying out peel strength, flex resistance and abrasion resistance tests. The test results showed significant improvement in the adhesion of nanofiber mats on woven fabric substrates due to atmospheric plasma pretreatment. The samples also exhibited good flex and abrasion resistance characteristics. XPS and water contact angle analyses indicate that plasma pretreatment introduces radicals, increases the oxygen content on the substrate surface, and leads to formation of active chemical sites that may be responsible for enhanced cross-linking between the substrate fabric and the electrospun nanofibers, which in turn increases the adhesion properties. The work demonstrates that the plasma treatment of the substrate fabric prior to deposition of electrospun nanofiber mats is a promising method to prepare durable functional materials.

Keywords: Adhesion, atmospheric pressure plasma, cross-linking, dielectric barrier discharge, electrospinning, water contact angle.

5.1 Introduction

Electrospinning technique is widely used to produce ultra-fine fibrous mat structures from many different polymers and the resultant nanofiber mats have found various applications including filtration, tissue engineering, catalytic reaction materials, electrochemical electrodes, affinity membranes, and nano-composites.[1,2] However, electrospun nanofiber mats are inherently weak, and they are often deposited on mechanically-strong substrates such as porous woven fabrics that can provide good structural support without altering the nanofiber characteristics.[3, 4] One major challenge of this approach is to ensure good adhesion of nanofiber mats onto the substrates and satisfactory durability of nanofiber mats against flexion and abrasion during practical use.

Atmospheric plasma treatment of polymer surfaces is an environmentally friendly process as compared to conventional chemical treatments.[5, 6] Plasma consists of highly active charged species; electrons, ions and radicals, and can create highly unusual environments to interact with material surfaces. Plasma treatment of polymer materials results in surface modification through various functionalizations such as etching, deposition, chain scission, and cross-linking.[7-12]

Plasma treatment has been used for: *i*) modifying the surface hydrophobic or hydrophilic characteristics,[13, 14] *ii*) etching and nano-texturing of polymer surfaces,[15-18] and *iii*) improving polymer mechanical properties depending on treatment conditions.[19] In addition,

plasma treatment has also been used to introduce various surface functional groups,[20-23] and improve surface bonding or adhesion of coatings onto various polymer materials.[24-32] In this work, plasma pretreatment of fabric substrates was investigated as a mechanism for improvement of adhesion and durability of nanofiber mats against flexion and abrasion.

5.2 Experimental

5.2.1. Materials

Nylon 6 pellets and 2, 2, 2-tri-fluoro ethanol (TFE) were purchased from Sigma-Aldrich and the reagents were used without further purification. Nylon 6,6/Cotton (50/50) woven fabric (mass per unit area 240 g/m^2) was acquired from Milliken & Company, USA. Nylon 6,6 (0.025 mm thickness) and Cellophane (0.031 mm thickness) films were purchased from Goodfellow Corporation, USA.

5.2.2. Atmospheric Plasma Pretreatment of Fabric Substrate

Prior to the deposition of electrospun nanofibers, the Nylon/Cotton fabric samples were treated in an atmospheric pressure audio frequency dielectric barrier discharge (DBD) plasma system (as illustrated in Figure 5.1), which was designed, manufactured and upgraded at North Carolina State University.[6] The plasma system consists of two parallel copper electrodes, each is embedded in a Lexan polycarbonate insulator. Stable and uniform plasma was achieved at a low frequency of 1.373 kHz during the operation. Either 100% helium (He) or mixture of 99% helium/1% oxygen (He-O_2) was used as plasma carrier gas. The gas

flow was 20 L/min for He and 0.3 L/min for O_2, respectively, which provide the 1% oxygen inclusion in the helium flow with the inclusion of the gas factor in the flow controller's calibration setup. The voltage across the electrode plates was maintained at 6.3 and 7.6 kVmax for the He plasma and 6.6 and 7.85 kVmax for the He-O_2 plasma. The fabric samples were placed on a nylon grid inside the test cell suspended in the middle of the plasma system to ensure complete and uniform exposure to plasma. The fabric samples were treated with either He plasma or He-O_2 plasma for 5 minutes, followed immediately by use as substrates for deposition of electrospun nanofiber mats.

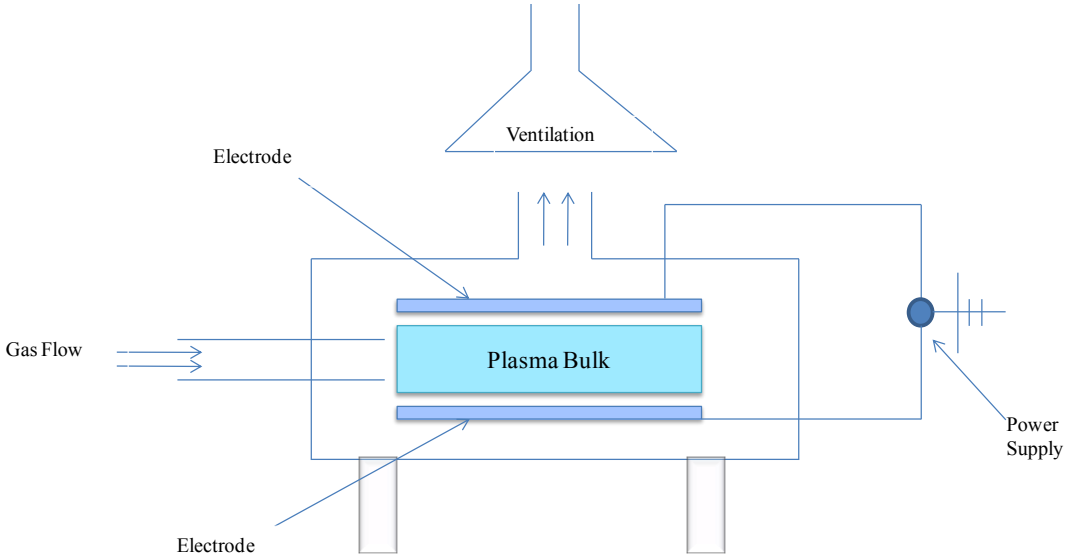

Figure 5.1 Schematic of atmospheric pressure plasma system.

5.2.3. Deposition of Nanofibers by Electrospinning

Nylon nanofibers were deposited onto plasma-pretreated fabric samples by the electrospinning process. The electrospinning set-up consists of a syringe pump, a rotating drum collector, and a high-voltage power supply (Figure 5.2). The plasma-treated fabric samples placed on aluminum foil were carefully fastened to the drum collector. The electrospinning syringe was filled with Nylon 6 solution (12 wt%) in TFE and placed in the pump. The pump feed rate was maintained at 1 ml/hr, the electrospinning voltage was 15 kV, and the needle-tip-to-collector distance was 15 cm. During electrospinning, the rotating speed of the drum collector was maintained at 20 rpm. For comparison, untreated fabric samples were also deposited with Nylon 6 nanofibers under the same conditions.

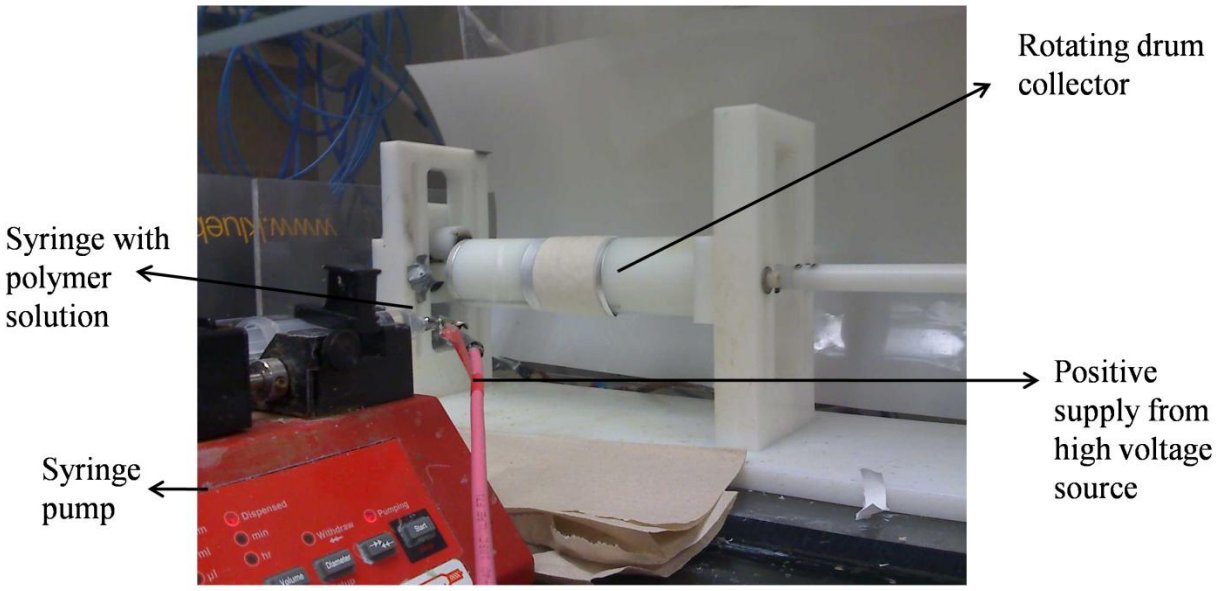

Figure 5.2 Electrospinning setup for depositing nanofiber mat onto fabric substrate.

5.2.4. Solution and Fiber Mat Characterizations

The zero shear viscosity of Nylon 6 solution was measured using a rheometer (StressTech HR, Rheologica Instruments AB) at 25 °C with the assistance of rheoExplorer V5 operating software. The ionic conductivity of Nylon 6 solution was measured using Orion model 164 conductivity meter (Orion Research Inc., Boston, MA). The morphology of the deposited Nylon 6 nanofiber mats was examined using JEOL JSM-6400F Field Emission Scanning Electron Microscopy (FESEM) (JEOL Ltd., Tokyo, Japan) at an accelerating voltage of 5 kV. The average fiber diameter was obtained by measuring the diameters of 100 nanofibers using the Revolution software provided by 4pi Analysis.

5.2.5. Water Contact Angles of Nylon 6,6 and Cellophane Films

To investigate the effect of plasma on the fabric surface, water contact angles (WCAs) were measured using Nylon 6,6 and Cellophane films as the model materials. The films (3 cm × 3 cm) were thoroughly washed in acetone for 30 minutes and dried. The films were treated using either He or He-O_2 plasma for 5 minutes. The untreated, He plasma-treated and He-O_2 plasma-treated samples were subjected to WCA measurement using an OCA 15 Plus Contact Angle Measuring Device (DataPhysics Instruments, GmbH). During the measurement, a 5 µL distilled water droplet was injected onto the film surface using a computer-aided micro-liter syringe. After 30 seconds, the WCA was measured using an optical microscope. The images of water droplets on film surfaces were also recorded. For each sample, at least 10

readings were taken at different spots using multiple specimens, and average WCA values including standard deviations were calculated.

5.2.6. XPS Analyses of Nylon 6,6 and Cellophane Films

Plasma treated Nylon 6 nanofibers, Nylon 6,6 films and Cellophane films were subjected to X-Ray Photoelectron Spectroscopy (XPS) analyses to investigate the changes in surface chemical composition before and after plasma treatment. The analyses were carried out using Axis Ultra (Kratos Analytical Ltd, UK) instrument. A mono-chromated Al K-alpha ray with 150W power was used and energy calibration was established by referencing to adventitious Carbon C1s (binding energy 284.5 eV). The work pressure in the analysis chamber was in the 2×10^{-8} Torr range. CASA XPS software was used for data analysis.

5.2.7. Adhesion Strengths of Nanofiber-Deposited Fabrics

The adhesion strength between electrospun fiber mat and fabric substrate was estimated by a peel test method based on ASTM 2261 *Standard Test Method for Tearing Strength of Fabrics by the Tongue Procedure* using an Instron® Tensile Tester. The peel test method allows the user to control the rate of nanofiber mat de-lamination from the fabric substrate and to estimate the adhesion strength in gram force (gf). During testing, the nanofiber mat (dimension: 50 mm × 10 mm, deposition time: 10 mins) was held by the movable grip of the Tensile Tester and the fabric substrate held by the stationary grip. To facilitate proper peeling and avoid grip slippage, short tapes were attached to the nanofiber mat and fabric substrate. These tapes were held by Instron tensile tester grips as shown in Figure 5.3. A 50

gm load cell was used to detect the maximum load required to remove the nanofiber mat from the fabric surface at a constant rate of 50 mm/min, using a 0.5 inch gauge length. The adhesion strength was estimated in terms of gram force and the average value of 20 test specimens was reported. Prior to testing, the nanofiber-deposited fabric samples were conditioned at standard temperature of 20 ± 1°C and relative humidity of 65 ± 2 % for at least 8 hours.

(a) (b)

Figure 5.3 Adhesion strength measurement between nanofiber mat and fabric; a) Nanofiber mat and fabric with short tape attached b) sample held in Instron instrument grips.

5.2.8. Flex Durability of Nanofiber-Deposited Fabrics

A Gelbo Flex test was conducted based on ASTM F392-93 *Standard Test Method for Flex Durability of Flexible Barrier Materials* in order to assess the durability of adhesion of the electrospun mat to the fabric substrate. Figure 5.4 shows a typical IDM Gelbo Flex Tester (IDM Instruments Ltd®). Nanofiber-deposited fabric samples (dimension: 50 mm × 10 mm; deposition time: 10 mins) were attached to the two circular clamping disks via hose clamps, and the samples were twisted and flexed for 1000 cycles. A qualitative assessment of adhesion was determined by observation of the electrospun nanofiber mat/fabric substrate interface via SEM. Prior to testing, the nanofiber-deposited fabric samples were conditioned at standard temperature of 20 ± 1°C and relative humidity of 65 ± 2 % for at least 8 hours.

Figure 5.4 Gelbo Flex Tester for evaluating the Flex durability of nanofiber mats deposited on fabric substrate.

5.2.9. Abrasion Resistance of Nanofiber-Deposited Fabrics

The abrasion resistance of nanofiber-deposited fabrics was evaluated on a Nu-Martindale test instrument (James H.Heal & Co Ltd, Halifax, England, UK) by using a modified ASTM D 4966-98 *Standard Test Method for Abrasion Resistance of Textile Fabrics*. Prior to testing, the prepared samples were conditioned at standard temperature of 20 ± 1°C and relative humidity of 65 ± 2 % for at least 8 hours. The nanofiber-deposited fabrics were cut to circular shapes (diameter: 38 mm) and were loaded on sample holders (Figure 5.5a). The sample holders were then placed face-down on an abrading worsted wool fabric surface using a spindle inserted through the instrument's top plate, as shown in Figure 5.5b.

(a) (b)

Figure 5.5 Nu-Martindale test instrument for evaluating abrasion resistance of nanofiber mats deposited on fabric substrate. (a) Abrasion test sample holder with sample loaded, and (b) overview of the abrasion test.

The combined weight of the specimen holder and spindle was 200 grams, which was equivalent to 17 cN/cm^2 of applied pressure on the specimen during testing. The top-plate of the Martindale instrument moved in the horizontal plane, driven by two reciprocating

mechanisms acting at right-angles to each other, and the resulting complex motion carried the test specimens in a constantly changing pattern across the abrading surfaces. The abrasion properties of nanofiber-deposited fabrics are represented by average numbers of rubbing cycles required to completely rupture the nanofiber mats.

5.3 Results and Discussion

5.3.1. Solution and Fiber Mat Characterizations

Table 5.1 shows the zero shear viscosity and ionic conductivity of 12 wt% Nylon 6 in TFE. The solution viscosity measured was 0.2 Pa·s and ionic conductivity was 3.1 μS/cm. The values are in the ranges that can produce a stable electrospinning process and lead to desirable nanofiber structure.[33, 34]

Table 5.1 Zero shear viscosity and ionic conductivity of Nylon 6 solution.

Polymer solution	Zero shear viscosity (Pa·s)	Ionic Conductivity (μs/cm)
Nylon 6 in TFE (12 wt %)	0.2	3.0 ± 0.1

Figure 5.6 shows a typical SEM image of Nylon 6 nanofibers electrospun directly on Nylon/Cotton fabric. It can be observed that the fibers have smooth surface texture and the fiber diameter was estimated to be 230 ± 40 nm. The nanofiber mat has random orientation

and a highly porous structure. These morphological characteristics are key factors in achieving high filtration efficiency with a low pressure drop across the nanofiber mat-deposited fabrics.[3]

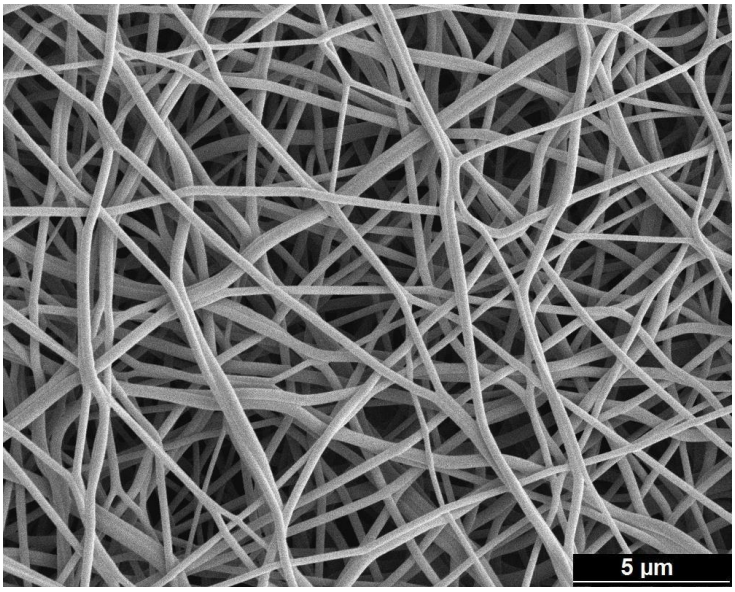

Figure 5.6 SEM micrograph of Nylon 6 nanofiber mat.

5.3.2. Water Contact Angles of Plasma-Treated Surfaces

Water contact angles (WCAs) were measured on plasma-treated surfaces to investigate the effect of plasma treatment on the surface characteristics. To avoid the complexity involved in surface characterization of Nylon/Cotton blend fabric and to analyze the actual effect on individual components, Nylon 6,6 and Cellophane films were chosen as the model materials to represent the nylon and Cotton in the blend fabric.

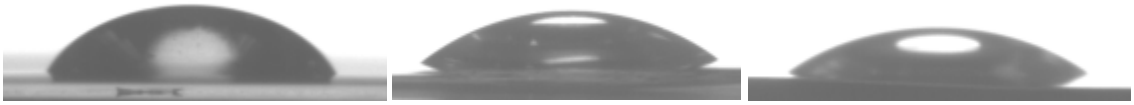

Untreated He plasma-treated He-O_2 plasma-treated

Figure 5.7 Photographs of water droplets on untreated and plasma-treated Nylon 6,6 films.

The photographs in Figure 5.7 show the water droplets on untreated and plasma-treated Nylon 6,6 films. The measured WCA values are shown in Table 5.2. The untreated Nylon 6,6 film has an average WCA of 58.1°. After He or He-O_2 plasma treatment, the average WCAs reduced to 39.6° and 41.6°, respectively.

Table 5.2 Water contact angles (^{o}) on untreated and plasma-treated Nylon 6,6 and Cellophane films.

Film substrate	Control	He Plasma	He-O_2 Plasma
Nylon 6,6	58.1 ± 3.7	39.6 ± 5.3	41.6 ± 3.9
Cellophane	0.0	0.0	0.0

The changes on WCAs confirm that the plasma treatment changes the surface characteristic of Nylon 6,6. Similar change is expected in the nylon component of the Nylon/Cotton blend fabric. Unlike Nylon 6,6, both untreated and plasma-treated Cellophane films were completely wetted within 30 seconds after placing the water droplets on them, and hence their WCAs are always zero (Table 5.2).

5.3.3. XPS Analyses of Nylon 6,6 and Cellophane Films

The elemental composition data and relative surface chemical bonds (%) of Nylon 6,6 films obtained from XPS analyses are reported in Tables 5.3 and 5.4, respectively. The elemental composition data suggest plasma treatment of films leads to increase in surface oxygen content. This might be due to radical creation and subsequent oxygen group formation on the surface of the films during atmospheric pressure plasma treatment. The relative surface chemical bond composition and C1s spectra of Nylon 6,6 films (Figure 5.8 and Table 5.4) suggest that plasma treatment significantly increases the C-O and CONH bonds, which could cause an increase in surface hydrophilic characteristic of the film. This trend was in agreement with the WCA value decrement trend of Nylon 6,6 films discussed in the previous section.

Cellophane film is composed of cellulose, which has high contents of C-OH and C-O-C surface chemical groups and hence makes it inherently hydrophilic. The elemental analysis of the plasma-treated Cellophane films (Tables 5.5 and 5.6) suggest significant increases in surface oxygen content. The C1s spectra of Cellophane films (Figure 5.9) confirms the formation of C=O and COOH groups.

Table 5.3 Elemental composition data of Nylon 6,6 films obtained from XPS analysis.

Nylon 6,6 film	C %	O %	N %	O/C	N/C
Untreated	78.39	10.66	10.95	0.14	0.14
He plasma	73.98	15.39	10.64	0.21	0.15
He-O_2 plasma	74.24	15.10	10.66	0.21	0.15

Table 5.4 Relative surface chemical bonds (%) on Nylon 6,6 film.

Nylon 6,6 film	C-C (284.5 eV)	C-N (285.4 eV)	C-O (286.5 eV)	CONH (287.5 eV)
Untreated	36.7	45.8	-	17.4
He plasma	31.2	39.4	5.6	23.8
He-O_2 plasma	60.2	17.4	2.1	20.3

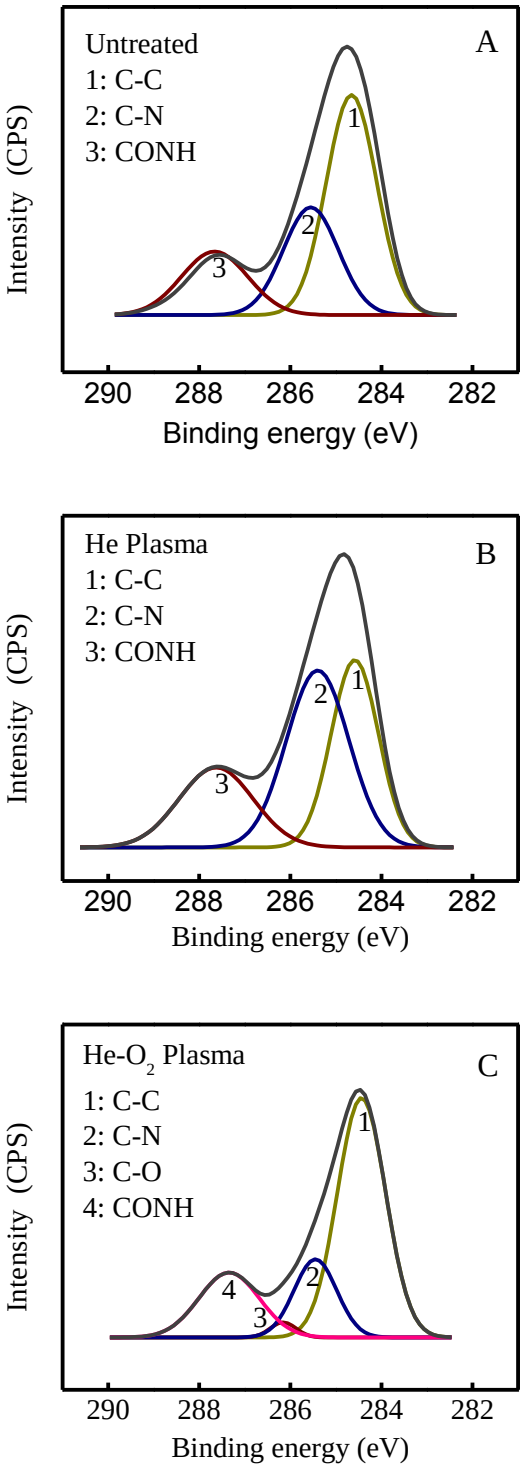

Figure 5.8 C1s spectra of Nylon 6 6 films: a) untreated, b) He plasma-treated, and c) He-O_2 plasma-treated.

Table 5.5 Elemental composition data of Cellophane films obtained from XPS analysis.

Cellophane film	C %	O %	O/C
Untreated	59.16	40.84	0.69
He plasma	57.09	42.91	0.75
He-O_2 plasma	55.78	44.22	0.79

Table 5.6 Relative surface chemical bonds (%) of Cellophane film.

Cellophane film	C-C (284.5 eV)	C-OH (286.2 eV)	C-O-C (287.2 eV)	C=O (287.6 eV)	COOH (288.5 eV)
Untreated	13.4	51.6	35.0	-	-
He plasma	3.1	49.4	43.1	4.4	-
He-O_2 plasma	4.4	70.9	22.2	-	2.5

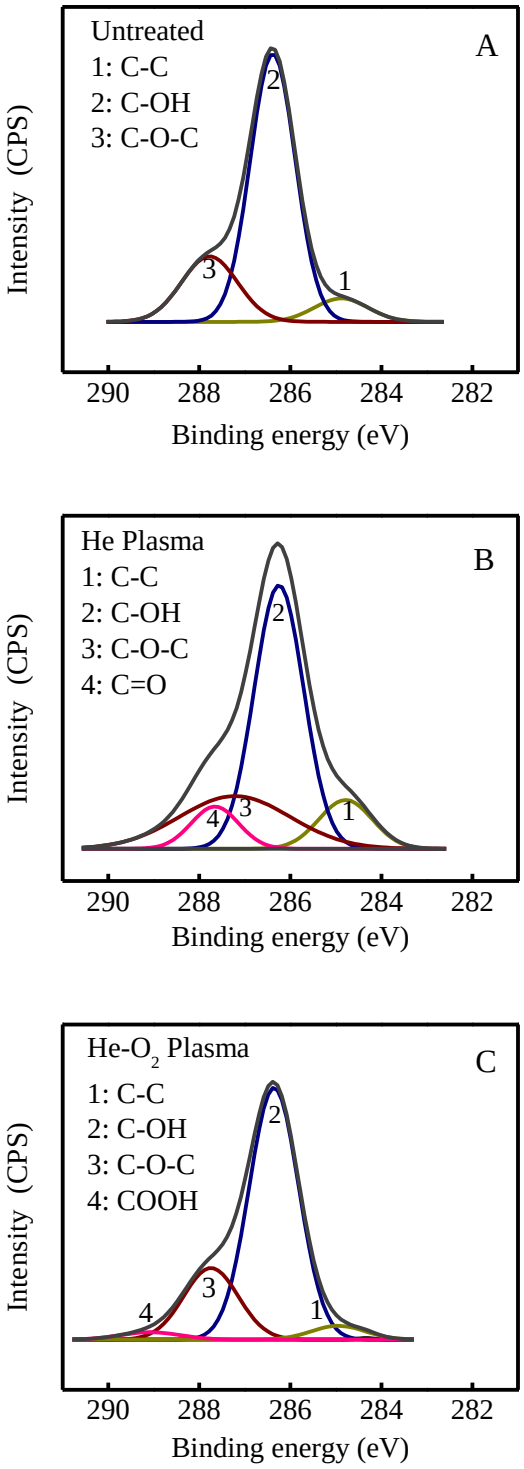

Figure 5.9 C1s spectra of Cellophane films: a) untreated, b) He plasma-treated, and c) He-O_2 plasma-treated.

5.3.4. Adhesion Strength

Table 5.7 shows the average adhesion strengths between electrospun Nylon 6 nanofiber mats and the Nylon/Cotton fabrics. It is seen that the average adhesion strengths of samples prepared with plasma-treated fabrics are higher than those prepared with untreated fabric. To verify the significance of improved adhesion strength values, a T-test was performed (95% confidence interval), and the results are also shown in Table 5.7. The T-test significances (*i.e.*, p values) for both He and He-O_2 treatments are less than 0.05. Therefore, the increases in adhesion strength caused by plasma treatment are statistically significant. This indicates that the radicals and active chemical species in the plasma interact with the fabric substrate to generate active surface sites, which help improve the bonding with the deposited nanofiber mats through possible chemical cross-linking with the substrate fabric.

Table 5.7 Adhesion strengths between Nylon/Cotton fabric and deposited nanofiber mats.

Fabric substrate	Adhesion strength (gf)	T-test significance (p value)
Untreated fabric	1.51 ± 0.3	-
He plasma-treated	2.84 ± 0.6	0.00006
He-O_2 plasma-treated	2.86 ± 0.5	0.00270

5.3.5. Repetitive Flex Resistance

Figure 5.10 shows the SEM images of Nylon 6 nanofiber-deposited Nylon/Cotton fabrics before and after Gelbo flex testing. When deposited on untreated fabric, the deposited nanofiber mat is almost completely destroyed after 1000 cycles (Figure 5.10b). However, when the nanofibers were deposited on He and He-O_2 plasma-treated fabrics, the nanofiber mats

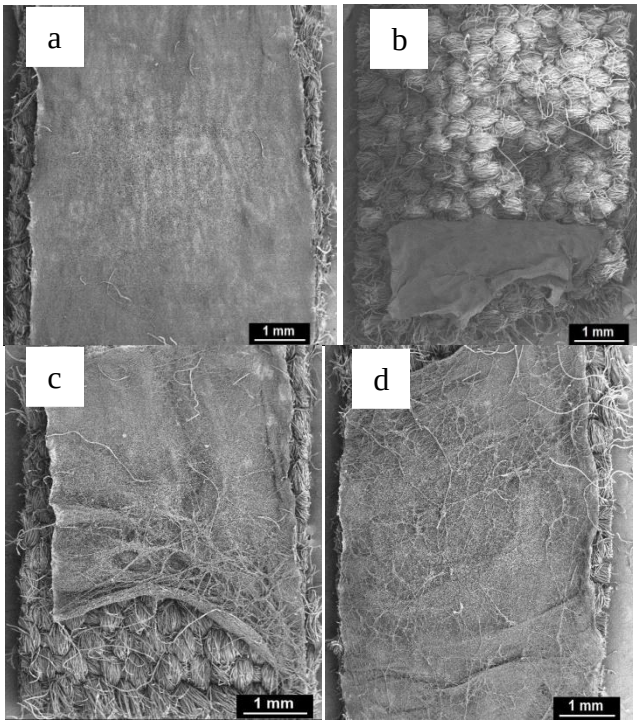

Figure 5.10 SEM micrographs of a) Nylon 6 nanofiber mat deposited on untreated Nylon/Cotton fabric before Gelbo flex test; b) Nylon 6 nanofiber mat deposited on untreated Nylon/Cotton fabric after Gelbo flex test; c) Nylon 6 nanofiber mat deposited on He plasma-treated Nylon/Cotton fabric after Gelbo flex test; and d) Nylon 6 nanofiber mat deposited on He-O_2 plasma-treated Nylon/Cotton fabric after Gelbo flex test.

showed better resistance to flex and they remained largely intact on the fabrics (Figures 5.10c and d). This indicates that the plasma treatment is effective in improving the adhesion and durability of nanofiber mats deposited on fabric surfaces.

5.3.6 Abrasion Resistance

Figure 5.11 shows photographs of a Nylon 6 nanofiber mat deposited on untreated Nylon/Cotton fabric after increasing cycles of rubs against standard abrading worsted wool fabric. It is seen that after 10 rubbing cycles, the nanofiber mat has a small aperture at the top left corner. After 20 cycles, the deterioration propagates and the aperture in the nanofiber mat is enlarged significantly. Complete damage of the nanofiber mat is observed after 30 cycles.

(a) (b) (c)

Figure 5.11 Photographs of Nylon 6 nanofiber-deposited untreated Nylon/Cotton fabric: (a) 10 rubs, damage initiated; (b) 20 rubs, half-damaged; (c) 30 rubs, completely damaged.

Figures 5.12 and 5.13 show the photographs of Nylon 6 nanofiber mats deposited on He plasma-treated and He-O_2 plasma-treated fabrics, respectively. Damages on the nanofiber mat can still be observed after 30 cycles. However, compared with Figure 5.9, it is seen that

the nanofiber mat on plasma-treated fabric has better abrasion resistance since more rubbing cycles are needed to damage the deposited nanofiber mats.

(a) (b) (c)

Figure 5.12 Morphology of Nylon 6 nanofiber-deposited He plasma-treated Nylon/Cotton fabric: (a) 30 rubs, damage initiated; (b) 50 rubs, half-damaged; (c) 60 rubs, completely damaged.

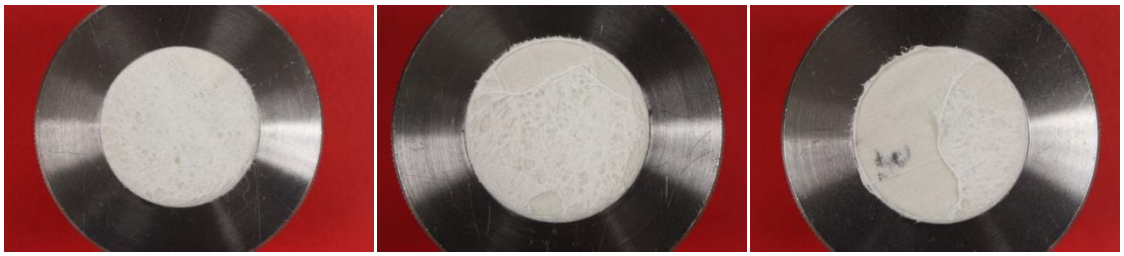

(a) (b) (c)

Figure 5.13 Morphology of Nylon 6 nanofiber-deposited He-O_2 plasma-treated Nylon/Cotton fabric: (a) 30 rubs, damage initiated; (b) 50 rubs, half-damaged; (c) 60 rubs, completely damaged.

Table 5.8 Abrasion resistance of nanofiber mats deposited on Nylon/Cotton fabrics.

Fabric substrate	Average rubbing cycles
Untreated fabric	28 ± 11
He plasma treated	64 ± 20
He-O_2 plasma treated	60 ± 16

Average numbers of rubbing cycles required to completely damage nanofiber mats are listed in Table 5.8 for untreated and plasma-treated fabrics. It can be seen that compared with nanofibers deposited on untreated fabrics, nanofibers deposited on plasma-treated fabrics can resist more than twice the rub cycles prior to complete failure. Due to increased adhesion, the nanofiber mats deposited on plasma-treated fabrics can remain on the fabric surface for a longer time during rubbing action and offer better resistance against the formation of tucks or ridges and subsequent apertures. In summary, the abrasion resistance of the nanofiber mats deposited on Nylon/Cotton 50:50 fabrics can be significantly improved by plasma pretreatment of the substrate fabrics.

5.4 Summary

Electrospun Nylon 6 nanofiber mats were deposited onto untreated and plasma-treated Nylon/Cotton fabric substrates. Two types of plasmas (*i.e.*, He and He-O_2) were used in this work. The adhesion strengths between nanofiber mats and fabric substrates were evaluated by a modified peel test. The results showed that the samples prepared with plasma-treated fabric substrates have higher adhesion strengths. The He-O_2 plasma showed slightly higher effectiveness in improving the adhesion strength than pure He plasma. In addition to the peel test, the samples were also subjected to Gelbo flex resistance and abrasion resistance tests. The results indicated improved flex resistance and abrasion resistance for samples prepared with plasma-treated fabric substrate. The effect of plasma treatment on polymer material was studied using Nylon 6,6 and Cellophane films as model substrates. The plasma-treated films

showed a decrease in WCA values and increase in surface oxygen chemical groups, which confirm the interaction of plasma species with the substrate surfaces, the formation of radicals, and subsequent introduction of active chemical groups. These active chemical groups might have led to the formation of crosslink bonds between fabric substrate and nanofiber mats. In summary, it was demonstrated that the plasma pretreatment of polymer fabrics increased the adhesion of deposited nanofiber mats. In future work, efforts will be made to plasma-treat electrospun nanofiber mats to further improve their adhesion on fabric substrates.

5.5 References

1. T. Subbiah, G. S. Bhat, R. W. Tock, S. Parameswaran, S. S. Ramkumar, Electrospinning of nanofibers, *J. Appl. Polym. Sci.* 2005, **96**, 557.
2. K. M. Sawicka, and P. Gouma, Electrospun composite nanofibers for functional applications, *J. Nanopart. Res.* 2006, **8**, 769.
3. N. Vitchuli, Q. Shi, J. Nowak, M. McCord, M. Bourham, X. Zhang, Electrospun ultrathin nylon fibers for protective applications, *J Appl Polym Sci* 2010, **116,** 2181.
4. Y. Matalov-Meytal, and M. Sheintuch, Catalytic fibers and cloths, *Appl. Catal., A,* 2002, **231**, 1.
5. F. S. Denes, S. Manolache, Macromolecular plasma-chemistry: an emerging field of polymer science, *Prog Polym Sci*, 2004, **29**, 815.
6. Y. J. Hwang, J. S. An, M. G. McCord, S. W. Park, and B. C. Kang, Effects of Helium Atmospheric Pressure Plasma Treatment on Low-Stress Mechanical Properties of Polypropylene Nonwoven Fabrics, *Text. Res. J.* 2005, **75**, 771.
7. Y. J. Hwang, Y. Qiu, C. Zhang, B. Jarrard, R. Stedeford, J. Tsai, Y.C. Park, M. G. McCord, Effects of atmospheric pressure helium/air plasma treatment on adhesion and mechanical properties of aramid fibers, *J. Adhes. Sci. Technol.* 2003, **17**, 847.
8. M. G. McCord, Y. J. Hwang, P. J. Hauser, et al., Modifying Nylon and Polypropylene Fabrics with Atmospheric Pressure Plasmas, *Textile Research Journal*, 2002, **72,** 491.

9. Jun Young Kim, Yongbeom Lee, Dae Young Lim, Plasma-Modified Polyethylene Membrane as a Separator for Lithium-Ion Polymer Battery, *Electrochim.Acta*, 2009, **54,** 3714.
10. L. I. Kravets, S. N. Dmitriev, A. B. Gil'man, Modification of Properties of Polymer Membranes by Low-Temperature Plasma Treatment, *High Energy Chemistry*, 2009, **43,** 181.
11. Dixon T. K. Kwok, Liping Tong, Che Yan Yeung, C. G. dos Remedios, Paul K. Chu, Hybrid Plasma Surface Modification and Ion Implantation of Biopolymers, *Surf.Coat.Technol.*, 2010, **204,** 2892.
12. B. Eliasson, and U. Kogelschatz, Nonequilibrium Volume Plasma Chemical Processing, *IEEE Trans. Plasma Sci.* 1991, **19**, 1063.
13. M. G. McCord, Y. J. Hwang, Y. Qiu, L. K. Hughes, M. A. Bourham, Surface Analysis of Cotton Fabrics Fluorinated in Radio-Frequency Plasma, *J Appl Polym Sci*, 2003, **88,** 2038.
14. W. Ren, C. Cheng, R. Wang, X. Li, Effect of fiber surface morphology on the hydrophilicity modification of cold plasma-treated polypropylene nonwoven fabrics, *J. Appl. Polym. Sci.* 2010, **116**, 2480.
15. S. R. Matthews, Y. J. Hwang, M. G. McCord, M. A. Bourham, Investigation into Etching Mechanism of Polyethylene Terephthalate (PET) Films Treated in Helium and Oxygenated-Helium Atmospheric Plasmas, *J Appl Polym Sci*, 2004, **94,** 2383.

16. M. G. McCord, Y. Qiu, C. Zhang, Y. J. Hwang, B. Bures, The effect of atmospheric pressure helium plasma treatment on the surface and mechanical properties of ultrahigh-modulus polyethylene fibers, *Adhes. Sci. Technol.* 2002, **16**, 99.
17. Zhiqiang Gao, Jie Sun, Shujing Peng, Lan YaoYiping Qiu, Surface Modification of a Polyamide 6 Film by He/CF4 Plasma using Atmospheric Pressure Plasma Jet, *Appl.Surf.Sci.,* 2009, **256,** 1496.
18. A. Hollaender, S. Kroepke, Surface Modification with Pressure Pulse Plasmas, *Plasma Process. Polym.* 2009, 6, 451.
19. A. L. Volynskii, D. A. Panchuk, Zh K. Sadakbaeva, A. V. Bol'shakova, L. M. Yaryshevam N. F. Bakeev, Evaluation of the Stress-Strain Properties of Surface Layers in Plasma-Treated Polymers, *High Energy Chemistry,* 2010, **44,** 341.
20. H. S. Yoo, T. G. Kim, T. G. Park, Surface-functionalized electrospun nanofibers for tissue engineering and drug delivery, *Adv. Drug Deliver. Rev.* 2009, **61**, 1033.
21. K. S. Siow, L. Britcher, S. Kumar, H. J. Griesser, Sulfonated Surfaces by Sulfur Dioxide Plasma Surface Treatment of Plasma Polymer Films *Plasma Process. Polym.* 2009, **6**, 583.
22. V. Švorčík, A. Chaloupka, P. Řezanka, P. Slepička, Z. Kolská, N. Kasálková, T. Hubáček, J. Siegel, Au-nanoparticles grafted on plasma treated PE, *Radiat. Phys. Chem.* 2010, **79**, 315.
23. F. Schwarz, B. Stritzker, Plasma immersion ion implantation of polymers and silver–polymer nano composites, *Surf. Coat. Tech.* 2010, **204**, 1875.

24. H. Krump, M. Simor, I. Hudec, M. Jasso, A. S. Luyt, Adhesion Strength Study between Plasma Treated Polyester Fibres and a Rubber Matrix, *Appl. Surf. Sci.,* 2005, **240,** 268.
25. N. Dumitrascu, C. Borcia, Adhesion Properties of Polyamide-6 Fibres Treated by Dielectric Barrier Discharge, *Surf. Coat. Technol.,* 2006, **201,** 1117.
26. L. Yenchun, F. Yenpei, Inductively Coupling Plasma (ICP) Treatment of Propylene (PP) Surface and Adhesion Improvement, *Plasma Science & Technology*, **11**, 704 (2009).
27. Yasuhiro Kurihara, Hiroyuki Ohata, Masahiko Kawaguchi, Shinichi Yamazaki, Kunio Kimura, Improvement of Adhesion Between Liquid Crystalline Polyester Films by Plasma Treatment, *J. Adhes. Sci. Technol.* **22**, 1985 (2008).
28. H. M. S. Iqbal, S. Bhowmik, R. Benedictus, Surface modification of high performance polymers by atmospheric pressure plasma and failure mechanism of adhesive bonded joints, *Int J Adhes Adhes*, **30**, 418 (2010).
29. S. Teodoru, Y. Kusano, N. Rozlosnik, P. K. Michelsen, Continuous Plasma Treatment of Ultra-High-Molecular-Weight Polyethylene (UHMWPE) Fibres for Adhesion Improvement, *Plasma Process. Polym.* **6,** S375 (2009).
30. K.N. Pandiyaraj, V. Selvarajan, R.R. Deshmukh, C. Gao, Adhesive properties of polypropylene (PP) and polyethylene terephthalate (PET) film surfaces treated by DC glow discharge plasma, *Vacuum*, 2009, **83**, 332
31. S. Erden, K.K.C. Ho, S. Lamoriniere, A.F. Lee, H. Yildiz, A. Bismarck, Continuous Atmospheric Plasma Oxidation of Carbon Fibres: Influence on the Fibre Surface and Bulk Properties and Adhesion to Polyamide 12**,** *Plasma Chem. Plasma Process.* 2010, **30**, 471.

32. A. Schutze, J. Y. Jeong, S. E. Babayan, R. F. Hicks, et. al., The Atmospheric-Pressure Plasma Jet: A Review and Comparison to Other Plasma Sources *IEEE Trans. Plasma Sci. 1998,* **26**, 1685.
33. E. Marsano, L. Francis, F. Giunco, Polyamide 6 nanofibrous nonwovens via electrospinning, *Journal of Applied Polymer Science*, 2010, **117**, 1754.
34. S. S. OJha, M. Afshari, R. Kotek, R. E. Gorga, Morphology of Electrospun Nylon-6 Nanofibers as a Function of Molecular Weight and Processing Parameters, *J Appl Polym Sci* 2008, **108**, 308.

CHAPTER 6

Plasma-Electrospinning Hybrid Process and Plasma Pretreatment to Improve Adhesive Properties of Nanofibers on Fabric Surface

Plasma-Electrospinning Hybrid Process and Plasma Pretreatment to Improve Adhesive Properties of Nanofibers on Fabric Surface

Abstract

Electrospun nanofiber mats are inherently weak, and hence they are often deposited on mechanically-strong substrates such as porous woven fabrics that can provide good structural support without altering the nanofiber characteristics. One major challenge of this approach is to ensure good adhesion of nanofiber mats onto the substrates and to achieve satisfactory durability of nanofiber mats against flexion and abrasion during practical use. In this work, Nylon 6 nanofibers were deposited on plasma-pretreated woven fabric substrates through a new plasma-electrospinning hybrid process with the objective of improving adhesion between nanofibers and fabric substrates. The as-prepared Nylon 6 nanofiber-deposited woven fabrics were evaluated for adhesion strength and durability of nanofiber mats by carrying out peel strength and flex resistance tests. The test results showed significant improvement in the adhesion of nanofiber mats on woven fabric substrates. The nanofiber-deposited woven fabrics also exhibited good resistance to damage under repetitive flexion. X-Ray photoelectron spectroscopy and water contact angle analyses were conducted to study the plasma effect on the nanofibers and substrate fabric, and the results suggested that both the plasma pretreatment and plasma-electrospinning hybrid process introduced radicals, increased oxygen contents, and led to the formation of active chemical sites on the nanofiber and substrate surfaces. These active sites helped in creating crosslinking bonds between

substrate fabric and electrospun nanofibers, which in turn increased the adhesion properties. The work demonstrates that the plasma-electrospinning hybrid process of nanofiber mats is a promising method to prepare durable functional materials.

Keywords: Adhesion, plasma, electrospinning, surface, nanofibers

6.1 Introduction

Electrospinning has been widely used to prepare ultra-fine fibrous mat structures from many different polymers and the resultant nanofiber mats have found various applications including filtration, tissue engineering, catalytic reaction materials, electrochemical electrodes, affinity membranes, and nano-composites.[1-2] However, electrospun nanofiber mats are inherently weak, and hence they are often deposited on mechanically-strong substrates such as porous woven fabrics that can provide good structural support without altering the nanofiber characteristics.[3-4] These nanofiber-deposited fabrics have potential uses as filters and protective clothing materials.[3] One major challenge of this approach is to ensure good adhesion of nanofiber mats onto the substrates and to achieve satisfactory durability of nanofiber mats against flexion and abrasion during practical use.

Plasma treatment of polymer surfaces is an environmentally friendly process as compared to conventional chemical treatments.[5-6] The plasma consists of highly active charged species, electrons, ions and radicals, and can create highly unusual environments to interact with material surfaces. Plasma treatment of polymer materials results in surface modification through functionalization, etching, chain scission, and cross linking.[7-12] Plasma treatment of textiles and polymers has been used for: *i*) modifying the surface hydrophobic or hydrophilic characteristics,[13-14] *ii*) etching and nano-texturing surfaces,[15-18] and *iii*) improving polymer mechanical properties depending on treatment conditions.[19] In addition, plasma treatment has also been used to introduce various surface functional groups [20-23] and improve surface

bonding or adhesion of various polymer materials.[24-32] Therefore, plasma can be used to enhance the adhesion of nanofiber mats onto the fabric substrates, and the simplest approach is to use plasma to treat the fabric surface and then deposit solidified nanofibers onto the plasma-pretreated fabric substrate. However, in this approach, there are no radicals or active species on the electrospun nanofibers, and hence the improvement in the adhesion between nanofibers and the fabric substrate is limited.

The plasma may have a larger impact if the treatment occurs during the electrospinning process and before the solidification of the polymer jets. Due to the large surface area of electrospun nanofibers, a large amount of active species can be generated *in-situ* during the electrospinning process, and hence the resultant plasma-treated nanofibers can have enhanced adhesion onto the fabric substrates. In this work, the electrospun nanofibers were subjected to *in-situ* plasma treatment through a plasma-electrospinning hybrid process. The *in-situ* plasma-treated nanofibers were deposited on a plasma-pretreated Nylon 6,6/cotton woven fabric and the adhesion and durability of nanofiber mats on the fabric substrate were investigated.

6.2 Experimental

6.2.1 Materials

Nylon 6 pellets and 2, 2, 2-tri-fluoro ethanol (TFE) were purchased from Sigma-Aldrich and the reagents were used without further purification. Nylon 6,6/Cotton (50/50) woven fabric

(mass per unit area: 240 g/m^2) was acquired from Milliken & Company, USA. Nylon 6,6 (thickness: 0.025 mm) and Cellophane (thickness: 0.031 mm) films were purchased from Goodfellow Corporation, USA.

6.2.2 Plasma pretreatment of fabric substrate

Prior to the deposition of electrospun nanofibers, the nylon/cotton fabric samples were pretreated in an atmospheric pressure audio frequency dielectric barrier discharge plasma system (Figure 6.1), which was designed and developed at North Carolina State University.[6]

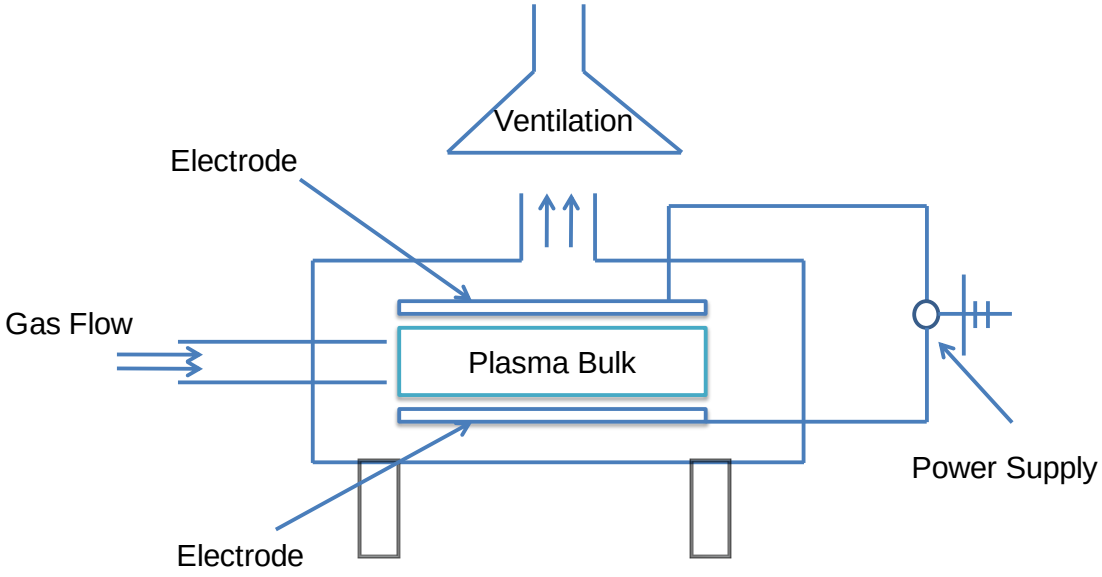

Figure 6.1 Schematic of atmospheric pressure plasma system.

The plasma system consists of two parallel copper electrodes, each embedded within a Lexan polycarbonate insulator. Stable and uniform plasma was achieved at a low frequency of

1.373 kHz during the operation. Either 100% helium (He) or a mixture of 99% helium/1% oxygen (He-O_2) was used as plasma carrier gas. The gas flows were 20 L/min for He and 0.3 L/min for O_2, respectively. The voltage between electrode plates was maintained between 6.3 and 7.6 kVmax for the He plasma and between 6.6 and 7.85 kVmax for the He-O_2 plasma. The fabric samples were placed on a nylon grid suspended in the plasma system cell to enable complete and uniform exposure of plasma onto them. The fabric samples were treated with either He plasma or He-O_2 plasma for 5 minutes, followed immediately by use as substrates for the deposition of electrospun nanofiber mats. For comparison, fabric samples without plasma pretreatment were also used for the deposition of nanofibers.

6.2.3 Deposition of nanofibers through plasma-electrospinning hybrid process

To carry out the *in-situ* plasma treatment of nanofibers during electrospinning, a plasma-electrospinning hybrid system was designed and developed at North Carolina State University for this research work.[33]

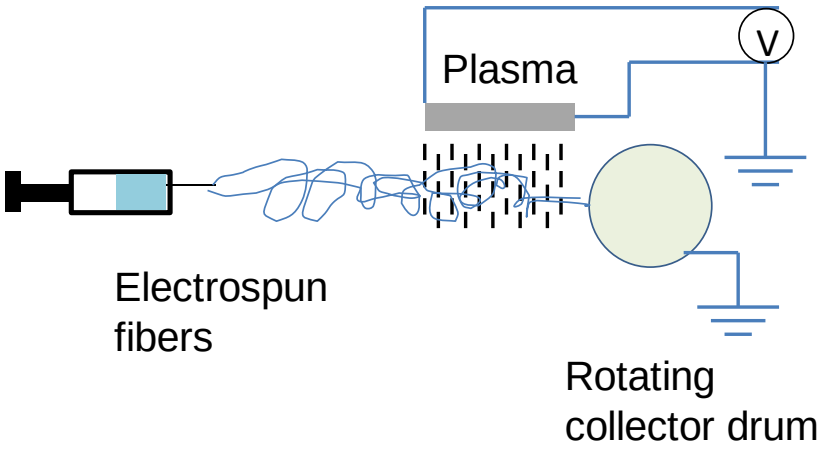

Figure 6.2 Schematic of atmospheric plasma-electrospinning hybrid processing set-up.

Figure 6.2 represents the schematic of the plasma-electrospinning hybrid processing device, which consists of a plasma generating device, electrospinning syringe pump, rotating drum collector, and high-voltage power supplies. The stable and uniform plasma was created with oscillating voltage (RMS voltage 3.48 kV and Peak voltage 5.1 kV) and current (RMS current 11.0 mA and peak current 17.25 mA) at a frequency of 11.24 kHz. The plasma carrier gases used included 100% He and mixture of 99% He/1% He-O_2. The gas flow rates were 28 L/min for He and 0.25 L/min for O_2, respectively.

For the deposition of electrospun nanofibers, the plasma-pretreated fabric samples placed on aluminum foil were carefully fastened to the drum collector. The rotating speed of the drum collector was maintained at 20 rpm. The electrospinning syringe was filled with Nylon 6 solution (12 wt%) in TFE and the feed rate was maintained at 1 ml/hr. The electrospinning voltage was 15 kV, and the needle-tip-to-collector distance was 15 cm. During the plasma-electrospinning hybrid process, the plasma was introduced in front of rotating drum collector (Figure 2). The electrospun fiber jets pass through the plasma, and are simultaneously treated and deposited on the fabric substrate. For comparison, nanofibers were also deposited without the presence of plasma under the same electrospinning conditions.

6.2.4 Solution and fiber mat characterizations

The zero shear viscosity of Nylon 6 solution was measured using a rheometer (StressTech HR, Rheologica Instruments AB) at 25 °C with the assistance of rheoExplorer V5 operating

software. The conductivity of Nylon 6 solution was measured using Orion model 164 conductivity meter (Orion Research Inc., Boston, MA). The morphology of the deposited Nylon 6 nanofiber mats was examined using a JEOL JSM-6400F Field Emission Scanning Electron Microscopy (FESEM) (JEOL Ltd., Tokyo, Japan) at an accelerating voltage of 5 kV. The average fiber diameter was obtained by measuring the diameters of 100 nanofibers using the Revolution software provided by 4pi Analysis.

6.2.5 Optical emission spectra of He and He-O_2 plasmas

Two Ocean Optics HR 2000 fixed grating spectrometers were used to obtain the spectra. Both spectrometers are fitted with a 600 line/mm grating, 25μm slit and Ocean Optics L2 internal lens to focus the light onto the charge coupled device. The grating of the Ultra Violet-Visible (UV-VIS) spectrometer is blazed at 500 nm and views the wavelengths between 244 nm and 700 nm. The Visible-Infra Red (VIS-IR) spectrometer has a range of 593 nm to 1025 nm with the grating blazed at 750 nm. Spectral data are transferred from the two spectrometers to a computer using an Ocean Optics software package. All spectra were taken inside the plasma source.

6.2.6 Water contact angles of Nylon 6,6 and Cellophane films

To investigate the effect of plasma pretreatment on the fabric surface, water contact angles (WCAs) were measured by using Nylon 6,6 and Cellophane films as the model materials. The films (3 cm × 3 cm) were thoroughly washed in acetone for 30 minutes and dried. The

films were then pretreated using either He or He-O_2 plasma for 5 minutes. The untreated, He plasma-pretreated and He-O_2 plasma-pretreated samples were subjected to WCA measurement using an OCA 15 Plus Contact Angle Measuring Device (DataPhysics Instruments, GmbH). During the measurement, a 5 µL distilled water droplet was injected onto the film surface using a computer-aided micro-liter syringe. After 30 seconds, the WCA was measured using an optical microscope. For each sample, at least 10 readings were taken at different spots using multiple specimens, and average WCA values were calculated. In addition, the images of water droplets on film surfaces were also captured.

6.2.7 XPS Analyses of Nylon 6,6 and Cellophane films

Nylon 6,6 and Cellophane films were subjected to X-Ray Photoelectron Spectroscopy (XPS) analyses to investigate the changes in surface chemical composition before and after plasma pretreatment. The analyses were carried out using Axis Ultra (Kratos Analytical Ltd, UK) with MgKα excitation (1254 eV). Energy calibration was established by referencing to adventitious Carbon (C1s line at 284.5 eV binding energy). A takeoff angle of 75° from the film surface was used with an X-Ray incidence angle of 20° and an X-ray source to analyzer angle of 55°. Base pressure in the analysis chamber was in the 10^{-10} Torr range. CASA XPS software was used for data analysis.

6.2.8 Adhesion strengths of nanofiber-deposited fabrics

The adhesion strength between the electrospun fiber mat and fabric substrate was estimated by a peel test method based on ASTM 2261 *Standard Test Method for Tearing Strength of Fabrics by the Tongue Procedure* using an Instron® Tensile Tester (Figure 6.3). During test, the nanofiber mat (dimension: 50 mm × 10 mm, deposition time: 10 mins) was held by the movable grip of the Tensile Tester and the fabric substrate held by the stationary grip. To facilitate proper peeling and avoid grip slippage, tapes were attached to the nanofiber mat and fabric substrate.

Figure 6.3 Adhesion strength measurement between nanofiber mat and fabric; a) Nanofiber mat and fabric with short tape attached b) sample held in Instron instrument grips.

A 50 gm load cell was used to detect the maximum load required to remove the nanofiber mat from the fabric surface at a constant rate of 50 mm/min, 0.5 inch gauge length. The

adhesion strength was estimated in terms of gram force and the average value of 20 test specimen was reported. Prior to testing, the nanofiber-deposited fabric samples were conditioned at standard temperature of 20 ± 1°C and relative humidity of 65 ± 2 % for at least 8 hours.

6.2.9 Flex durability of nanofiber-deposited fabrics

A Gelbo Flex test was conducted based on ASTM F392-93 *Standard Test Method for Flex Durability of Flexible Barrier Materials* in order to assess the durability of the electrospun mats on the fabric substrate using an IDM Gelbo Flex Tester (IDM Instruments Ltd®). Nanofiber-deposited fabric samples (dimension: 50 mm × 10 mm; deposition time: 10 mins) were attached to the two circular clamping disks via hose clamps, and the samples were twisted and flexed for 1000 cycles. A qualitative assessment of adhesion was determined by observing the electrospun nanofiber mat/fabric substrate interface via SEM. Prior to test, the nanofiber-deposited fabric samples were conditioned at standard temperature of 20 ± 1°C and relative humidity of 65 ± 2 % for at least 8 hours.

6.3 Results and discussion

6.3.1 Solution and fiber mat characterizations

Table 6.1 shows the zero shear viscosity and ionic conductivity of 12 wt% Nylon 6 in TFE. The solution viscosity measured was 0.2 Pa·s and ionic conductivity was 3.1 μS/cm. The values are in the ranges that can produce a stable electrospinning process and lead to

desirable nanofiber structures.[34-35] Figure 6.4 shows a typical SEM image of Nylon 6 nanofibers deposited directly on nylon/cotton fabric using the plasma-electrospinning hybrid process. It is seen that the fibers have smooth surface texture and the average fiber diameter was estimated to be 230 ± 40 nm. The nanofiber mat has random fiber orientation and a highly porous structure. These morphological characteristics are key factors in achieving high filtration efficiency with a low pressure drop across the nanofiber-deposited fabrics. The filtration performance of nanofiber-deposited fabrics has been published somewhere else.[3]

Table 6.1 Zero shear viscosity and ionic conductivity of Nylon 6 solution.

Polymer solution	Zero shear viscosity (Pa·s)	Ionic Conductivity (μs/cm)
Nylon 6 in TFE (12 wt %)	0.2	3.0 ± 0.1

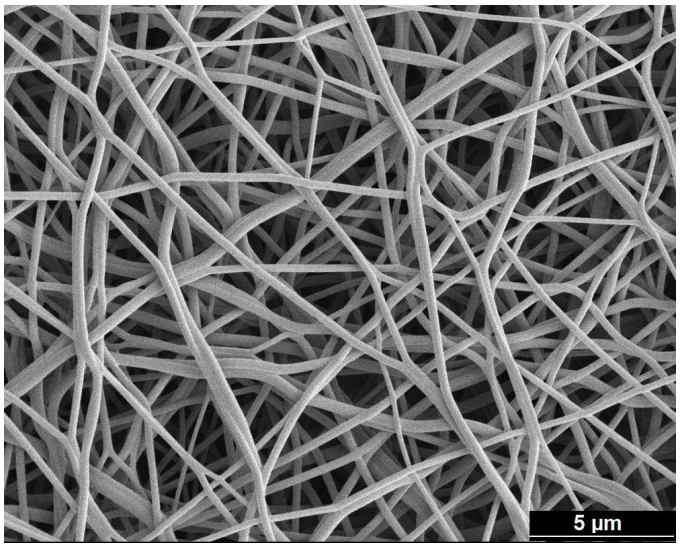

Figure 6.4 SEM micrograph of Nylon 6 nanofiber mat.

6.3.2 Spectral analyses of plasma

The UV-VIS and VIS-IR spectral data of the plasma sources are shown in Figure 6.5. The peaks at wavelengths of 656.6 nm and 486.3nm represent Hα and Hβ line respectively. The Hα and Hβ lines peaks indicate the formation of excited hydrogen species.

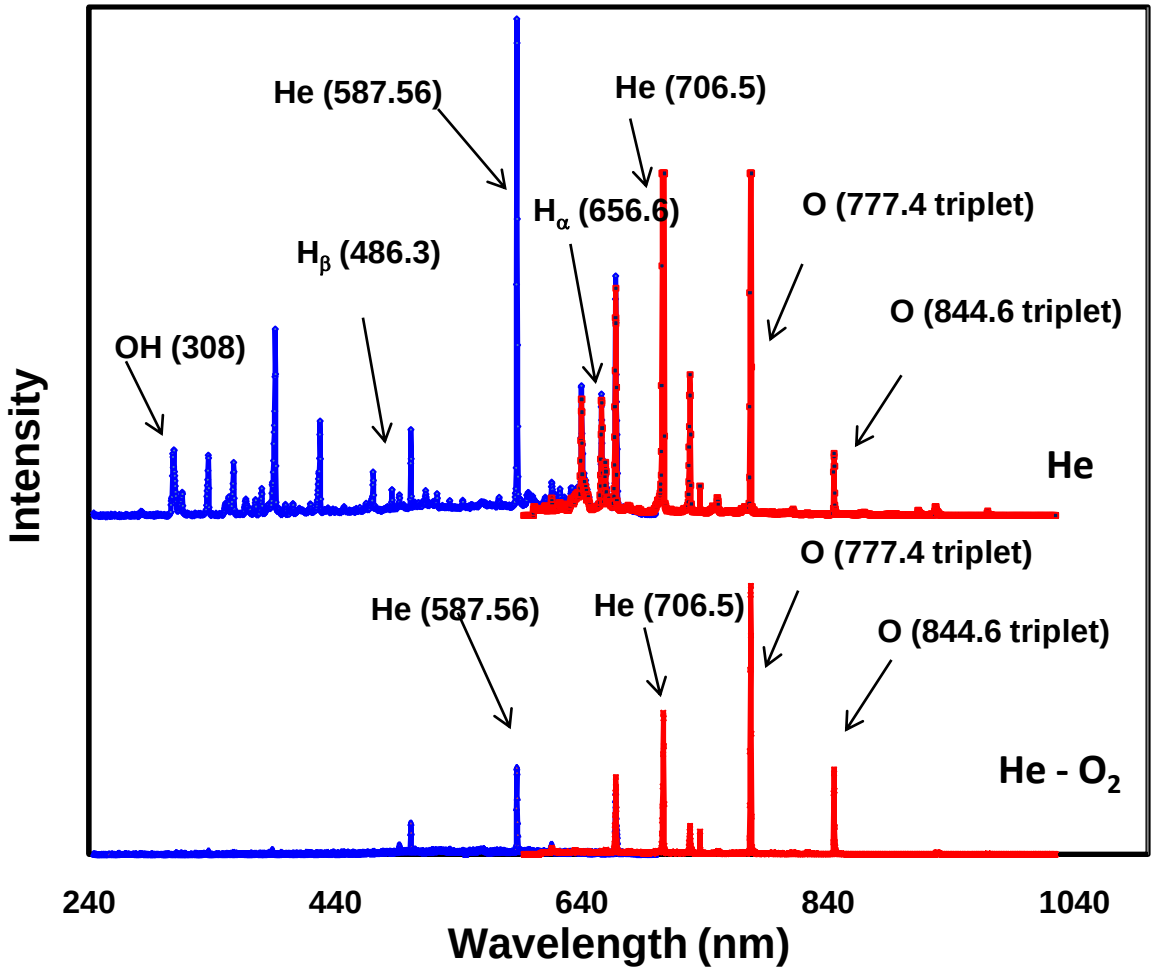

Figure 6.5 The UV-VIS and VIS-IR spectral data of He and He-O_2 plasma.

The peak at wavelength of 308nm represents the formation of hydroxyl species in plasma which might be due to the reaction between excited hydrogen atoms and oxygen molecules

present in atmospheric air. The interaction between these hydroxyl species and polymer surface might lead to the increased hydrophilic nature of plasma treated polymer surface s and the formation of other active species, as discussed in the following sections. The peaks at wavelengths 777.4 nm and 844.6 nm represent the formation of active atomic oxygen species in plasma due to the dissociative excitation process as shown in the following equations.[36]

$$e + O_2 \rightarrow O + O^* + e \rightarrow 2O + e + h\nu$$

$$e + O \rightarrow O^* + e \rightarrow O + e + h\nu$$

These active atomic oxygen species created in He-O_2 plasma might cause the formation of other active oxygen groups on the surface of the plasma-treated nanofibers, which is also discussed in the subsequent sections.

6.3.3 Water contact angles of plasma-pretreated surfaces

To avoid the complexity involved in surface characterization of nylon/cotton blend fabric and to analyze the actual effect of plasma on individual components, Nylon 6,6 and Cellophane films were used as the model materials to represent the nylon and cotton in the blend fabric and their WCAs were measured.

Table 6.2 Water contact angles (^{o}) on untreated and plasma-pretreated Nylon 6,6 and Cellophane films.

Film substrate	Control	He Plasma	He-O_2 Plasma
Nylon 6,6	58.1 ± 3.7	39.6 ± 5.3	41.6 ± 3.9
Cellophane	0.0	0.0	0.0

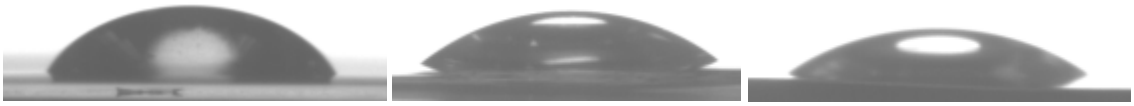

Untreated He plasma-treated He-O_2 plasma-treated

Figure 6.6 Photographs of water droplets on untreated and plasma-pretreated Nylon 6,6 films.

The photographs in Figure 6.6 show the water droplets on untreated and plasma-pretreated Nylon 6,6 films. The measured WCA values are shown in Table 6.2. The untreated Nylon 6,6 film has an average WCA of 58.1°. After He or He-O_2 plasma treatment, the average WCA reduces to 39.6° and 41.6°, respectively. The WCA results confirm that the plasma treatment changes the surface characteristic of Nylon 6,6. Similar WCA change is expected in the nylon component of the nylon/cotton blend fabric. Unlike Nylon 6,6, both untreated and plasma-pretreated Cellophane films were completely wetted within 30 seconds after placing the water droplets on them, and hence their WCAs are not measurable, indicating their extremely high hydrophilicity (Table 6.2).

6.3.4 XPS analyses of plasma-pretreated surfaces

The elemental composition data and relative surface chemical bonds (%) of untreated and plasma-pretreated Nylon 6,6 films obtained from XPS analyses are reported in Tables 6.3 and 6.4, respectively. Figure 6.7 shows the corresponding C1s spectra. The elemental composition data suggest that plasma pretreatment leads to increased surface oxygen content. This might be due to the creation of radicals and the subsequent formation of oxygen groups on the surface of the Nylon 6,6 films during atmospheric plasma pretreatment. The relative surface chemical bond composition (Table 6.4) and C1s spectra of Nylon 6,6 films (Figure 6.7) suggest that plasma pretreatment significantly increases the C-O and CONH bonds, which could cause an increase in surface hydrophilicity. This trend is in agreement with the WCA value decrement trend of Nylon 6,6 films discussed in the previous section.

Tables 6.5 and 6.6 show the elemental composition data and relative surface chemical bonds (%) of untreated and plasma-pretreated Cellophane films, respectively. Figure 6.8 shows the corresponding C1s spectra. Cellophane film is composed of regenerated cellulose, which has high contents of C-OH and C-O-C surface chemical groups that make it inherently hydrophilic. The elemental analysis (Table 6.5) of untreated and plasma-pretreated Cellophane films suggests further increases in surface oxygen content. The relative surface chemical bond composition (Table 6.6) and C1s spectra (Figure 6.8) of Cellophane films confirms the formation of C=O and COOH groups.

Table 6.3 Elemental composition data of Nylon 6,6 films obtained from XPS analysis.

Nylon 6,6 film	C %	O %	N %	O/C	N/C
Untreated	78.39	10.66	10.95	0.14	0.14
He plasma	73.98	15.39	10.64	0.21	0.15
He-O_2 plasma	74.24	15.10	10.66	0.21	0.15

Table 6.4 Relative surface chemical bonds (%) on Nylon 6,6 film.

Nylon 6,6 film	C-C (284.5 eV)	C-N (285.4 eV)	C-O (286.5 eV)	CONH (287.5 eV)
Untreated	36.7	45.8	-	17.4
He plasma	31.2	39.4	5.6	23.8
He-O_2 plasma	60.2	17.4	2.1	20.3

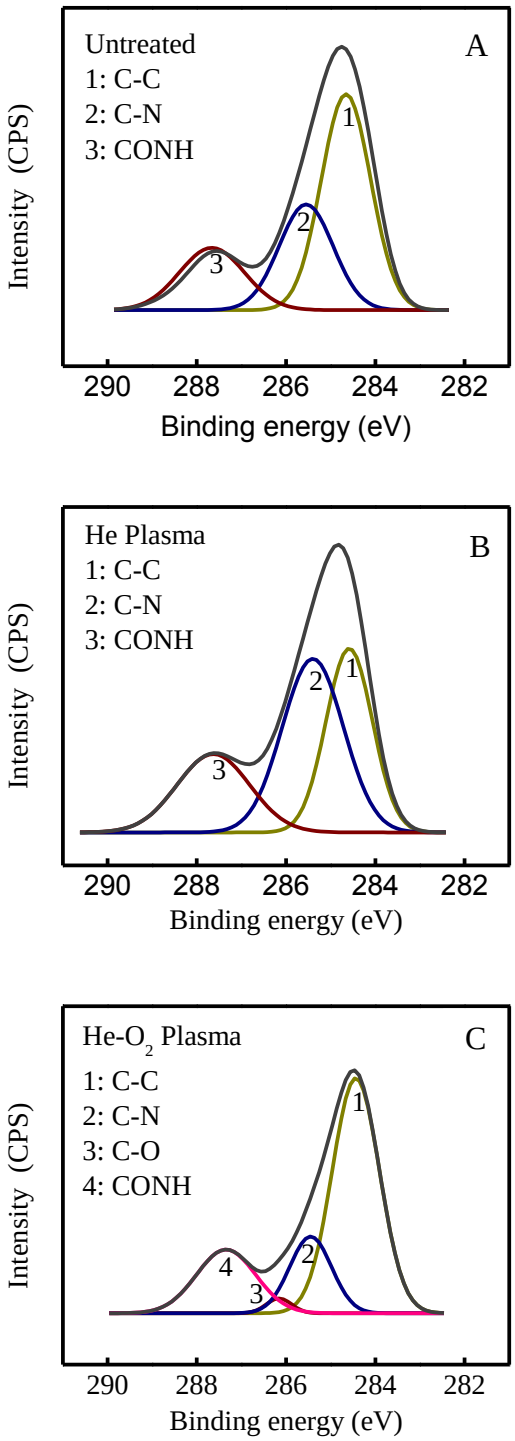

Figure 6.7 C1s spectra of Nylon 6 6 films: a) untreated, b) He plasma-treated, and c) He-O_2 plasma-pretreated.

Table 6.5 Elemental composition data of Cellophane films obtained from XPS analysis.

Cellophane film	C %	O %	O/C
Untreated	59.16	40.84	0.69
He plasma	57.09	42.91	0.75
He-O_2 plasma	55.78	44.22	0.79

Table 6.6 Relative surface chemical bonds (%) of Cellophane film.

Cellophane film	C-C (284.5 eV)	C-OH (286.2 eV)	C-O-C (287.2 eV)	C=O (287.6 eV)	COOH (288.5 eV)
Untreated	13.4	51.6	35.0	-	-
He plasma	3.1	49.4	43.1	4.4	-
He-O_2 plasma	4.4	70.9	22.2	-	2.5

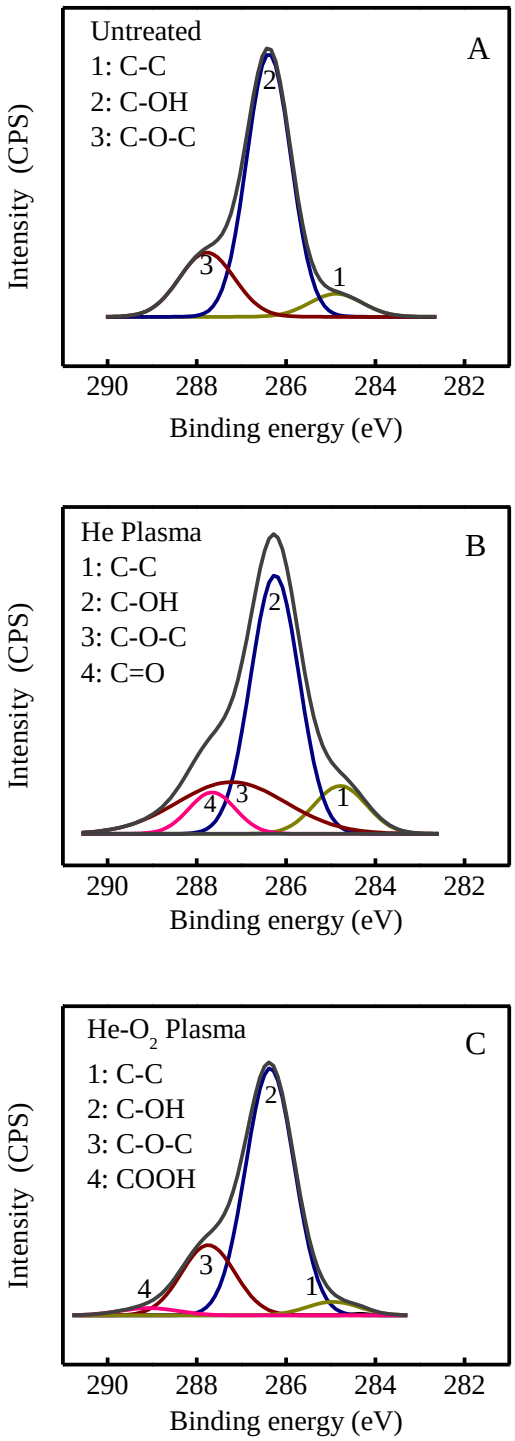

Figure 6.8 C1s spectra of Cellophane films: a) untreated, b) He plasma-treated, and c) He-O_2 plasma-pretreated.

6.3.5 XPS analyses of Nylon 6 nanofibers

The elemental composition data and relative surface chemical bonds (%) of Nylon 6 nanofibers prepared using the plasma-electrospinning hybrid process are listed in Tables 7 and 8 respectively. The C1 spectra of these Nylon 6 nanofibers are shown in Figure 9. For comparison, the XPS analysis results of Nylon 6 fibers prepared solely by electrospinning were also shown. From the XPS data shown in Tables 7, 8 and Figure 8, it is seen that Nylon 6 nanofibers prepared by electrospinning have C-C, C-N and CONH bonds on the surface. These bonds are also present in nanofibers prepared by plasma-electrospinning hybrid process. In addition to these chemical groups, C-O bonds are found in Nylon 6 nanofibers prepared by He plasma-electrospinning hybrid process, while both C-O and O-C=O bonds are found in nanofibers prepared by He-O_2 plasma-electrospinning process. This might be due to active atomic species present in the plasma (Figure 5), which leads to the formation of more active chemical sites on the as-prepared nanofibers.

In addition, compared to Nylon 6 nanofibers prepared solely by electrospinning, nanofibers prepared by plasma-electrospinning hybrid process have decreased percentage of C-N and CONH groups. This suggests that the presence of plasma during electrospinning causes possible breakage of C-N and CONH bond links at the fiber surface. This effect seems to be more severe in the case of He-O_2 plasma, in which CONH content decreases tremendously. Hence, it can be summarized that the plasma-electrospinning hybrid process of Nylon 6

nanofibers can cause possible breakage of C-N and CONH bond links and increased contents of C-O and O-C=O bonds, which in turn improve the reactivity of nanofiber surfaces.

Table 6.7 Elemental composition data of Hybrid plasma treated Nylon 6 fibers obtained from XPS analysis.

Nylon 6 nanofiber	C %	O %	N %	O/C	N/C
Untreated	78.1	11.1	10.8	14.2	13.8
He plasma	77.2	10.8	12	14	15.5
He-O_2 plasma	72.5	16.6	10.9	23	15.1

Table 6.8 Relative surface chemical bonds (%) on hybrid plasma treated Nylon 6 fibers.

Nylon 6 fiber	C-C (284.5 eV)	C-N (285.4 eV)	C-O (286.5 eV)	CONH (287.5 eV)	O-C=O (288.5 eV)
Untreated	39.3	33.2	-	27.5	-
He plasma	44.8	26.3	17.4	11.4	-
He-O_2 plasma	23.8	5.5	45.4	5.7	19.6

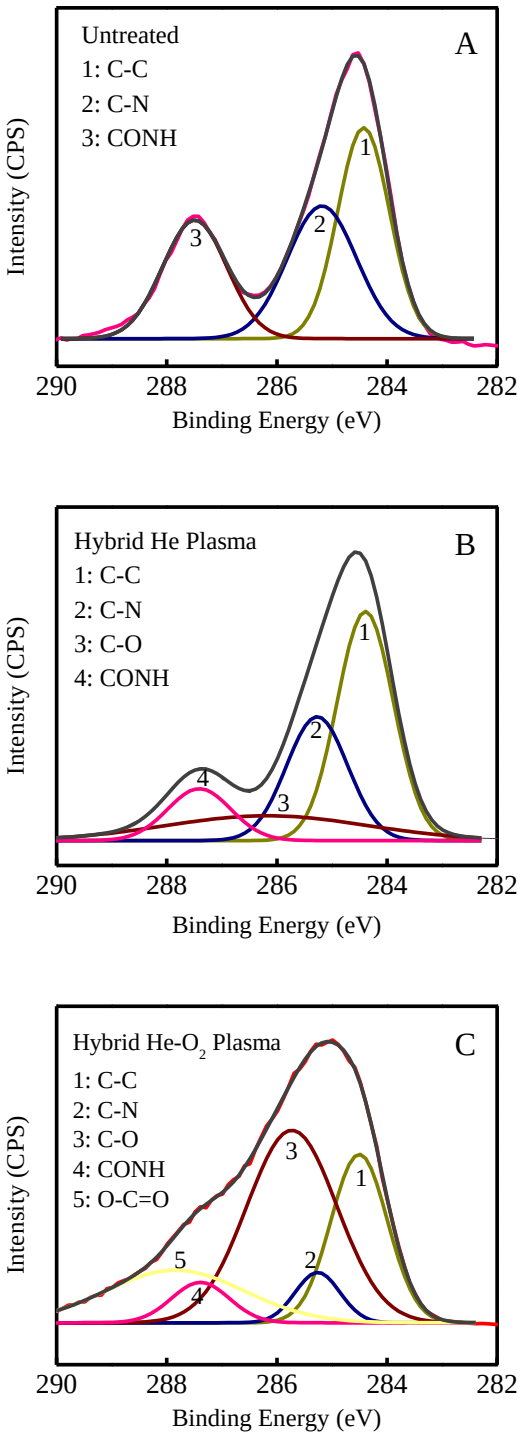

Figure 6.9 XPS spectra of Nylon 6 nanofibers prepared by: a) electrospinning, b) He plasma-electrospinning, and c) He-O_2 plasma-electrospinning hybrid process.

6.3.5 Adhesion Strength

Figure 6.10 shows the schematic of possible plasma effects on the polymer surface. Plasma treatment results in the formation of active surface chemical groups on the polymer surface, which is beneficial for the improvement of adhesion strength at the polymer interface.[37-38]

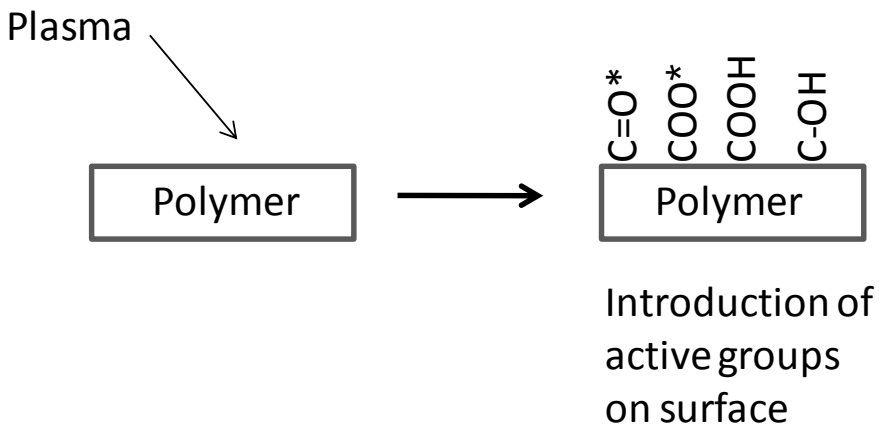

Figure 6.10 Schematic of plasma effect on polymer surface.

Table 6.9 shows the average adhesion strengths between Nylon 6 nanofiber mats and Nylon 6,6/cotton fabric substrates. It is seen that the average adhesion strengths of samples prepared with the plasma-electrospinning hybrid process are higher than those with solely electrospinning. This indicates the possible formation of covalent bonds and crosslinking between nanofibers and fabric surfaces, which is a result of the active species that have been created on plasma-pretreated fabrics and nanofibers produced by the hybrid process. From Table 6.9, it is also seen that for the He plasma-electrospinning hybrid process, nanofibers deposited on He and He-O_2 plasma-pretreated fabrics have higher adhesion strength than

those deposited on untreated substrate fabrics. However, in the case of the He-O_2 plasma-electrospinning hybrid process, the plasma pretreatment of the substrate does not have beneficial effect on the adhesion strengths.

Table 6.9 Adhesion strengths (gf) between Nylon/Cotton fabric and deposited nanofiber mats.

	Electrospinning	He Plasma-Electrospinning Hybrid Process	He-O_2 Plasma-Electrospinning Hybrid Process
Untreated Fabric	1.51 ± 0.3	2.74 ± 0.6	3.69 ± 0.9
He Plasma-Pretreated Fabric	2.84 ± 0.6	3.32 ± 0.4	2.3 ± 0.5
He-O_2 Plasma-Pretreated Fabric	2.86 ± 0.5	3.87 ± 1.7	3.55 ± 1.7

Table 6.10 Statistical t-Test data obtained for adhesion strength of different samples.

	Electrospinning	He Plasma-Electrospinning Hybrid Process	He-O_2 Plasma-Electrospinning Hybrid Process
Untreated Fabric	-	0.000008	0.000006
He Plasma-Pretreated Fabric	0.000003	0.000000	0.000351
He-O_2 Plasma-Pretreated Fabric	0.000001	0.000455	0.001564

Table 6.10 shows the t-test ($p<0.05$) data obtained for the adhesion strength values. The t-test is a statistical hypothesis test for assessing whether the means of two groups are statistically different from each other. Independent t-test with one tail distribution and threshold significance value of 0.05 was carried out for adhesion strength data with unequal population and unequal variance. From Table 10, it is seen that all t-test values are less than 0.05, suggesting that the adhesion strength improvement discussed above is statistically significant.

6.3.6 Repetitive flex resistance

Figure 6.11 shows the SEM images of a Nylon 6 nanofiber-deposited nylon/cotton fabric before and after 1000 cycles of Gelbo flex testing. The fabric was not pretreated by plasma and the nanofiber deposition was carried out by electrospinning without the presence of plasma. It is seen that the nanofiber mat is destroyed after of the Gelbo Flex test.

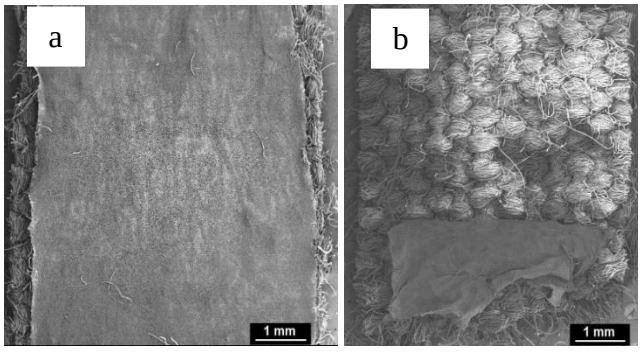

Figure 6.11 Typical SEM images of electrospun Nylon 6 nanofibers deposited on untreated Nylon/Cotton fabrics a) before and b) after Gelbo Flex test, respectively.

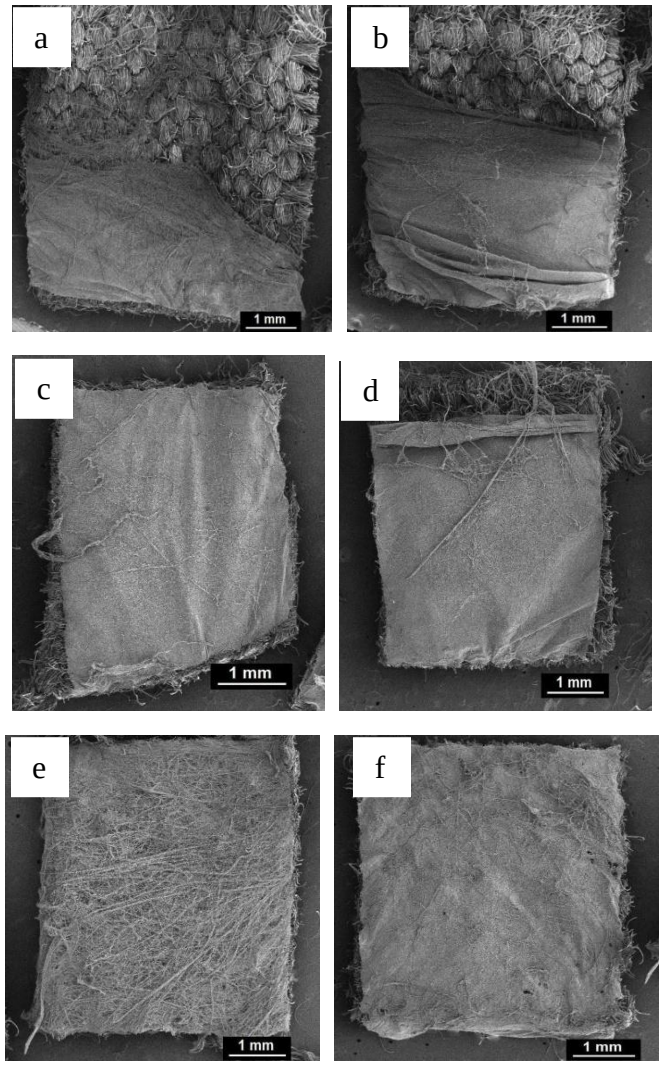

Figure 6.12 Typical SEM images of Nylon 6 nanofibers deposited by using (a,c, and e) He plasma-electrospinning and (b,d, and f) He-O_2 plasma-electrospinning hybrid processes after Gelbo Flex test. Nanofibers were deposited on (a and b) untreated, (c and d) He plasma-pretreated, and (e and f) He-O_2 plasma-pretreated fabrics.

Figure 6.12 shows SEM images of Nylon 6 nanofibers deposited using the plasma-electrospinning hybrid process on both untreated and plasma-pretreated fabrics, after 1000 cycles of Gelbo Flex testing. Comparing Figures 12a and b with Figure 11b, it is seen that when the nanofibers were deposited using the He or He-O_2 plasma-electrospinning hybrid

process, the nanofiber mats show better resistance to flex and more nanofibers remain on the fabric surface (Figures 12a and b). When the nanofibers were deposited using the hybrid process on He and He-O_2 plasma-pretreated fabric substrates, they exhibit significantly improved Gelbo Flex resistance. For these samples, the SEM images (Figures 12c, d, e, and f) show that the nanofiber mats remain intact on the fabric substrates without significant damage after 1000 cycles of twisting and flex. This indicates that both substrate fabric pretreatment in plasma and the use of the plasma-electrospinning hybrid process are effective in improving the adhesion and durability of nanofiber mat-deposited fabrics.

6.4 Summary

The effects of plasma pretreatment of substrate fabrics and the use of a novel plasma-electrospinning hybrid process on the adhesion and durability of nanofiber mats on Nylon6/cotton substrate fabrics were investigated. Nylon 6 nanofiber mats were deposited onto plasma-pretreated or untreated nylon/cotton fabric substrates through either conventional electrospinning or the plasma-electrospinning hybrid process. Two types of plasmas (*i.e.*, He and He-O_2) were used in this work. Peel-test results showed that the samples prepared with the plasma-electrospinning hybrid process have higher adhesion strengths. The Nylon 6 nanofiber-deposited fabrics were also subjected to Gelbo flex testing and the results indicated improved durability against repeated twist and flex force. The effect of plasma pretreatment on fabric substrates was studied using Nylon 6,6 and Cellophane films as model substrates. The plasma-pretreated films showed decreased WCA values and

XPS analyses indicated increases in oxygen-containing surface groups. The XPS analyses also showed increased oxygen content and the formation of functional chemical groups on nanofibers produced by the plasma-electrospinning hybrid process. The active chemical groups created on nanofibers and fabric surfaces might have led to the formation of crosslink bonds between them during the plasma-electrospinning hybrid process, which might be responsible for improved durability of nanofiber-deposited fabrics. In summary, it was demonstrated that both the plasma pretreatment of fabric surfaces and plasma-electrospinning hybrid process of nanofibers could increase the adhesion between fabric substrate and deposited nanofibers.

6.5 References

1. T. Subbiah, G. S. Bhat, R. W. Tock, S. Parameswaran, S. S. Ramkumar, Electrospinning of nanofibers, *J. Appl. Polym. Sci.* 2005, **96**, 557.
2. K. M. Sawicka, and P. Gouma, Electrospun composite nanofibers for functional applications, *J. Nanopart. Res.* 2006, **8**, 769.
3. N. Vitchuli, Q. Shi, J. Nowak, M. McCord, M. Bourham, X. Zhang, Electrospun ultrathin nylon fibers for protective applications, *J Appl Polym Sci* 2010, **116,** 2181.
4. Y. Matalov-Meytal, and M. Sheintuch, Catalytic fibers and cloths, *Appl. Catal., A,* 2002, **231**, 1.
5. F. S. Denes, S. Manolache, Macromolecular plasma-chemistry: an emerging field of polymer science, *Prog Polym Sci*, 2004, **29**, 815.
6. Y. J. Hwang, J. S. An, M. G. McCord, S. W. Park, and B. C. Kang, Effects of Helium Atmospheric Pressure Plasma Treatment on Low-Stress Mechanical Properties of Polypropylene Nonwoven Fabrics, *Text. Res. J.* 2005, **75**, 771.
7. Y. J. Hwang, Y. Qiu, C. Zhang, B. Jarrard, R. Stedeford, J. Tsai, Y.C. Park, M. G. McCord, Effects of atmospheric pressure helium/air plasma treatment on adhesion and mechanical properties of aramid fibers, *J. Adhes. Sci. Technol.* 2003, **17**, 847.
8. M. G. McCord, Y. J. Hwang, P. J. Hauser, et al., Modifying Nylon and Polypropylene Fabrics with Atmospheric Pressure Plasmas, *Textile Research Journal*, 2002, **72,** 491.

9. Jun Young Kim, Yongbeom Lee, Dae Young Lim, Plasma-Modified Polyethylene Membrane as a Separator for Lithium-Ion Polymer Battery, *Electrochim.Acta*, 2009, **54,** 3714.
10. L. I. Kravets, S. N. Dmitriev, A. B. Gil'man, Modification of Properties of Polymer Membranes by Low-Temperature Plasma Treatment, *High Energy Chemistry*, 2009, **43,** 181.
11. Dixon T. K. Kwok, Liping Tong, Che Yan Yeung, C. G. dos Remedios, Paul K. Chu, Hybrid Plasma Surface Modification and Ion Implantation of Biopolymers, *Surf.Coat.Technol.*, 2010, **204,** 2892.
12. B. Eliasson, and U. Kogelschatz, Nonequilibrium Volume Plasma Chemical Processing, *IEEE Trans. Plasma Sci.* 1991, **19**, 1063.
13. M. G. McCord, Y. J. Hwang, Y. Qiu, L. K. Hughes, M. A. Bourham, Surface Analysis of Cotton Fabrics Fluorinated in Radio-Frequency Plasma, *J Appl Polym Sci*, 2003, **88,** 2038.
14. W. Ren, C. Cheng, R. Wang, X. Li, Effect of fiber surface morphology on the hydrophilicity modification of cold plasma-treated polypropylene nonwoven fabrics, *J. Appl. Polym. Sci.* 2010, **116**, 2480.
15. S. R. Matthews, Y. J. Hwang, M. G. McCord, M. A. Bourham, Investigation into Etching Mechanism of Polyethylene Terephthalate (PET) Films Treated in Helium and Oxygenated-Helium Atmospheric Plasmas, *J Appl Polym Sci*, 2004, **94,** 2383.

16. M. G. McCord, Y. Qiu, C. Zhang, Y. J. Hwang, B. Bures, The effect of atmospheric pressure helium plasma treatment on the surface and mechanical properties of ultrahigh-modulus polyethylene fibers, *Adhes. Sci. Technol.* 2002, **16**, 99.
17. Zhiqiang Gao, Jie Sun, Shujing Peng, Lan YaoYiping Qiu, Surface Modification of a Polyamide 6 Film by He/CF4 Plasma using Atmospheric Pressure Plasma Jet, *Appl.Surf.Sci.,* 2009, **256,** 1496.
18. A. Hollaender, S. Kroepke, Surface Modification with Pressure Pulse Plasmas, *Plasma Process. Polym.* 2009, 6, 451.
19. A. L. Volynskii, D. A. Panchuk, Zh K. Sadakbaeva, A. V. Bol'shakova, L. M. Yaryshevam N. F. Bakeev, Evaluation of the Stress-Strain Properties of Surface Layers in Plasma-Treated Polymers, *High Energy Chemistry,* 2010, **44,** 341.
20. H. S. Yoo, T. G. Kim, T. G. Park, Surface-functionalized electrospun nanofibers for tissue engineering and drug delivery, *Adv. Drug Deliver. Rev.* 2009, **61**, 1033.
21. K. S. Siow, L. Britcher, S. Kumar, H. J. Griesser, Sulfonated Surfaces by Sulfur Dioxide Plasma Surface Treatment of Plasma Polymer Films *Plasma Process. Polym.* 2009, **6**, 583.
22. V. Švorčík, A. Chaloupka, P. Řezanka, P. Slepička, Z. Kolská, N. Kasálková, T. Hubáček, J. Siegel, Au-nanoparticles grafted on plasma treated PE, *Radiat. Phys. Chem.* 2010, **79**, 315.
23. F. Schwarz, B. Stritzker, Plasma immersion ion implantation of polymers and silver–polymer nano composites, *Surf. Coat. Tech.* 2010, **204**, 1875.

24. H. Krump, M. Simor, I. Hudec, M. Jasso, A. S. Luyt, Adhesion Strength Study between Plasma Treated Polyester Fibres and a Rubber Matrix, *Appl. Surf. Sci.,* 2005, **240,** 268.
25. N. Dumitrascu, C. Borcia, Adhesion Properties of Polyamide-6 Fibres Treated by Dielectric Barrier Discharge, *Surf. Coat. Technol.,* 2006, **201,** 1117.
26. L. Yenchun, F. Yenpei, Inductively Coupling Plasma (ICP) Treatment of Propylene (PP) Surface and Adhesion Improvement, *Plasma Science & Technology*, **11**, 704 (2009).
27. Yasuhiro Kurihara, Hiroyuki Ohata, Masahiko Kawaguchi, Shinichi Yamazaki, Kunio Kimura, Improvement of Adhesion Between Liquid Crystalline Polyester Films by Plasma Treatment, *J. Adhes. Sci. Technol.* **22**, 1985 (2008).
28. H. M. S. Iqbal, S. Bhowmik, R. Benedictus, Surface modification of high performance polymers by atmospheric pressure plasma and failure mechanism of adhesive bonded joints, *Int J Adhes Adhes*, **30**, 418 (2010).
29. S. Teodoru, Y. Kusano, N. Rozlosnik, P. K. Michelsen, Continuous Plasma Treatment of Ultra-High-Molecular-Weight Polyethylene (UHMWPE) Fibres for Adhesion Improvement, *Plasma Process. Polym.* **6,** S375 (2009).
30. K.N. Pandiyaraj, V. Selvarajan, R.R. Deshmukh, C. Gao, Adhesive properties of polypropylene (PP) and polyethylene terephthalate (PET) film surfaces treated by DC glow discharge plasma, *Vacuum*, 2009, **83**, 332
31. S. Erden, K.K.C. Ho, S. Lamoriniere, A.F. Lee, H. Yildiz, A. Bismarck, Continuous Atmospheric Plasma Oxidation of Carbon Fibres: Influence on the Fibre Surface and Bulk Properties and Adhesion to Polyamide 12**,** *Plasma Chem. Plasma Process.* 2010, **30**, 471.

32. A. Schutze, J. Y. Jeong, S. E. Babayan, R. F. Hicks, et. al., The Atmospheric-Pressure Plasma Jet: A Review and Comparison to Other Plasma Sources *IEEE Trans. Plasma Sci. 1998,* **26**, 1685.
33. E. Marsano, L. Francis, F. Giunco, Polyamide 6 nanofibrous nonwovens via electrospinning, *Journal of Applied Polymer Science*, 2010, **117**, 1754.
34. S. S. OJha, M. Afshari, R. Kotek, R. E. Gorga, Morphology of Electrospun Nylon-6 Nanofibers as a Function of Molecular Weight and Processing Parameters, *J Appl Polym Sci* 2008, **108**, 308.

CHAPTER 7

Conclusions and Recommendations

7.1 Conclusions

In the preceding chapters, the deposition of electrospun nanofibers on woven fabric to improve barrier properties and the fabrication of multifunctional nanofibers to detoxify C-B agents were discussed. The atmospheric pressure plasma pretreatment of fabric substrate and plasma-electrospinning hybrid process to improve adhesion between electrospun fibers and fabric were also explored. The major findings of the above experiments are summarized as follows.

- A thin layer of electrospun nanofiber mat was deposited on woven fabric substrate at controlled rate. The electrospinning parameters such as polymer solution concentration, applied voltage, deposition time were studied on the barrier performance behavior against submicron aerosol particles. The filtration efficiency of nanofiber mat was influenced by fiber diameter and mat structure. Decrease in polymer solution concentration and increase in electrospinning voltage resulted in finer fiber diameter and higher filtration efficiency. A small increment of deposited nanofiber mat areal density significantly improved the filtration efficiency to maximum level. The barrier performance characterization of electrospun Nylon 6 nanofiber mat-deposited fabric exhibited a maximum filtration of over 99.99%. The deposition of nanofiber mat on fabric did not affect the air permeability or pressure drop values.

- ZnO-Nylon 6 nanofiber mats were fabricated through electrospinning-electrospraying hybrid process which involves simultaneous electrospinning of nanofibers and

electrospraying of nanoparticles on a single target collector plate. In this process the ZnO particles were dispersed on the surface of Nylon 6 nanofibers. The fabricated ZnO-Nylon 6 mats were subjected to performance evaluation against simulants of chemical-biological warfare agents. Qualitative and quantitative antibacterial tests were conducted using gram negative and gram positive types of bacteria. In addition, the catalytic detoxification tests of paraoxon, a simulant of nerve agent were carried out. The result showed impressive antibacterial efficiency of over 99.99% against *E.coli* and *B.cereus* pathogens and very good detoxifying ability of over 95% against paraoxon.

- Plasma pretreatment of Nylon/Cotton blend fabric substrates in atmospheric pressure plasma chamber were carried out using helium or mixture of helium and oxygen as the plasma carrier gas. Electrospun nanofiber mats were deposited at controlled rate on the plasma pretreated fabric substrates. The prepared samples were subjected to adhesion strength tests by a modified peel test method. The peel test results showed significant improvement of adhesion strength due to plasma pretreatment of fabric substrate. The samples were also subject to flex resistance and abrasion resistance tests. These results exhibited prominent improvement of nanofiber adhesion and durability on fabric substrate against repeated twist and rubbing actions. The effect of plasma pretreatment on fabric substrate was analyzed through water contact angle and XPS tests. The results suggested that plasma pretreatment introduced surface etching and active chemical groups on polymer surface. These active chemical groups might have led to possible cross-linking between fabric substrate and nanofiber mat to assist adhesion improvement.

- Electrospun nanofibers were deposited on plasma pretreated Nylon/Cotton blend fabric substrates through plasma-electrospinning hybrid process. Helium or mixture of helium and oxygen was used as plasma carrier gas. The effects of plasma treatment on electrospun nanofibers and fabric substrate were analyzed through water contact angle and XPS tests. The results suggested that plasma pretreatment introduced surface etching and active chemical groups on polymer surface. The active chemical groups might have led to possible cross-linking between fabric substrate and nanofiber mat to assist adhesion improvement. The plasma-electrospinning hybrid process in combination with plasma pretreatment of fabric substrate has shown better improvement in adhesion strength of nanofiber mat. The flex resistance tests results also showed improvement in nanofiber adhesion and durability on fabric substrate against repeated twist and flexion actions.

7.2 Recommendations

In this dissertation research, the fabrication of multifunctional nanofibers, deposition of electrospun fibers on woven fabric to improve barrier properties and improvement of nanofiber mat adhesion on fabric substrate through atmospheric pressure plasma application were examined. Some of our recommendations for future research are discussed below.

7.2.1 Reactive polymers

In Chapter 4, multifunctional ZnO/Nylon 6 nanofibers fabrication and its detoxifying abilities were discussed. The scope of polymer nanofibers with self detoxifying ability could be

explored to reactive polymeric materials as evidenced in recent studies on oximation of polyacrylonitrile fibers.[1,2] Oxime chemical compounds belong to imines with general formula $R_1R_2C=NOH$ and they have strong hydrolytic action against nerve agents. Bromberg and coworkers [1] have reported blending polyacrylamidoxime compound with polyacrylonitrile polymer in electrospun fibers. The resultant reactive polymer nanofibers exhibited hydrolytic action against simulant of nerve agents. However the blending of polyacrylamidoxime is a tedious chemical process and the obtained nanofibers are specific to detoxify nerve agent. As an alternate, polymer could be made multifunctional by introducing active chemical compounds such as redox enzymes of oxidase, peroxidase, hydrolase, and N-alkyl 4-pyridinium.[3,4] It has been reported that polyethyleneimine compound is effective against various types of pathogens and has moderate detoxifying ability against nerve agents.[5,6] In view of these literature reports, it is worthwhile to investigate the possible fabrication of functional fibers by using these reactive polymers.

7.2.2 Plasma Carrier Gas

In Chapter 5 and 6, the plasma treatment of fabric substrate and electrospun Nylon 6 fibers were discussed. He or He-O_2 was used as plasma carrier gas. The XPS analyses showed that the introduction of oxygen gas might have assisted in the formation of more active chemical groups. The active chemical groups on polymer surfaces facilitate the formation of cross-linking between nanofibers and fabric substrates, and improve adhesion strength. The possibilities of other plasma carrier gases such as N_2, CO_2 and NH_3 could be explored for creation of more active chemical groups on polymer surfaces. Epaillard et.al reported the use

of CO_2 as plasma carrier gas to introduce COOH groups on hydrophobic polymers surfaces such as polypropylene and polystyrene.[7] The use of N_2 and NH_3 as plasma carrier gases were also reported to introduce C=N or NH_2 polar groups.[8-10] These highly polar chemical groups could lead to formation of hydrogen, ionic and cross-linking bonds between plasma treated polymer surfaces. So we recommend use of different plasma carrier gases and study the effect of active chemical group formation of surfaces of plasma treated nanofibers and fabric substrates.

7.2.3 Electrospun fibers and fabric substrate

In this research, Nylon 6 polymer was used as electrospinning polymer and Nylon/Cotton blend woven fabric as substrate. It has been reported about electrospinning of various polymer nanofibers such polyethylene terephthalate, polyurethane, polyacrylonitrile, polypropylene, etc.[11] These fibers are inherently hydrophobic and have limited adhesive behavior with other material interface. However, each polymer material has distinctive properties and could be tailored for specific end use. For example, polyurethane is well known for its high flexibility and elastic or shape recovery properties.[12] Polyurethane fibers deposited on fabric could serve excellent flex resistance. Low temperature plasma treatment of various hydrophobic polymer fibers to improve adhesion on other material surface have been reported.[13-15] So we recommend use of polyurethane polymer to electrospun nanofibers and deposit on different fabric surfaces and study the durability performances.

7.3 References

1. L. Chen, L. Bromberg, H.S. Gibson, J. Walker, T.A. Hatton, G.C. Rutledge, Chemical protection fabrics via surface oximation of electrospun polyacrylonitrile fiber mats, *J. Mater. Chem.*, 2009, **19**, 2432.
2. L. Bromberg, H.S. Gibson, W.R. Creasy, D.J. McGarvey, R.A. Fry, T.A. Hatton, Degradation of Chemical Warfare Agents by Reactive Polymers, *Ind. Eng. Chem. Res.* 2009, ***48***, 1650.
3. G. Amitai, H. Murata, J.D. Andersen, R.R. Koepsel, A.J. Russell, Decontamination of chemical and biological warfare agents with a single multi-functional material, *Biomaterials*, 2010, 31, 4417.
4. Borkar, C.Z. Dinu, G. Zhu, R.S. Kane, J.S. Dordick, Bionanoconjugate-Based Composites for Decontamination of Nerve Agents, *Biotechnol. Prog.*, 2010, **26**, 6.
5. S. Sundarrajan, A. Venkatesan, S. Ramakrishna, Fabrication of Nanostructured Self-Detoxifying Nanofiber Membranes that Contain Active Polymeric Functional Groups, *Macromol. Rapid Commun*. 2009, **30**, 1769.
6. B. Gao, X. Zhang, Y. Zhu, Studies on the preparation and antibacterial properties of quaternized polyethyleneimine *J. Biomater. Sci.*, 2007, **18**, 531.
7. M.Wang, Y. Chang, F.P. Epaillard, Acid and basic functionalities of nitrogen and carbon dioxide plasma-treated polystyrene *Surf. Interface Anal.* 2005, **37**, 348.
8. N. Me´dard, J. Soutif, F.P. Epaillard, CO2, H2O, and CO2/H2O Plasma Chemistry for Polyethylene Surface Modification Langmuir 2002, **18**, 2246.

9. M. M. Hossain, J. Mussig, A.S. Herrmann, D. Hegemann, Ammonia/Acetylene Plasma Deposition: An Alternative Approach to the Dyeing of Poly(ethylene terephthalate) Fabrics at Low Temperatures, *Journal of Applied Polymer Science*, 2009, **111**, 2545.
10. Brigitte Mutel Polymer Functionalization and Thin Film Deposition by Remote Cold Nitrogen Plasma Process, *Journal of Adhesion Science and Technology*, 2008, **22,** 1035.
11. Z. Huang, Y.Z. Zhang, M. Kotaki, S. Ramakrishna, review on polymer nanofibers by electrospinning and their applications in nanocomposites, *Composites Science and Technology* 2003, **63**, 2223.
12. Y. Zhu, J. Hu, L. Yeung, Y. Liu, F. Ji, K. Yeung, Development of shape memory polyurethane fiber with complete shape recoverability, 2006, *Smart Mater Struct*, **15** 1385.
13. K.N. Pandiyaraj, V. Selvarajan, R.R. Deshmukh, C. Gao, Adhesive properties of polypropylene (PP) and polyethylene terephthalate (PET) film surfaces treated by DC glow discharge plasma, *Vacuum*, 2009, **83**, 332.
14. H. Krumpa,*, M. Sˇimorb, I. Hudecc, M. Jasˇsˇoc, A.S. Luyta Adhesion strength study between plasma treated polyester fibres and a rubber matrix, *Applied Surface Science*, 2005, **240**, 268.
15. C. Dai, T. Tsui, Y. Cheng, Adhesion of PET/PSMA Interfaces Reinforced with Plasma Treatment, *Surface Review and Letters*, 2006, **13**, 265.